QUANTIFYING SPATIO-TEMPORAL SOIL WATER CONTENT USING ELECTROMAGNETIC INDUCTION

by

Judith Amarachukwu Edeh

A dissertation submitted in accordance with the requirements for the degree

Magister Scientiae Agriculturae

In the Department of Soil, Crop and Climate Sciences

Faculty of Natural and Agricultural Sciences

University of the Free State

Bloemfontein, South Africa

Supervisor: **Dr JH Barnard**

Co-supervisor: **Prof LD van Rensburg**

2017

DECLARATION

I, Judith Amarachukwu Edeh, hereby declare that;

- this research dissertation, submitted for the Degree Magister Scientiae Agriculturae qualification in Soil Science Department, at the University of the Free State is my own independent work and has not previously in its entirety or in part been submitted by me to any other University.

- I also agree that the University of the Free State has the sole right to the publication of this dissertation.

Judith Amarachukwu Edeh

_____

Signature

TABLE OF CONTENTS

ACKNOWLEDGEMENTS

- My utmost gratitude to the Lord God Almighty. The Author of my life and he, who knows it all; to you I return all thanks.

- I humbly declare my heartfelt gratitude to my brother Dr C.J. Ede who supported and financed my stay in South Africa thus far. He was there for me both in payment of school fees, feeding and accommodation.

- I would like to sincerely thank my supervisor Dr. J.H. Barnard for his efforts and contributions to the successful completion of this thesis. He devoted a tremendous amount of time and effort to help me redefine the statistical part of this study, his efforts helped to the finalization of this thesis.

- Heartfelt gratitude to my co-supervisor and mentor Prof. L.D. Van Rensburg for his enduring patience, advice, full support and painstaking attention to details and accuracy in field procedures and academic writing. He saw my eagerness to learn and assigned me to this project with full support and motivation, taking every step with me in achieving the set goals.

- I would like to thank the University of the Free State for the free registration offered to me during the extension of this project, and also the Department of Soil, Crop and Climate Sciences at the University of the Free State, for offering me financial assistance.

- I would like to gratefully acknowledge the support of Dr. S.S. Mavimbela, Dr. B. Kuenene and Dr. P. Dlamini that took their time in identifying the different soil forms within the selected layout at Paradys Experimental Farm of the University of the Free State. Also, Dr Z.A. Bello, Dr W.A. Tesfuhuney and Mr C. Tfwala, for their friendly advice and contributions.

- I am also very thankful to Anneline Bothma for her time, effort and contribution in proof-reading my work, including the final editing, making sure that the entire piece of work is readable. Special thanks to your family for the accommodation towards the final stage of writing this thesis; if not you, it wouldn't have been easy.

- I must thank the technicians Mr Sandile, Mr Elias and Mr Fegan for their valuable help in instrumentation and facilitating equipment installation, and their field work assistance in measurements and data collection.

- Special thanks to my friends and colleagues who may have assisted me in any way with profound inputs.

- Finally, I must thank my entire family, my beloved mother, sisters and brothers, for their generous support, calls and encouragement.

LIST OF TABLES

LIST OF FIGURES

LIST OF APPENDICES

QUANTIFYING SPATIO-TEMPORAL SOIL WATER CONTENT USING ELECTROMAGNETIC INDUCTION

by

Judith Amarachukwu Edeh

ABSTRACT

Water scarcity is still a global concern, and the fact that water is not evenly distributed within the soil remains a case study in agriculture. Apparent electrical conductivity (EC_a) measured with the EM38 devices have been consequently used to distinguished areas of water management in precision agriculture, before irrigation planning. However, to efficiently use EM38 and its newer model "EM38-MK2" required site specific calibration. This involves collecting soil samples for volumetric water content the same time the device is used. Repeated soil sampling over time series have been reportedly stated to be time consuming and destructive. Therefore, this thesis proposed to use DFM capacitance probes that only need to be installed once in the soil to continuously record water content. The study presented three main objectives to: (i) examine the influence of DFM probes, and other possible obstructions including neutron water meter galvanized-steel access tubes and profile pits on EC_a measurements with the EM38-MK2, (ii) calibrate the EM38-MK2 using DFM probes installed in the field, and (iii) spatially characterize soil water content estimated from multiple EM38-MK2 surveys.

On relative homogenous soils of Kenilworth Experimental Farm and with DFM probes, steel access tubes and profile pits consecutively inserted into the soil, EM38-MK2 was moved towards these interferences, over it and away from it without zeroing the EM-device. Results showed that while trenches had no effect, both DFM and steel tubes influenced EC_a readings when the EM-device was closer than 1 m to these instruments. This effect was inconsistent with large values that were either negative or positive. After encountering the interferences and without EM zeroing, EC_a readings were either less stable (only at vertical mode for the DFM) or reduced. Although the instability was statistically significant, the mean EC_a before and after the probe-interference were not significantly different. The decreases in mean EC_a values at horizontal mode for DFM and at both modes for steel tubes were all relatively small (< 2 mS m^{-1}). This study concluded that the EM38-MK2 can be used together with DFM probes, but keeping the EM-device at least 1 m away from the probes. On a practical level, there should be no need to re-zero the EM38-MK2 after an encounter with such metal-containing interferences. Rather, re-zeroing is advised after extended use in the field as suggested by other researchers.

On the heterogeneous soils of Paradys Experimental Farm comprising of four diverse soil forms, field calibration of DFM probes and EM38-MK2 were performed under both dry and wet conditions. The calibrated capacitance probes accurately predicted water content that spatially explained on average, up to 96% of the observed water content. The DFM estimated soil water values on individual plots were consistent and were used for site-specific calibration of EM38-MK2. EC_a-based estimated water content for individual plot models explained on average, 97% and 90% of variation in soil water content, at 0.38 m and 0.75 m depth, respectively. With the general models EC_a values could predict 74% and 69% of the volumetric soil water content at 0.38 m and 0.75 m, respectively. This was regarded as satisfactory, especially considering the heterogeneity of the soils on the experimental site. Therefore, the models developed in this study, performed well both at individual plot and over spatial scales.

When the general models were applied on spatial scale, EC_a-based estimated water content was temporally stable. The spatio-temporal soil water maps produced an accurate representation of topographical effects on soil water distribution over the area. Therefore, the proposed use of the DFM capacitance probe method for site specific-calibration of EM38-MK2 was successful and could be adopted for future research.

Keywords: EMI, EM38-MK2, EC_a interference, soil water content, calibration, soil heterogeneity, site-specific calibration, spatial and temporal water characterization, mapping.

CHAPTER 1. GENERAL INTRODUCTION

Water scarcity is a global concern due to the extremely limited amount of accessible fresh water suitable for use in agriculture. It is estimated that 7100 km^3 of water is consumed globally each year to produce food (Kosseva & Webb, 2013). Approximately 77% of this estimate is utilized in rain-fed production systems, while the remaining 1600 km^3 is applied in irrigated production systems yearly (CA, 2007; De Fraiture *et al.*, 2007). To sustain food production, while ensuring optimal use of rain and irrigation water, requires the best soil water management practices. This begins with accurate quantification of soil water at different spatial and temporal scales within the plant root zone.

The standard and direct way to accurately quantify soil water content is via the gravimetric method, which involves collection of soil samples and calculation with soil bulk density. This method is expensive, time-consuming, labour intensive and too destructive to use repeatedly at the same location (Hendrickx, 1990). Where soil water measurement is required over large field scales on a regular basis, electromagnetic induction (EMI) methods (Chapter 2) have become popular. The advantages of EMI methods are based on their measurement depths (McNeil, 1980; Gebbers *et al*., 2009), fast application on larger field scales (Misra & Padhi, 2014), temporal stability in soil spatial surveying (Western *et al*., 2004) and their use for soil mapping (Lesch *et al*., 1992; Lesch *et al*., 2005).

The EM38 instruments (Geonics Limited, Mississauga, Ontario, Canada) are the most widely used EMI sensors in agriculture (Sudduth *et al.*, 2001; Corwin *&* Lesch, 2003). Like other EMI instruments, EM38 devices are non-invasive, relatively easy to use, and can record a large volume of data in a short period of time. Large field scales can be surveyed through mobile means directed by Global Positioning System (GPS) and data can be automated to a Geographical Information System (GIS). The EM38 produces soil water variability maps with much higher spatial resolution (Lesch *et al*., 1992; Lesch *et al*., 2005; Misra & Padhi, 2014), compared to the conventional mapping method involving several points or grid sampling (Batte, 2000; Brevik *et al*., 2003, 2012). The EM38 also maintain good sensitivity and remain well adapted for soil water mapping even under drier soil conditions (Lahoche *et al*., 2002). The newer model “EM38-MK2”, developed in 2008 (Doolittle & Brevik, 2014), has been proven capable for near surface application in agriculture (Gebbers *et al.*, 2009). The EM38-MK2 is equipped with double receiver coils, allowing both shallow and deep soil measurements that correspond to most agricultural crop root zones. The instrument also has built-in temperature compensation circuitry that improves temperature-related drift characteristics associated with previous models (Geonics, 2012). This device can be used without installation or any

destructive soil sampling and is more productive on a highly heterogeneous soil (Heil & Schmidhalter, 2012, 2015).

Like other EMI sensors, the EM38-MK2 measures apparent electrical conductivity (EC_a) for a bulk soil volume directly beneath the soil surface. This is a sensor-based measurement that reflects from the cumulative current applied by the instrument over a specific depth range (McNeill, 1980). It is an indirect measure of soil water, since it incorporates some soil physicochemical properties that are highly dependent on soil water into its measured values. However, geospatial EC_a measurements can be used to quantify if not all, one dominant soil property when information on other contributing soil properties are known or can be estimated (Sudduth *et al.*, 2005). This measure has been used to develop soil water maps (Lesch *et al*., 1992; Lesch *et al*., 2005; Misra & Padhi, 2014) and characterize variation in several soil properties including soil water content (Sheets & Hendrickx, 1995; Triantafilis *et al.*, 2002; Corwin *et al*., 2003b; Sudduth *et al.*, 2005) on large spatial scales.

There are two major drawbacks in the use of EM38-MK2 in agriculture. First is the fact that the instrument requires site-specific calibration with soil sampling every time the instrument is used. Calibration is performed to obtain a function that accurately describes the relationship between EC_a and volumetric soil water content (Corwin & Lesch, 2005b). However, sampling the soil for gravimetric soil water estimation every time the instrument is used is not practical on a large field scale. Literature has reported the use of intermediate methods, such as a neutron water meter (NWM) (Sheet & Hendrickx, 1995; Reedy & Scanlon, 2003) and electrical resistivity tomography (ERT) (Lavoue *et al*., 2010) to calibrate the EM38 for mapping EC_a variation on a large scale. The problem with the NWM is based on its radioactive source that is unsafe for human health. Possible limitations of ERT are that it uses a large number of electrodes and provides EC_a measurements on a smaller scale. This measure can be influenced by any soil attribute in the same manner as with the EM38.

The second major drawback is the sensitivity of the EM38 to metallic objects in the soil (Bevan, 1998). When the instrument encounters metallic objects, it causes drift and the instrument needs recalibration to avoid instability in EC_a readings. Therefore, the presence of soil water sensors, such as capacitance probes and steel NWM access tubes are likely to influence readings of the EM38-MK2. In preliminary studies, it was observed that current flow from the EM38-MK2 may also be influenced by large trenches like profile pits, that are often used on research farms to characterize soil.

This study therefore wants to explore the use of a different reliable, indirect method that is also less destructive and less laborious, to calibrate the EM38-MK2. The use of capacitance

sensors (DFM probes) is one accurate indirect method for determining soil water content (Zerizghy *et al*., 2013). DFM capacitance probes are point measurement instruments that need to be installed only once into the soil, to continuously measure apparent relative dielectric permittivity of the soil for soil water estimation (Kelleners *et al.*, 2005; Kizito, 2008).

Evidence of whether EC_a-directed soil surveys will provide a temporally stable calibration functions that can be used to estimate water content from measured EC_a on a rangeland, is still limited. The ultimate goal of this dissertation was to quantify spatio-temporal soil water content at field scale with the specific objectives allocated to Chapters 2 to 6:

- Chapter 2 was dedicated to the literature review with the purpose of presenting a theoretical background of EM38-MK2, its operational principles and application of field measured EC_a.

- Chapter 3 was devoted to distinguish the various soil forms on the selected experimental sites, to characterize the morphological, physical and chemical properties of each individual soil form. An important outcome of this was to verify the homogeneity or heterogeneity of the experimental sites.

- Chapter 4 was structured to achieve two objectives. Firstly, to determine at what distance to place the EM38-MK2 from obstructions, including trenches, DFM capacitance probes and NWM steel access tubes, during field surveys, since EC_a readings should preferably be taken as close as possible to soil water measurement points. Secondly, to examine accuracy and stability of EC_a readings after the EM38-MK2 encountered the various interferences, in order to determine whether instrument re-zeroing would be required.

- Chapter 5 dealt with the evaluation of the EM38-MK2 to infer soil water content on a heterogeneous soil. The first objective was to conduct field calibration of the DFM probes readings to volumetric water content. The second objective focused on calibrating the EM38-MK2 for soil water estimation using calibrated DFM probe output. To develop a general EC_a model equation that can be used over time to characterize soil water content on a spatio-temporal scale.

- Chapter 6 aimed to provide a summary of all results from the above experiments, making final conclusions and suggestions for future research.

CHAPTER 2. LITERATURE REVIEW

2.1 Introduction

In the quest to estimate soil water variability both at field and landscape scales, electromagnetic induction (EMI) has been used with success (Corwin, 2008; Toushmalani, 2010). The principle of EMI was first introduced by Michael Faraday in the early 19th century. This principle is incorporated into many devices or sensors for soil surveying. Commercially available EMI sensors used in agriculture for soil investigation include: the DUALEM sensors (Dualem, Inc., Milton, Ontario), the Profiler EMP-400 (Geophysical Survey Systems, Inc., Salem, New Hampshire) and the EM38 sensors such as EM38, EM38-DD, EM38-MK2-1 and EM38-MK2 sensors (Geonics Limited, Mississauga, Ontario, Canada) (Gebbers *et al*., 2009; Doolittle & Brevik, 2014).

Sudduth *et al*. (2003) stated that each of these commercial sensors has their own operational advantages and disadvantages. The DUALEM sensors were developed with multiple coils and orientations, hence it provides information at different depth ranges but has not been as widely used as the EM38 instruments. The Profiler EMP-400 is an electromagnetic profiling sensor that uses multiple frequencies, allowing the user to select the frequencies that provide the best results for the intended application (Doolittle & Brevik, 2014). The Profiler was designed for maximum structural and thermal stability, but is limited to shallow depth application (Doolittle & Brevik, 2014). The EM38 sensors were reported as the most widely used EMI sensors in agriculture due to its shallow depth application (Sudduth *et al.*, 2001).

EMI sensors are tools for assessing both subsurface and groundwater information of a soil (Brune & Doolittle, 1990; McNeill, 1996; Bowling *et al.*, 1997; Eigenberg & Nienaber, 1998; Eigenberg *et al.*, 1998). With these sensors, measurements can be done with ease, a variety of ground conditions can be surveyed under dry and wet conditions, and vertical separation of geophysical properties can also be viewed through digital soil mapping. The depth at which each EMI sensor can assess soil informaion is controlled by the orientation of the instrument, intercoil spacing, height of the instrument above the soil and the frequency of the induced current (Gebbers *et al.*, 2007). All EMI sensors record the apparent electrical conductivity (EC_a) of a soil, which is the reflected current from that applied by the sensor.

Although these EMI sensors have a great time-saving advantage over direct soil sampling for estimating water content, they still require calibration of the instrument reading with the standard volumetric method. This involves soil sampling and deriving the volumetric water content for the surveyed sites. Because this standard method is too tedious and time

consuming to be applied on large field scale, several studies have shown the possibility of using a two-step calibration process that involves the use of water content estimated by other indirect methods (Sheet & Hendrickx, 1995; Reedy & Scanlon, 2003; Lavoue *et al*., 2010) for fast and accurate calibration.

This chapter will provide in detailed description of the EM38-MK2, including its principles of operation. The factors influencing EC_a measured with the EM38, different approaches for field calibration of the instrument, as well as application and field protocols for EC_a measurements will also be reviewed.

2.2 Description and operation of the EM38-MK2

The EM38-MK2 sensor was developed for use on the ground, air and boreholes (Daniels *et al.*, 2008). The standard EM38-MK2 (Figure 2.1) is 1.05 m in length and 3.5 kg in weight. This sensor is a hand held instrument, also mountable on a mobile and directed by a Global Positioning System (GPS) as data are automatically logged into a Geographical Information System. Data recording is either via RS-232 serial port or Bluetooth (Jaynes *et al.*, 1993; Geonics, 2012). The EM-device is powered by a single 9 volt battery with a battery life of up to 20 hours, or an external rechargeable battery. The specifications of EM38 sensors are detailed in the Geonics catalogue (Geonics, 2012), while the operating instructions of the EM38-MK2 are given in the operating manual by Geonics (2010).

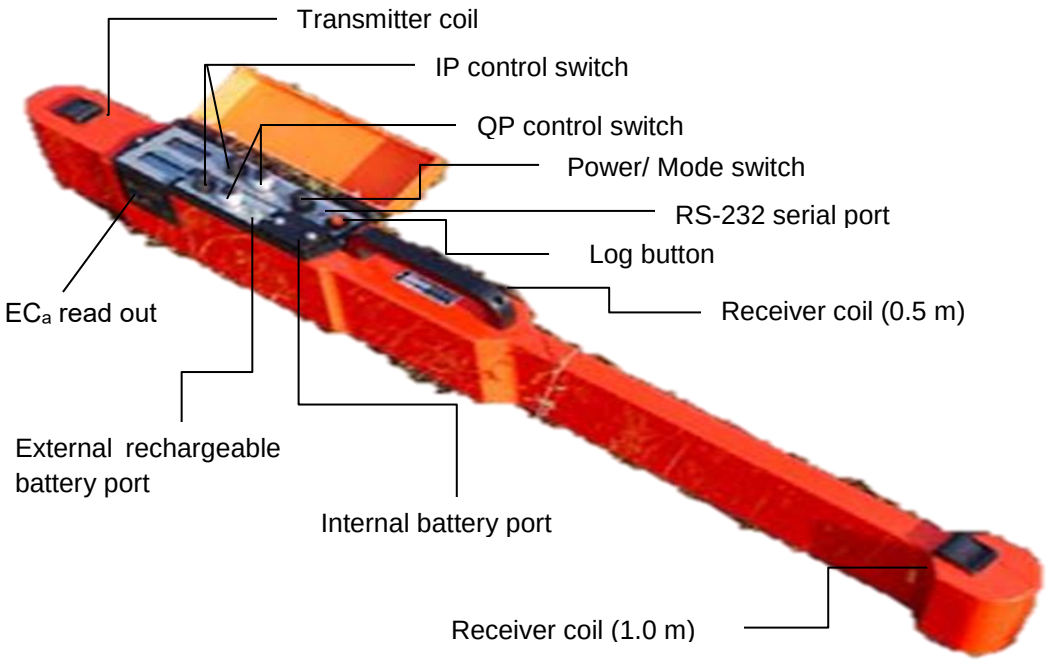

Figure 2.1 The EM38-MK2 manufactured by Geonics Limited and the functions of some important parts.

All EM38 instruments measure soil EC_a on both horizontal (H-mode) and vertical (V-mode) dipole modes. The original EM38 instrument has one receiver and one transmitter coil with a 1 m intercoil spacing, while the EM38-MK2 (Figure 2.1) has one transmitter and two receiver coils that are situated 1 m and 0.5 m from the transmitter. As a result of the additional receiver coil, the EM38-MK2 provides EC_a measurements at two distinct depths of 0.375 m and 0.75 m in the H-mode, and 0.75 m and 1.5 m in the V-mode. This EC_a measure is the ground electrical conductivity of the soil recorded as QP (Quad-phase) on the EM38-MK2 read-out screen. The QP readings are also accompanied by an In-phase (IP) reading, which is a measure of the magnetic susceptibility of the soil (Geonics, 2003).

Quad-phase (QP): This is the measured ground electrical conductivity of the soil known as the apparent electrical conductivity (EC_a). The QP measures in milliSiemens per meter (mS m^{-1}) with a measuring range of 100 mS m^{-1} and 1000 mS m^{-1} for 0.5 m and 1 m intercoil spacing, respectively. The noise level for the QP reading is 0.5 mS m^{-1}. Note that the QP measured values can also be expressed in dS m^{-1} when multiplied by 100.

In-phase (IP): The IP reading is a self-generated signal expressed by the EM device as a result of magnetizable objects or metals within the soil that react to the presence of the electrical current applied by the EM device. This reading is in relation to the variability of the earth's magnetic field near the surface, which senses any metallic obstruction or artificial objects buried within the soil profile. It reads in parts per thousand (ppt) with a measuring range of ± 7 ppt and ± 28 ppt for 0.5 m and 1 m coil separations, respectively (Geonics, 2012). The noise level for the IP reading is 0.02 ppt. The EM device requires a proper check after an encounter with a metallic object, in order to null out this IP effect within the field when carrying out a ground conductivity survey. IP readings should be maintained at zero using the controls on the EM38-MK2 (Geonics, 2003).

2.2.1 Instrument zeroing

For accuracy when using the EM38-MK2, an instrument check is required each time prior to field measurement. This involves a battery test, in-phase nulling (to cancel or null the large primary signal from the transmitter so that it does not overload the electronic circuitry) and instrument zeroing. A complete guide on field EM device calibration to null the effect of IP was published by Geonics (2003) and this procedure is the same for all EM38 devices. Following is a summary of these instructions given by the manufacturer (Geonics, 2003):

The first step is to carry out a battery check at the beginning of the operation. A good battery reads above 720 units, below this the battery needs to be replaced. It is advised to switch on the EM device and allow it to warm-up for approximately 5 to 15 minutes before setting up the

device. The idea is to allow the EM device to get used to the area temperature, especially when it is transported from a storage house with different room temperature. With the EM device still on the ground, the QP and IP controls are set to zero using the control switch and a clockwise rotation of IP switch should not change the QP readings.

For step two, the EM device is placed at a height of 1.5 m above the ground, because at this height the device seizes to respond to ground conductivity. Placing the EM device in the horizontal operation mode and with the switch mode at 1 m, the QP and IP controls are set to read zero (Figure 2.1). Following the work examples in Table 2.1, with the EM device still in the H-mode, the QP is adjusted to read to a number “H1” (where H is the reading in the horizontal orientation of the EM device) that when the device is rotated to the V-mode (still at 1.5 m height), the QP reads a value “V1” (V is the reading at the vertical orientation of the EM device). Note that the value for H1 is an arbitrary number which means that there are no principles in choosing the value for H1, but the rule is to obtain V = 2H at the end of instrument zeroing.

For the EM38-MK2 to be properly calibrated to satisfy V = 2H, the EM device is returned back to the H-mode. With the EM device still reading “H1”, the QP zero control needs to be adjusted a second time by a value “C” (difference between V1 and H1) to form “H”, such that repositioning the device to the V-mode, the new QP will read the new “V” double the “H” which satisfies V = 2H. Table 2.1 gives a mathematical illustration on how to obtain V = 2H.

If “C” is the adjustment value and

$$\frac{V_1}{H_1} = \frac{V + C}{H + C} = 2 \qquad 2.1a$$

then,

$$C = V - 2H \qquad 2.1b$$

Table 2.1 Mathematical illustration for field EM38-MK2 instrument zeroing

If H1 = 12 mS m $^{-1}$, V1 = 32 mS m $^{-1}$ thus, C = 32 – (2 x 12) 32 – 24 = +8 mS m $^{-1}$. Therefore, H = H1 + C = 12 + 8 = 20 mS m $^{-1}$. And V = 2H V = 40 mS m^{-1} Note: when C is positive the reading is in the direction of higher conductivity	But if: H1 = 50 mSm^{-1} and V1 = 53 mS m $^{-1}$; thus, C = 53 – (2 x 50) 53 – 100 = - 47 mS m $^{-1}$. Therefore, H= H1 – C = 50 – 47 = 3 mS m $^{-1}$. And V = 2H V = 6 mS m $^{-1}$ Note: when C is negative the reading is in the direction of lower conductivity

At this stage, it means the zero is correctly set. But if conductivity values obtained when the EM device is in the V-mode are the same as when it is in H-mode after zeroing, it means that the soil on which calibration is conducted is so resistive that at 1.5 m height, the EM38 could not respond to conductivity. In this case, the QP control is adjusted to zero.

The third step is the final In-phase nulling which helps to null out the large primary signal from the transmitter so that it does not overload the electronic circuitry. After performing the procedures in step two and the EM device is brought down to the ground, the magnetic susceptibility of the soil causes an additional signal to be picked up by the receiver coil. The residual signal arising from this magnetic susceptibility is nulled out at this stage by zeroing the in-phase control switch. After this, the EM device is set for use (Geonics, 2003).

2.2.2 Principles of operation

The EM38-MK2 sensor works on the principle of electromagnetic induction (EMI), using a transmitter and two receiver coils. When the EM device is placed on the soil surface, carried, or mobilized within the field, the transmitter coil sends an alternating current at a fixed audio frequency of 14.5 KHz and temperature range of -30°C to +50°C (Geonics, 2003), creating a primary magnetic field "H_p" (Figure 2.2).

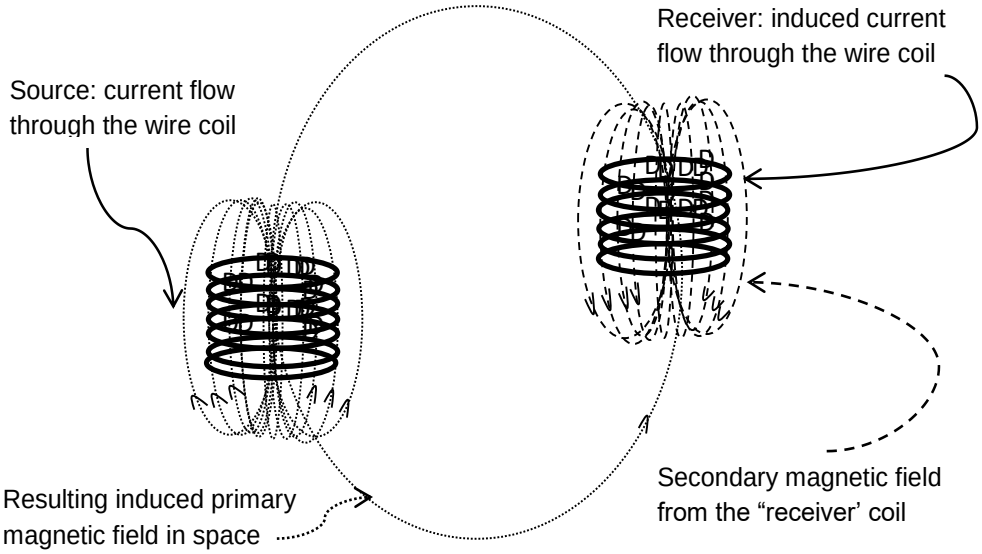

Figure 2.2 The principles of induction, showing the combination of Ampere's and Faraday's laws as used in geophysical electromagnetic equipment (Daniels *et al.*, 2008).

This primary magnetic field propagates through the soil spaces "μ_o", and induces an eddy current on any conductive soil materials within itself. The induced eddy current on the conductors now radiates a secondary magnetic field "H_S" by combining the intercoil space "s"

covered by the magnetic field, the frequency "f" at which the current was applied and the ground conductivity "σ" (i.e. ability of the soils around the sensor to conduct electricity), defined at low values of induction number. This is given in Equation 2.2 according to McNeill (1980).

The ratio of both primary and secondary magnetic fields is sensed by the receiver coils (McNeill, 1980) as the apparent electrical conductivity (EC_a) (Corwin, 2008). The measured EC_a when the EM device is located at the soil surface is given in Equation 2.3 (Corwin, 2008).

$$\frac{H_S}{H_p} \simeq \frac{i\omega\mu_o\ \sigma s^2}{4} \qquad 2.2$$

$$EC_a = \frac{4}{2\pi f\mu_0\ s^2}\left(\frac{H_S}{H_p}\right) \qquad 2.3$$

where, $\omega = 2\pi f$ and

$I = \sqrt{-1}$

μ_o = Permeability of free space $(4\pi \times 10^{-7}\ Hm^{-1})$

σ = Ground conductivity

S = Intercoil spacing (m)

H_S = Secondary magnetic field at the receiver coil

H_p = Primary magnetic field at the receiver coil

2.3 Apparent electrical conductivity (EC_a)

The EC_a measured with the EM38-MK2 is a sensor-based measurement that reflects from the cumulative current applied by the device over a specific depth range (McNeil, 1980). This is the averaged value of several conductive earth materials over a certain soil depth, depending on the dipole mode of the EM device. In South Africa, the values of EC_a are in standard units of milliSiemens per meter (mS m^{-1}) while other countries reports EC_a in deciSiemens per meter (dS m^{-1}). The principle soil features that determine EC_a measurements are soil water content, soil salinity, the amount of clay in a soil, cation exchange capacity (CEC) and temperature (McNeil, 1980; James *et al*., 2000; Friedman, 2005). Other soil properties associated with EC_a are bulk density, soil organic content, soil nutrients and the concentration of ions in a solution. The condition of these additional properties controls how the earth materials determine the EC_a measured. Most of these properties are among the factors influencing EC_a measured by EMI sensors (Friedman, 2005).

2.3.1 Factors influencing EC_a measurement

Soil water content

Studies have found that soil water content is the single most important of all the factors known to influence EC_a (Brevik & Fenton, 2002; Huth & Poulton, 2007) since current flow within a soil mainly depends on water content. As a result of charge displacement from the water molecules, water flowing down the soil creates a pathway for electric current flow (Williams & Hoey, 1987; Sudduth & Kitchen, 1993; Doolittle *et al.*, 1994). As water moves within the soil, it affects soil properties. Sometimes water movement removes or translocates soluble chemical components and suspended colloids through a recharge process, while other times, they are added through a discharge process (Richardson *et al.*, 1992). In this same process, salts can be easily dissolved or activated and heat conduction (λ) increased, leading to soil temperature increase. Using EM38-MK2 under these conditions will result in high variation in EC_a values and more contributions from other soil properties as well.

A soil that is extremely dry will definitely influence EC_a because soil chemical reactions and current flow will seize under such conditions. This has been confirmed by Johnson *et al.* (2001) after finding poor correlation between EC_a and a number of soil properties on a no-till dryland. Also, if soil water content changes during a survey (after a rainfall episode for example) the values of EC_a will also change (Brevik *et al*., 2006) and if rain has been excessive, there is a possibility that one will not be able to discriminate between low level variation in EC_a values (Clay, 2005).

Soil salinity

Salinity of a soil is caused by the accumulation of salts. It is quantified in the laboratory as electrical conductivity (EC) using saturated paste extraction (EC_e) method or 1:1 ($EC_{1:1}$), 1:2 ($EC_{1:2}$) and 1:5 ($EC_{1:5}$) soil to water ratio methods, and is expressed either in dS m^{-1} or mS m^{-1}. The soil water solution extracted under suction from a saturated soil paste contains several electrolytes (Salts), and under wet soil conditions, they dissolve and increase the ability of a soil to conduct an electrical current. The higher the concentration of the dissolved salts, the higher the electrical conductivity of the soil solution. Despite the stress with this saturated paste extraction method, it is an accurate measure of soil salinity (McNeil, 1992) in the laboratory. The measured EC_e from the paste extract is the field equivalent of EC_a measured with the EM38-MK2 (Nadler & Frenkel, 1980). However, the conversion between EC_e and EC_a only required a calibration function (Vlotman, 2000). On a low conductive soil, the relationship between these two variables is reduced. Rhoades (1989) illustrated a number of EC_a and EC_e relationships, for different soil types and found that, EC_a values increases in proportion to the

percentage clay in each soil type. On high conductive soil, salinity can influence the measured EC_a readings. When excess salts dissolved within a soil, it affects soil-water balance, causes the water table to rise by capillarity, and exposes the salts within the soil surface to be readily detectable (Rhoades & Corwin, 1981) more than the proposed soil property under study.

Soil texture

Soil texture is the proportion of various particle sizes in a soil. Each particle size has a range of electrical charge that results in the particle surface holding ions. Clay particles has a larger surface area and can retain soil water and dissolved solids, therefore they are associated with high electrical conductivity. On the other hand, silt and sand particles have low electrical conductivity (Lund, 1999; Grisso *et al.*, 2009). Lund (1999) stated that the primary contributor to soil electrical conductivity in a non-saline field is soil texture. A study by Mckenzie *et al*. (1988) on the effect of soil texture, temperature and soil water on EC_a measurements, showed that the coarser the soil is, the more variation in the measured field EC_a values. Also, a study has shown that EC_a has its greatest potential to differentiate between soil types under wet conditions (Brevik *et al.*, 2006), but due to complexity in high-clay soils, a different result could be expected (Sudduth *et al*., 2003). This is because, high-clay soil acts as a storage medium for soil water contents, soil nutrients and exchangeable cations and expands under wet conditions, increasing the volume of the soil which might influence EC_a measurements.

Cation exchange capacity (CEC)

Cation exchange capacity is the measure of the ability of the soil to hold positively charged ions, such as: calcium (Ca^{2+}), magnesium (Mg^{2+}), sodium (Na^{+}) and potassium (K^{+}) generally known as the base cations (Rayment & Higginson, 1992). The CEC of a soil differs, depending on the clay percentage, type of the clay, soil pH and the amount of organic matter in the soil. Soils rich in clay minerals have negatively charged ions on their surface; hence, during the formation of clay through weathering, positively charged ions (cations) are adsorbed to the surface area. These cations are loosely held to the surface and can subsequently be exchanged for other cations, or essentially go into solution if the clay is mixed with water. For this reason they are called exchangeable cations. Thus, the CEC of the soil is a measure of the number of cations that are required to neutralize the clay particle as a whole. A high exchange capacity indicates a high electric conductivity potential. However, clay particles are very small, and because the surface area per unit volume is very large, a large number of cations are absorbed. These absorbed cations can contribute significantly to the electrical conductivity of the soil, which then becomes a function of the clay content. Shainberg *et al*. (1980) studied the effect of CEC and exchangeable sodium percentage (ESP) on EC_a and found that conductivity increased as CEC increases, with a nonlinear relationship.

Temperature

Temperature is another factor influencing EC_a measurements (Sudduth *et al*., 2001; Brevik *et al.*, 2004; Robinson *et al.*, 2004). This includes both atmospheric temperature and soil temperature. Atmospheric temperature heats directly on the EM38 (Sudduth *et al*., 2001), warming up the device and this may impose short-term EC_a measurement drift. Soil temperature, resulting from the climatic changes between solar radiation, time of the day, vegetation and soil, may also influence EC_a readings. Soil temperature affects physical processes such as: soil water and soluble movement, diffusion of gasses and reaction coefficients of soils. It also governs the type of reactions that takes place in the soil profile (Hillel, 1998), as the natural chemical processes present in the soil profile can be doubled their reactions for each 10°C the soil temperature rises (Campbell, 1985). A small increase in water content of a dry soil causes an increase in heat conduction (λ). It has been reported that soil EC increases by 1.9% for every degree centigrade (°C) rise in temperature (Corwin & Lesch, 2005a). Friedman (2005) stated that "under conditions of low solution conductivity, the temperature response of soil EC_a tends to be stronger than that of its free solution".

Jury *et al*. (1991) reported that soil temperature variations are usually greater at shallow depths of 0.05 and 0.1 m than at greater depths of 0.3 m. This is because the heat from the atmosphere penetrates slowly into the soil due to low values of heat diffusivity and damping depth. Thus, the combination of heat in the surface area with a relatively low heat capacity results in a rapid rise of the soil surface temperature during the day. In the case of a frozen ground, soil particles move further apart and when soil particles separate, soil EC potentials decreases. Below freezing point, soil pores become increasingly insulated from each other, however, the overall soil EC_a declines rapidly (Mckenzie *et al*., 1988). Large diurnal temperature fluctuations tend to explain why EM38 instruments were confirmed to be more sensitive to horizontal mode readings (Geonics, 2003).

Studies have reported on the effect of temperature on EC_a measurements. Bevan (1998) found that, EC_a rises as the temperature changes during the day. Sudduth *et al*. (2001) also reported that an increase in ambient temperature (23ºC to 35ºC) caused an increase in EC_a values (32.2 mS m^{-1} to 42.3 mS m^{-1}), but only in experiments where a stationary EM38 device was elevated above the soil level. Sudduth *et al*. (2001) concluded that EC_a measured with the EM38 could drift as much as 3 mS m^{-1} per hour. This may be up to 10% of the total EC_a variation, a potentially large effect on soils with low conductivity. In the case of temporal studies, it has been shown that changes in temperature over a time period of several weeks to months can significantly influence EC_a measured with EM38 (Nugteren *et al.*, 2000; Sudduth *et al*., 2001; Brevik & Fenton, 2002).

Due to these effects, it has been advised to correct measured EC_a to a reference temperature of 25°C using Equation 2.4, as given by the U.S. Salinity Laboratory Staff (1954):

$$EC_{25} = f_T \times EC_T \ , \qquad 2.4$$

where, EC_T = EC_a measured at a particular temperature

EC_{25} = EC corrected temperature

f_T = Temperature conversion factor

Temperature conversion models for EC_a data: Models for the temperature conversion factor (f_T) are in various forms as shown in Table 2.2. These models has been analyzed and compared based on consistency and accuracy (Corwin & Lesch, 2005a; Ma *et al.*, 2010). A review by Ma *et al.* (2010) explained that, the ratio model has the best fit within a temperature range of 3 to 47°C but with a high residue error of 0.7%. The polynomial model by Rhoades *et al.* (1999) was accurate for a temperature range of 15 to 35°C, while the Wraith polynomial model was found more accurate for temperatures near 25°C.

All exponential models were reported to be consistent within a 15 to 35°C temperature range, except Well's original model and the corrected Sheet and Hendrickx's model (Corwin & Lesch, 2005a). Both these models produced smaller average residual error (0.26% and 0.14%, respectively) within a wider temperature range of 3 to 47°C. The corrected Sheet and Hendrickx model was reported as the most accurate correction factor commonly substituted in Equation 2.4 to convert EC_a readings to EC_{25}. Hence, the exponential equation in Table 2.2 should be used as a correction factor for measured EC_a values.

Table 2.2 Literature compilation of several forms of temperature conversion models

Models	Equations	References
Ratio model	$EC_{25} = \frac{EC_T}{1+\delta\,(T-25)}$; $\delta = 0.0191°C^{-1}$	Scollar *et al.* (1990); Heimovaara *et al.* (1995); Persson & Berndtsson (1998); Hayashi (2004); Dalliger (2006); Barry *et al.* (2008); Besson *et al.* (2008)
Exponential model	$f_T = 0.4470 + 1.4034e^{-T/26.815}$	Wells (1978); Sheets & Hendrickx (1995); Durlesser (1999); Auerswald *et al.* (2001); Eijkelkamp (2003); Corwin & Lesch (2005); Luck *et al.* (2005)
Polynomial model	$f_T = 1 - 0.20346(T_a) + 0.03822(T^2{}_a) + 0.00555(T^3{}_a)$	Stogryn (1971); Rhoades *et al*. (1999); Wraith & Or (1999)
Power function model	$f_T = \left(\frac{T_{ref}}{T_m}\right)^s$	Besson *et al.* (2008)

Other suggestions on unexplained EC_a variation

Soil pollution is another possible factor that can affect soil EC_a measurements. Polluted soils often contain high amounts of heavy metals that are also a source of electrical conductivity (Seifi *et al*., 2010). These metals may be residues from industrial mining or from soil management practices in agriculture. When measuring EC_a under such conditions the EM38 devices can easily detect these metals, thereby introducing error in readings. Most polluted soils are also filled with metallic debris such as art-craft or long forgotten metallic pipes. Such metallic objects including electric fences and wires, wrist watches and other form of metals can be easily dictated by the EM38. In respect to this, the manufacturer (Geonics, 2003) suggested removing all metallic objects on the operator's body during an EC_a field survey. Bevan (1998) performed conductivity tests on metal objects using EMI sensors (EM38 and EM31), excluding soil property effects. Electromagnetic signatures of several metal objects were tested using both EM devices and it was found that a large iron artillery shell produced a very strong response when passed under the coils of the EM38, while smaller iron fragments produced a weaker response. It was also noted that while both instruments were capable of detecting large metal objects, only the EM38 could detect small metal objects.

It should be noted that EM38 devices uses an open signal collector, therefore, the device can easily pick up environmental noise that can influence EC_a readings. Overhead power lines, fences (especially electric fences), as well as variation due to bouncing of a trailer mounted EM38 when travelling across rough areas, may cause fluctuation in the recorded EC_a or a drift in readings (Clay, 2005). The accuracy of the EM38 in measuring EC_a for precision agriculture was reported in Sudduth *et al*. (2001). The report showed that the distance of sensor from the ground level (i.e. when EM38 device is placed at some height above the ground) and the operating speed causes minor variations in EC_a measurements.

Dabas *et al*. (2003) recognized an error in positioning of the instrument and in EC_a data processing. This error in positioning could originate from the GPS offset (Friedman, 2005), bad calibration of EM38, disturbances from temperature effect (Robinson *et al*., 2004), vibrations (Clay, 2005) and the presence of scattered metal objects (Bevan, 1998) detailed earlier.

Possible precautions during field EC_a survey:

When performing an EC_a survey in the field, using an EM38 device, the following procedures may help to reduce error in readings:

- Always warm up the EM38 sensors before calibration to minimize drift and the effects of temperature in general (Bevan, 1983; Sudduth *et al*., 2001).

- The EM38 devices should be protected against direct sun rays by carrying the device in an envelope constructed of sheet foam 0.9 cm thick (Bevan, 1998). During data dumping and field breaks, the device should be insulated and shielded from the sun.
- Robinson *et al*. (2004) suggested conducting surveys when temperatures are below 40ºC. Alternatively, measurements should be taken during mid-morning (Huth & Poulton, 2007).
- Near surface conductivity and depth sensitivity can be muted by carrying the EM38 device 0.1 to 0.3 m (15 to 30 cm) above ground surface during a field survey.
- Avoid surveying if rainfall is expected in the middle of a survey (because of the possible effect of both the rain and lightning that might occur) (Clay, 2005).
- Avoid making measurements when soils are too dry to a depth of 0.3 to 0.4 m (30 to 40 cm) as conductivity is significantly reduced and readings are more variable. Take EC_a measurements when the soil is neither excessively moist nor very dry (Grisso *et al*., 2009).
- Avoid metal interferences with EM38 devices by keeping a distance from any electric fence, nearby vehicles, buried metal objects and wires. This can be accomplished by careful placement of the EM device beneath a high-clearance vehicle or on a custom-made cart constructed of non-metallic materials when performing a mobile field survey (Grisso *et al.*, 2009).

The soil properties mentioned from Section 2.3.1 influences EC_a in a complex and interrelated way in contributing to EC_a variation in a field survey and this varies from one site to another (Gardner, 1986). Banton *et al.* (1997) found a stronger correlation between texture classes and EC_a under dry than under wet soil conditions; while under wet soil conditions, Dalgaard *et al*. (2001) reported very strong correlation between EC_a and clay content. Therefore, one will expect EC_a variation within a field to correlate with these soil properties. However, when the targeted field EC_a survey is to characterize soil water variation, other soil properties are likely to impose some values on the EC_a measure if taken on very sunny days, swelling clays or saline soils. Studies have shown that there is a relationship between these properties and EC_a measure (Johnson *et al.*, 2001). However, using EC_a to quantify or characterize any of these properties is only achievable through calibration to relate EC_a measured to that dominant property (Reedy & Scanlon, 2003). The strength of the correlation will depend on how dominant one property is on conductivity relative to other soil properties, the method of operation, data analysis or on interpolation techniques applied if mapping is involved (Fulton *et al.*, 2011).

2.3.2 Calibration of EM38-MK2 for soil water

Calibration of the EM38-MK2 is site specific due to soil differences from one site to another and this is required each time the device is used, to correlate what the instrument measured to the more dominant soil properties. The standard way of calibrating EM38-MK2 for soil water

estimation involves, sampling the soil each time EC_a measurement is made with the device. Considering this process on a very large field scale or for time series soil management, it is very time consuming, labour-intensive and costly to collect soil samples, and it is also destructive to repeat sampling on the same piece of land. However, studies have successfully used various intermediate methods other than the standard gravimetric method to calibrate EC_a measured with EM38 devices (Kachanoski *et al*., 1990; Reedy & Scanlon, 2003; Stanley *et al*., 2014).

Time-domain reflectometry has been used as an intermediate to relate EC_a values to soil water content taken at the exact point of EC_a measurement on a non-saline soil with low conductivity (Kachanoski *et al*., 1988). Results showed that EC_a measured with an EM38 explained approximately 96% of the soil water content as measured with TDR up to 0.5 m soil depth, with no significant relationship deeper than 0.5 m.

Kachanoski *et al*. (1990) compared water content measured with neutron soil water meter (NWM) access tubes installed at 10 m intervals along a 660-m transect to EC_a measured with the EM38 at 2 m distance away from the probes. It was found that EC_a could explain 70% of the water content measured with the NWM. Sheet & Hendrickx (1995) conducted a similar study with 65 NWM access tubes at 30 m intervals, with the EM31 placed 10 m away from the tubes for 16 monthly EC_a measurements. It was recorded that EC_a explained 58% and 64% of the soil water content as measured with the NWM. The lower percentage water estimated was attributed to the 10 m distance between measuring points of EC_a and soil water content and the depth penetration of the EM31 (4 m) relative to that of water content measurement (1.5 m). Reedy & Scanlon (2003) investigated both spatial and temporal aspects of soil water monitoring over 3 years using 10 NWM access tubes, taking EM38 measurements at the location of the tubes (2.1 m soil depth). This study recorded approximately 73% of the combined spatial and temporal variability in water content at the top 0.75 m and 90% at 1.5 m, soil depths. Stanley *et al*. (2014) also used the same method to calibrate EM38 response to soil water content, but used polyethylene NWM access tubes and operated the EM38 directly over the same points where the NWM was used and recorded a strong relationship explaining 94% of water content as measured with the NWM.

EC_a measured with the EM38 has also been successfully correlated to EC_a measured by electrical resistivity tomography (ERT) for estimating soil water content (Lavoué *et al*., 2010).

2.3.3 Agricultural applications of EC_a measurement

The EC_a measurement have been in use since the early 20th century to locate geological features, including the determination of bedrock type and depth, location of aggregate and clay

deposits, measurement of groundwater extent, detection of pollution plumes in groundwater, location of geothermal areas and characterization of archaeological sites. Increased interest in precision agriculture has led to the vast application of EC_a in agriculture. The theoretical basis relating EC_a and soil properties was developed by Rhoades *et al*. (1989b).

EC_a as a surrogate measure of soil properties

***Soil-salinity assessment*:** Soil EC_a was regarded as the best method to spatially determine soil salinity (Williams & Baker, 1982; Wollenhaupt *et al.*, 1986; Rhoades *et al.*, 1989a; Triantafilis *et al.*, 2002). Soil electrical conductivity and the total salt concentration in a solution are closely correlated. Hence, EC_a measurements are frequently used as an expression of the total concentration of salt in a soil (Rhoades *et al.*, 1999). The first EC_a application in agriculture was to access soil salinity in an area of salt affected soils, where 65 to 70% of the EC_a variations were explained by the concentration of soluble salts (Williams & Baker, 1982). Also, Lesch *et al.* (1995a, b) was able to quantify within-field variations in soil salinity under a uniform soil where other soil properties were reasonably homogenous. On the other hand, in non-saline soils EC_a is a function of soil texture, soil water content and CEC (Rhoades *et al.*, 1976) and research has been conducted that introduces additional uses of EC_a in precision agriculture (Sudduth *et al.*, 2005).

Soil-water assessment: Several investigators have confirmed the relationship between soil water content and EC_a (Rhoades *et al.*, 1976; Hendricks *et al.*, 1992). Brevik *et al*. (2006) reported that EC_a was linearly related to soil water content. With EC_a measured with the EM38, Kachanoski *et al.* (1990) was able to record more than 80% of soil water storage variation in a moderately fine-textured, calcareous soil. Also, Padhi & Misra (2011) investigated the sensitivity of EM38 in determining soil water distribution in an irrigated wheat field and found both linear and non-linear functions that explain 70% to 81% of water content.

Yield assessment: Studies have also evaluated EC_a to describe several soil properties that can possibly influence crop yield and are ecologically important (Johnson *et al.*, 2001; Corwin *et al*., 2003a). Johnson *et al*. (2001) correlated EC_a measured based on a stratified soil sampling design with a small data set of soil properties, and found positive correlation between EC_a and clay, EC and bulk density within 0.3 m soil depth, and a negative correlation with soil water and organic matter. To assess soil quality of a saline-sodic soil, Corwin *et al*. (2003a) used a response surface soil sample design and found positive correlation between EC_a and EC_e, but not with clay, bulk density, CEC, exchangeable N^+, K^+ Mg^+ and total N. Corwin *et al*. (2003b) went further to integrate crop yield into EC_a-directed sampling approach and was able to identify those properties responsible for the spatial variation in cotton yield. On a soil with highly dissimilar soil drainage classes, Jaynes *et al.* (1993) reported negative correlation

between EC_a and grain yield during a wet year, with no correlation during a normal rainfall season. Sudduth *et al.* (1995) on clay pan soils, reported that EC_a and grain yield were negatively correlated during dry years. This confirms the precautions stated earlier in this Chapter that EC_a survey should be avoided when soils are extremely wet or dry. Soil organic matter has been indirectly assessed by the EC_a (Jaynes, 1996). Also, EC_a has been applied in field quality assessment and soil management zones where each zone is more homogeneous in terms of soil properties than the whole field (Fulton *et al.*, 2011). According to Audun *et al*. (2003), study of EC_a variations showing differences in soil organic matter (SOM), would provide useful information for the farmer in making decisions concerning site-specific fertilization.

Soil particle size assessment: Soil EC_a has been used in identifying highly uniform soil properties within a field (Brevik *et al*., 2012). Sudduth *et al*. (2005) related EC_a to soil properties across north-central USA and observed that clay content and CEC correlated much higher, with $r^2 \geq 0.55$, than other soil properties.

Soil EC_a measure has also been applied in soil depth studies. Brus *et al*. (1992) uses EC_a to identify depth to boulder clay soil. Soil EC_a has also been applied in estimating depth to clay pan (Kitchen *et al.*, 1999; Sudduth *et al*., 1995). It has been used to estimate depth of sand deposited after a flooding event (Kitchen *et al*., 1996) and soil drainage classes (Kravchenko *et al.*, 2002; Triantafilis *et al.*, 2004; Kravchenko, 2008). These properties were able to correlate with EC_a, because they are conductive body or in one way or the other contribute to those properties that affect EC_a measured. Therefore, the relationship between soil EC_a and some important soil properties depends spatially on individual soil condition and temporally on climatic differences.

EC_a in soil spatial and temporal studies

The variability of EC_a within a field is due to the depth-weighed summarized response of all properties influencing electrical conductivity of a soil. Emphasis has been laid on the need for long term measurement of soil water content to study its spatial variability at larger scales over several time series (Bell *et al.*, 1980). The reason is that, the effect most soil properties imposed on EC_a are to an extent fixed; while, some exhibit seasonal changes. Thus, EC_a measure has been consecutively applied to understand soil variability, both spatially and temporally (Brocca *et al.*, 2009, 2010). Eigenberg *et al.* (2002) related time series EC_a data to temporal changes with the hypothesis that EC_a measurements might be used as an indicator of soluble nitrogen gain and loss in the soil over time. It has been proven potential in predicting variation in crop production due to soil water unevenly distribution (Heermann *et al.*, 2000). Also, spatial and temporal application of EC_a measurement has helped to determine the extent and on what condition the spatial pattern of soil water variability are stable (Eagleson, 1978;

Porporato *et al.*, 2001). It may interest to know that, soil variability within an area in time and space is likely to be the same than variability on the entire field scale (Singh & Fiorentino, 1996), as most soils are highly heterogeneous. In order to have a clear view of variation within the surveyed area, EC_a data were found capable of producing high quality soil maps (Herrero *et al.*, 2003; Doolittle *et al.*, 2008, 2009; White *et al.*, 2012), when compared to the conventional soil mapping methods

EC_a in mapping soil variability

Increased interest in precision agriculture has led to the need for more detailed and accurate soil mapping techniques (Batte, 2000). The conventional method of soil mapping is not only expensive and time consuming, but it provides only descriptive spatial information and does not infer the location of each map unit. Furthermore, the conventional method requires a large amount of information. However, the use of EM38 device in connection with Digital Global Positioning System (DGPS) is a digital method of soil mapping that uses only a selected number of sampling points. Zhu *et al.* (2010) investigated the use of repeated EMI surveys, in combination with depth to bedrock and terrain attributes, to improve soil mapping in a 19.5 ha agricultural landscape. The relationship that exists between EC_a and several soil properties makes the EC_a map a potential tool to be used as a guide in decision making in precision agriculture (Lesch *et al.*, 2005). Maps produced from EC_a are time-invariant, implying that an EC_a survey can be conducted at any time of the year (Neuderker *et al.*, 2001). EC_a mapping has been used to map groundwater contaminant plumes associated with elevated chloride, sulphate and nitrate levels (Jaynes, 2008). Most importantly, EC_a maps has been useful in characterizing soil water variations, designing on-farm trials to optimize crop yield, identifying crop productivity and yield variation, as well as in developing soil management zones to control flood (Topp *et al.*, 1980). It has also been used in solute transport modelling and as a guide to soil sampling. In some cases, EC_a maps may also be used to evaluate differences in soil organic matter to assist in making decisions concerning site-specific fertilization and other crop treatments (Audun *et al.*, 2003).

EC_a for delineating site-specific management units

Another EC_a application involves its use in delineating Site-Specific Management Units (SSMUs) (Corwin *et al.*, 2008). SSMU is a new farming concept mostly used in spatial soil studies to account for existing soil property variations (Figure 2.4). The concept of SSMUs aims to identify sampling locations through the EC_a map and analyze each location based on the sampling plan, in order to characterize how soil properties affecting crop yield and quality were spatially distributed within the soil. This gives the farmer an idea of what treatment to apply, at what rate and at which location the management is needed most, based on the spatial pattern

of geo-referenced data collected, instead of assuming treatment over the whole field area (Long, 1998). This allows crop productivity to be tracked on temporal bases. The first step in generating SSMU's is to determine variations through EC_a field survey.

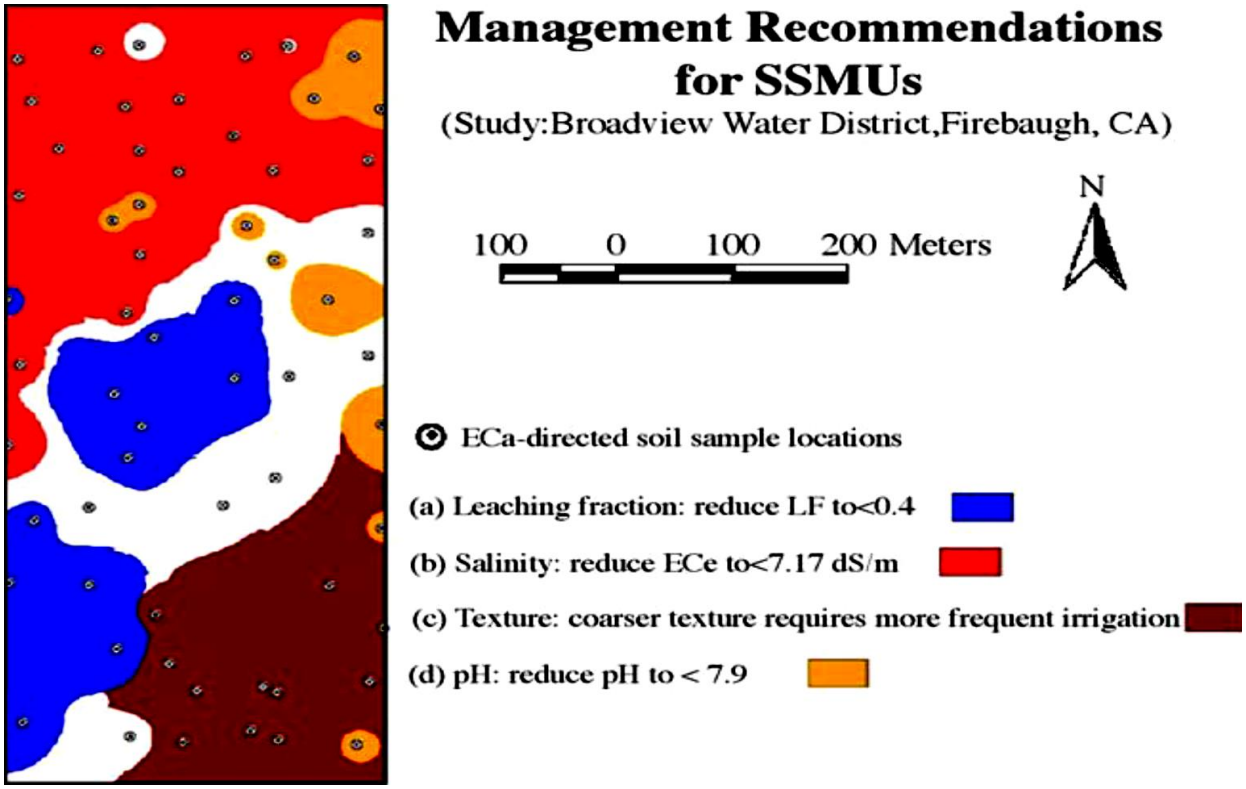

Figure 2.3 Site-specific management units showing the distribution of soil properties and possible recommendations to manage the: (a) leaching fraction, (b) salinity, (c) texture and (d) soil pH (Corwin & Lesch, 2005a).

Protocol for EC_a field survey: There are three important considerations in choosing a statistic when working with EC_a data. These include sample design, sample size and the properties contributing to EC_a within the surveyed field. A survey procedure for EC_a-directed soil sampling was developed by Corwin & Lesch (2005b) and has been followed to characterize spatial soil variability. These procedures are as follows:

- Site description and EC_a survey design
- Geo-reference EC_a data collection
- Soil sampling design based on geo-referenced EC_a data (analyzing EC_a data in ESAP software)
- Soil sample and soil core collection based on design
- Laboratory analysis of relevant soil properties based on project objectives
- Calibration of EC_a to soil water content
- Statistical and spatial analysis of properties influencing EC_a measurements

- GIS database development and graphic display of spatial distribution of soil water.

The hypothesis behind this was that if a relationship exists between EC_a and a soil property, then the range and variability of such property can be identified using an EC_a-directed soil sampling approach. On this assumption, EC_a is also useful in choosing soil sampling locations prior to field-survey (Kitchen *et al.*, 1999).

2.4 Analysis for spatio-temporal EC_a measurement

Due to the complexity of spatial EC_a measurements with respect to not knowing which property is responsible for the EC_a variation (Li & Heap, 2011). Several approaches have been employed to explain EC_a measurement either for spatio-temporal characterization or for map production through interpolation. The EC_a variations in soil water content at multiple depths across scales can be analyzed either by using the statistical methods (Brocca *et al*., 2012), non-geostatistics or deterministic methods and geostatistics or stochastic approaches.

2.4.1 Statistical approach

The concept of temporal or time stability, as proposed by Vachaud *et al.* (1985), is a measure of the rank stability of long-term mean soil water conditions (Martinez-Fernandez & Ceballos, 2003). The hypothesis is that if a soil is repeatedly surveyed for soil water content, there is a probability that the spatial variation in soil water within a field in one time series will remain the same at another time series (Hu *et al.*, 2013). Time stability involves describing the overall similarity of the spatial pattern between measurements and the time-invariance of the relative soil water content of the surveyed area. The most common way to describe time stability is through Spearman's rank correlation (r_S) analysis in Equation 2.5 (Vachaud *et al.*, 1985).

$$r_S = 1 - \frac{6 \sum_{i=1}^{n} (R_{it} - R_{it^2})^2}{n(n^2 - 1)} \qquad 2.5$$

where, n = Number of observations
i = Observation location
t and t' = Different observation periods

This is a non-parametric measure that explains how well to describe the relationship of spatial soil water content between two time series (R_{it} and R_{it^2}) by ranking, which linearize nonlinear relationships making this statistics more sensitive to nonlinear correlations. The coefficient of r_S are between -1 and 1. The closer r_S is to '1', the more stable the spatial pattern of soil water content, and r_S of '1' implies no change in the rank of the observed values. Martini *et al.* (2016)

used this analysis to investigate the temporal stability of the spatial pattern of EC_a and daily average water content over seven days repeated survey and recorded $r_S \geq 0.9$.

Secondly, is the Pearson correlation (r) analysis (Cosh *et al.*, 2004), which is strictly for linear relationships. The Pearson correlation coefficient *($r_{t,\dot{t}}$),* of spatial soil water content collected from two time series *t* and *t'* can be defined by Equation 2.6.

$$r_{t,\dot{t}} = \frac{\sum_i \left(\theta_{vt}(i) - \hat{\theta}_{vt}\right)\left(\theta_{v\dot{t}}(i) - \hat{\theta}_{v\dot{t}}\right)}{\sqrt{\sum_i \left(\theta_{vt}(i) - \hat{\theta}_{vt}\right)^2}\ \sqrt{\sum_i \left(\theta_{v\dot{t}}(i) - \hat{\theta}_{v\dot{t}}\right)^2}} \qquad 2.6$$

where, $\theta_{vt}(i)$ and $\hat{\theta}_{vt}$ = Water content at location 'i' and its spatial means at time 't'

$\theta_{v\dot{t}}(i)$ and $\hat{\theta}_{v\dot{t}}$ = Water content at location 'i'' and its spatial means at another time 't''

This stability analysis has been used to identify points where soil water is considered to be most representative of the spatial mean soil water within a field scale (Teuling *et al.*, 2006; Brocca *et al.*, 2010). The analysis is on the basis of the parametric test of the relative differences and does not provide information on the varying spatio-temporal characteristic of the scale surveyed.

2.4.2 Deterministic or non-geostatistical approach

This is a calibration technique that uses mathematically inversion algorithm based on geophysical theories to convert EC_a into salinity (EC_e) by assuming all model parameters are known; thus, deterministic models are "*static*". One example is the dual pathway parallel conductance (DPPC) model (Equation 2.7), developed by Rhoades *et al*. (1989, 1990) for salinity studies, to convert field measured EC_a to EC_e. This model explained that EC_a can be reduced to a non-linear function of several physico-chemical properties such as: EC_e, saturation percentage (SP), volumetric water content (θv), bulk density (ρ_d) and soil temperature (Equations 2.8 to 2.13), when it was further expanded in Lesch and Corwin (2003).

$$EC_a = \left(\frac{(\theta_{SS} + \theta_{WS})^2 \times EC_{WS} \times EC_{SS}}{(\theta_{SS} \times EC_{WS}) + (\theta_{WS} \times EC_S)}\right) + (\theta_W - \theta_{WS}) \times EC_{WC} \qquad 2.7$$

$$\theta_W = \frac{(PW \times \rho_d)}{100} \qquad 2.8$$

$$\theta_{WS} = 0.639\theta_W + 0.011 \qquad 2.9$$

$$\theta_{SS} = \frac{\rho_d}{2.65} \qquad 2.10$$

$$EC_{SS} = 0.019(\mathrm{SP}) - 0.434 \quad 2.11$$

$$EC_W = \left[\frac{\mathrm{EC_e} \times \rho_d \times SP}{100 \times \theta_b}\right] \quad 2.12$$

$$\mathrm{SP} = 27.25 + 0.76\,(\%\mathrm{Clay}) \quad 2.13$$

The model was found capable in accessing the degree at which each of these soil properties influenced the EC_a measured in a field (Corwin & Lesch, 2003; Lesch *et al*., 2000). In view of that, by measuring soil EC_e, SP, PW, and ρ_d from the laboratory results and using Equation 2.7 through 2.13, the EC_a values can be estimated. The use of this approach in near surface EC_a data is limited. This is because the approach assumes that, there are multiple conductivity readings from each survey point, and there are differences within the near-surface soil horizon. Therefore, it requires knowledge of additional soil properties. Other reference on EC_a to EC_e conversion is that of McKenzie *et al*. (1989).

Deterministic method for ECa-directed soil sampling

Deterministic approach can also be applied in the field measured EC_a, to delegate soil sampling locations. This involves the use of design-based (probability-based) sampling methods like the simple random, stratified random, multistage, cluster and network sampling schemes (Corwin *et al*., 2008; McRoberts, 2010). This approach has a well-developed underlying theory and is designed with an in-built randomization principle (Cox & Hinkley, 1974) for drawing statistical inference. But, the approach avoids incorporating parametric modelling assumptions and more often, data quality is to an extent difficult to analyze.

2.4.3 Stochastic or geostatistical approach

This is a statistical modelling technique that uses soil sample data collected during field survey to directly predict EC_e from EC_a values; thus, stochastic models are “dynamic”. This approach relates soil properties, with EC_a values to develop a prediction model that can be used to infer variability at the non-sampled measurement points. The method makes use of spatial scales with co-ordinates, time series, EC_a survey data, prediction models and other possible information that will aid in linking both spatial and temporal distributed data. Common examples are the geostatistical (generalized universal Kriging and co-kriging models) and spatially referenced regression models.

Geostatistical methods analyzed soil spatial and temporal variability using generalized universal kriging model commonly referred to as “spatial linear” or “spatial random” models (Christensen *et al*., 1992). Corwin and Lesch (2005b) stated that, this is the most accurate

statistical calibration method, so long as there's enough sampling points (n ≥ 50). This model is used in regional scales but rarely used for field scale studies (Corwin & Lesch, 2005b). This is due to the large number of samples required for calibration therefore, making this approach economically impractical. Spatial referenced regression model is the same as a regression equation that includes the soil property that was calibrated with EC_a. This model is popularly applied and more practical because it requires a small number of soil samples (n < 15).

Stochastic method for ECa-directed soil sampling

Model-based (prediction-based) soil sampling approach uses non-random identification strategy that depends on the principles of conditionality to select a set of calibration sites with desirable spatial and statistical properties (Cox & Hinkley, 1974). The model uses a response surface sampling technique, RSSD, (ESAP, Software program) together with space filling algorithm (Muller, 2001), to generate sampling points where the soil seems to differ from each other. This software was developed by Lesch *et al.* (2000) specifically for EC_a measurements hence; it will be adopted for the proceeding studies. The two main advantages with this software include a reduction in the number of samples needed to estimate a calibration function and the fact that the approach was specifically for estimating a regression model with EC_a field survey. It also selects sampling locations based on observations derived from a random variable, whose values are considered a realization from a distribution of possible values. With this approach, the average separation between two sampling locations is maximized thereby, minimizing the prediction error effect (Corwin & Lesch, 2010) produced by the calibration function. In doing so the approach simultaneously ensures that the independent regression model residual error assumption remains approximately valid, which makes it possible to use the regression model to predict soil water content at all the non-sampled locations (Corwin & Lesch, 2005b).

2.5 Conclusion

When working with the EM38-MK2, it is of vital important that the basic concepts of the instrument and calibration procedures are understood, in order to avoid unreliable results and false information from the experiment. The preceding review included a detailed description of the EM38-MK2. The calibration and applications of EM38-MK2 in field surveys and definitions of some basic terms in EC_a measurement were described.

The strength of the induced current when an EM38-MK2 is placed on the soil is determined by the EC_a of the soil which is a function of several soil properties, including soil water content. Studies have shown that these soil properties influence EC_a in a very complex and

interchangeable manner. Increase in soil water content was reported to cause conductivity rise and to a more significant variation in EC_a measurements under a high water table above wilting point. However, it was suggested avoiding EC_a field surveys during rainfall, and when the soil is excessively moist or dry. It was also recorded that temperature changes significantly influence EC_a readings obtained with EM38 sensors. It was suggested that practitioners should use the corrected Sheets and Hendrickx or ratio models to correct EC_a readings to a reference temperature of 25°C.

EC_a can be seen as a surrogate measure of various soil properties that requires proper *in situ* calibration in order to either characterize these properties or determine one dominant factor when the values of other contributing factors are available or constant. An EC_a soil survey allows the establishment of workable management zones and also allows surveyors to anticipate the magnitude and range of soil EC_a readings expected for a given soil series.

Based on the results and conclusions of past researches, the EM38 devices still remain an appropriate instrument for monitoring of spatial and temporal variation of soil water distribution with a depth concentration that corresponds to the crop root zone. Hence, there is a need to examine most agricultural field tools used in conjunction with the EM38-MK2 for instrument interference. After an extensive literature search, no information was found on the interaction of EM38 devices with the DFM capacitance probes for soil water determination. Also, more studies are needed on the calibration of EM38 sensors under rangeland conditions and over diverse soil types.

CHAPTER 3. FIELD DESCRIPTION AND SOIL CHARACTERIZATION OF EXPERIMENTAL SITES

3.1 Introduction

The type and condition of the soil is very important in field surveying with EMI instruments (Corwin & Lesch, 2013). The distance that the medium wave transmitted from the EM38-MK2 can travel, does not only depend on its power, frequency and the ground conductivity, but also on the ground condition. This implies that soil apparent electrical conductivity (EC_a) measured with the EM38-MK2 is influenced, either directly or indirectly, by factors such as solutes, particle size, cation exchange capacity, water content, temperature, bulk density and porosity of the soil (Auerswald *et al*., 2001; Johnson *et al*., 2003; Friedman, 2005). Several studies confirmed that most of these soil properties correlate well with EC_a measurements (Lesch & Corwin, 2003; Sudduth *et al*., 2005), because these factors have the ability to influence the transmission of an electrical charge within a soil. In general, soil water is the main factor that accentuates other properties associated with EC_a measured values. The interpretation of EC_a depends on the most dominant of these factors.

Soil EC_a has been employed to spatially determine and map various soil properties (Williams & Baker, 1982; Lesch *et al*., 1992, 1995a, b; Neuderker *et al*., 2001; Domsch & Giebel, 2004); including soil water variability (Kachanoski *et al*., 1988; Perry & Nieman, 2008). It has also been used as an indicator of soil textural class (Williams & Hoey, 1987; Waine *et al*., 2000; Robinson *et al*., 2008) with strong correlation. This is due to the capacity of each textural class to hold a certain amount of water. Brevik *et al*. (2006) confirmed that EC_a has its greatest potential to differentiate between soil types when soils are wet. This is more visible in high-clay soils. Most clay has charged surfaces and the water they retain has a relatively high concentration of dissolved solids compared to sandy soil. Hence, clay soils tend to show high EC_a readings (Sudduth *et al*., 2005; Triantafilis & Lesch, 2005).

Field measured EC_a values vary from one measurement point to another, especially on a heterogeneous soil. At the time of a field survey with the EM38-MK2, the property or properties responsible for EC_a variations is not known. Hence, knowledge of the spatial distribution of these properties within a field can provide useful information on what actually contributes to EC_a variations for the benefit of decision making in agriculture. To use EM38-MK2 for soil water studies, soil classification is very important, especially information on soil texture. If no relationship exists between measured EC_a and soil water content, however, a correlation may still be made with any other soil property to determine the cause of EC_a variation.

In this chapter, complete descriptions of the field experimental sites, where EM38 studies were conducted, are presented. Information is given in terms of location, climate, topography and soils. This chapter aimed to distinguish the various soil forms on the selected experimental areas, to characterize the morphological, physical and chemical (EC of the paste extract and cations) properties of each individual soil form. An important outcome of this will be to verify the homogeneity or heterogeneity of the experimental sites. Most of the analyses were done specifically for the present studies, however, some information was sourced from previous studies. Finally, the general outcome of the soil classification and analysis will be used to calculate the range of EC_a values to be expected for the soils in this study.

3.2 Site description

3.2.1 Location

Two sites were selected near Bloemfontein in the Free State Province (Figure 3.1a), South Africa. Soils on one of the sites are relatively homogenous, while soils on the other site are more heterogeneous. Site 1 is located at Kenilworth Experimental Farm (Figure 3.1b); latitude 29º01'47.6"S, longitude 26º08'58.3"E and altitude 1366 m. Site 2 is located at Paradys Experimental Farm (Figure 3.1c); latitude 29º13.375'S, longitude 026º12.527'E and altitude 1422 m. Both experimental farms belong to the University of the Free State (UFS). Kenilworth is located 15 km northwest of the UFS, close to Tempe Airport. Paradys is located 14 km southeast of the UFS, between the N1 road to Colesberg and N6 to Reddersburg.

3.2.2 Climate

The two experimental sites (Figure 3.1) are less than 40 km apart, with the UFS at the center, therefore the climate may be regarded as similar for the area (Walker & Tsubo, 2003). The climate of Bloemfontein is classified by the Köppen-Geiger Classification System as BSk and is influenced by its local steppes. This implies that it is a semi-arid zone (BS) found in the mid-latitudes and is affected by high elevation (k), which limits the amount of moisture supplied from the ocean. Bloemfontein is known for its dry-grassland climate with an aridity index of 0.23 (mean annual evaporation demand of 2198 mm and mean annual rainfall of 543 mm). Summers are hot (October to April), while winter periods are cold and dry (May to August). Rainfall in this area is very low during the winter period from May to August (Figure 3.2). During these months, the temperature often falls below freezing point overnight, especially in July. Summer days may come with rain, starting from October, increasing to a peak in January where after, it decreases as winter approaches.

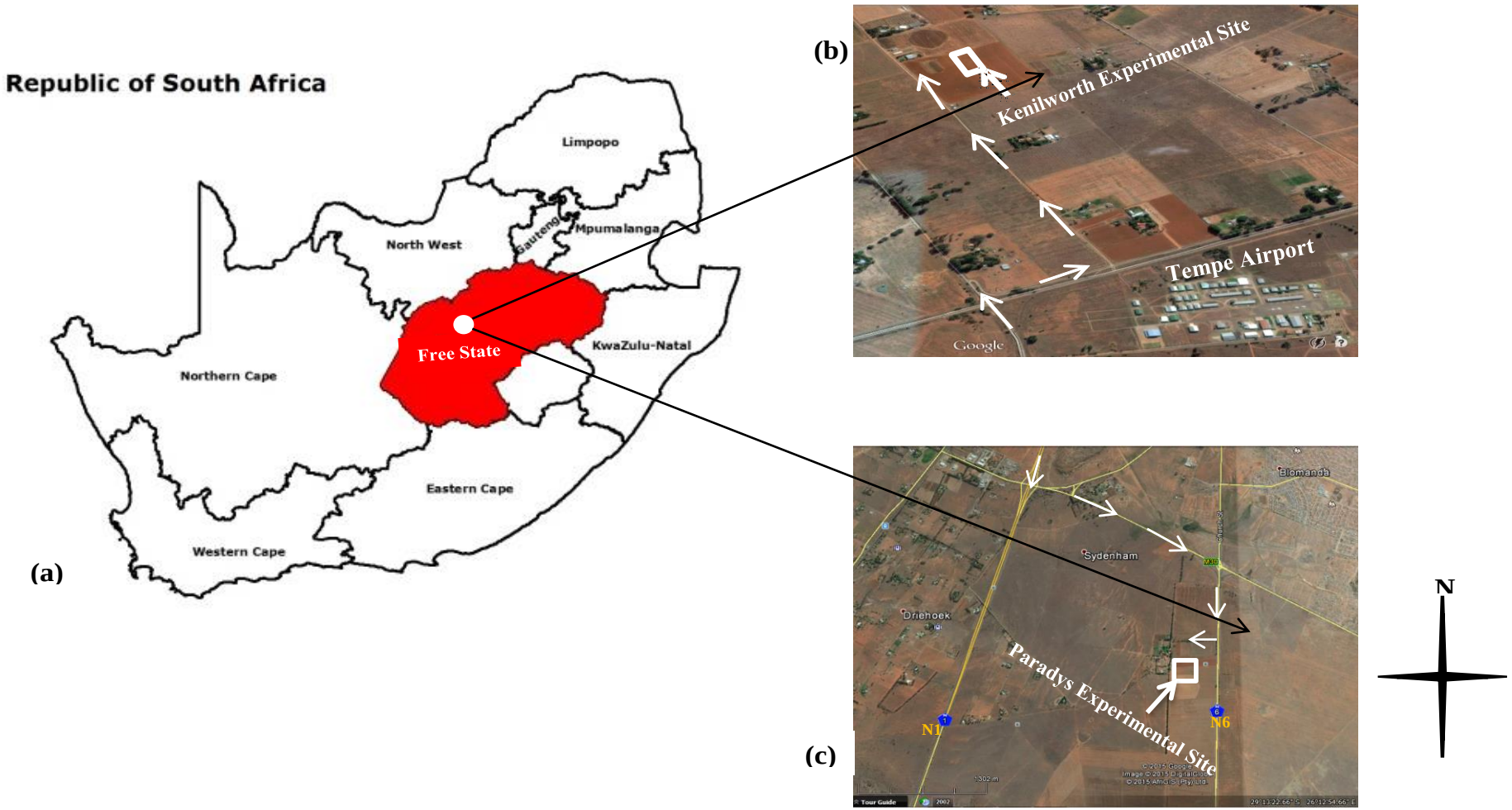

Figure 3.1 Location of the experimental sites (a) near Bloemfontein in the Free State Province. (b) Site 1 is located at Kenilworth Experimental Farm and (c) site 2 at Paradys Experimental Farm (Source: Google imagery, 2012).

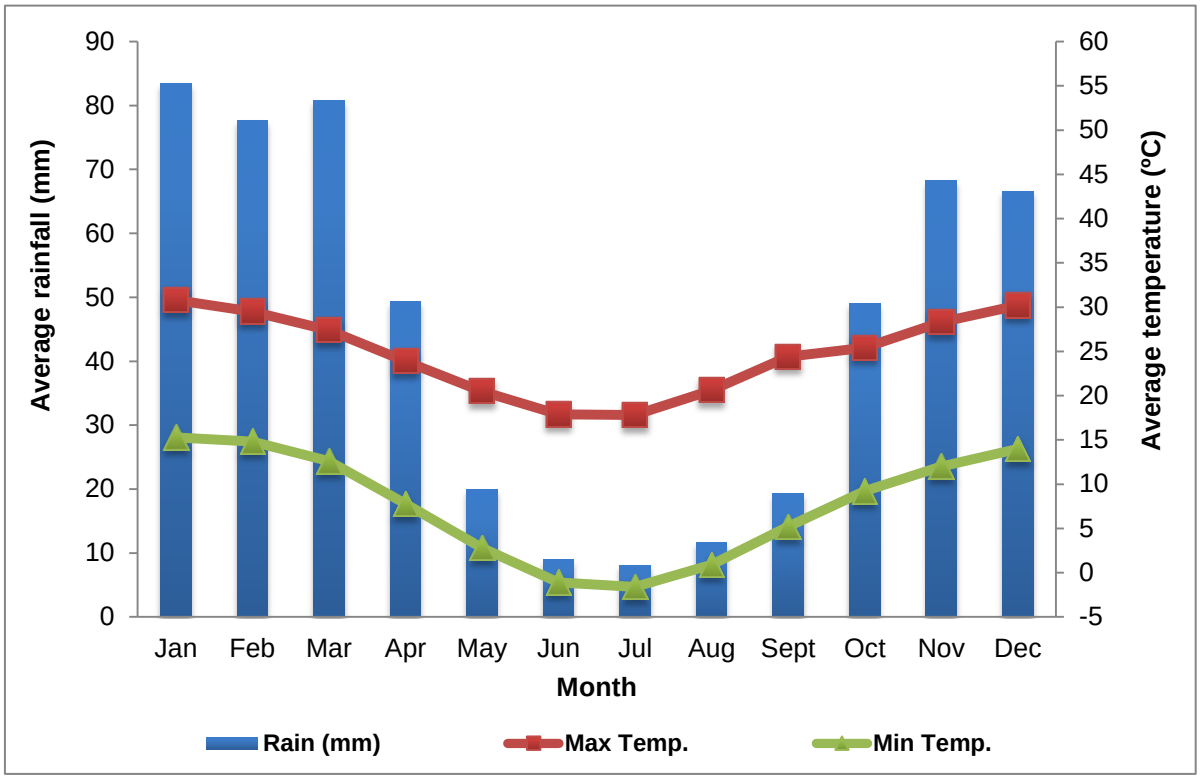

Figure 3.2 long-term average monthly rainfalls, with average maximum and minimum monthly temperatures for Bloemfontein (data sourced from Fraenkel, 2008).

3.2.3 Topography

Site 1 is positioned at terrain unit 5 with a gentle slope of less than 1% facing northwest. Due to the flat surface area of this landform, runoff from rainfall is not encouraged. Site 2 is positioned at the mid-slope terrain unit 3, with a linear convex slope of 0.3% facing in an eastern direction (Figure 3.3). The slope encourages runoff during rain periods and this result in the huge variation in soil properties in this landscape.

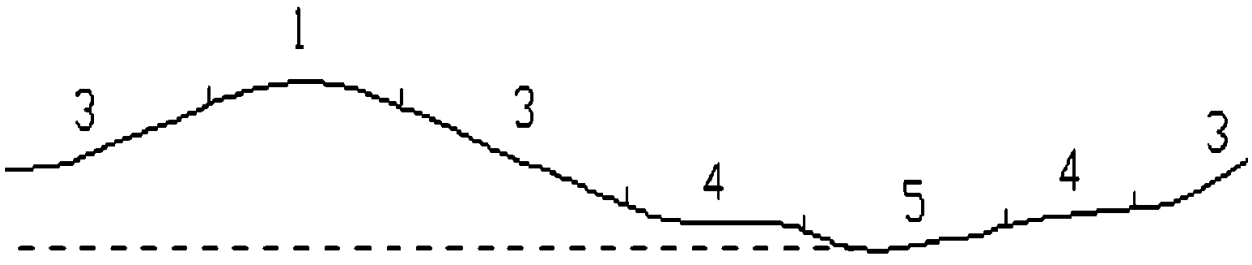

Figure 3.3 The landscape, showing the terrain units of the experimental sites (Fraenkel, 2008).

3.3 Methodology for soil analyses

3.3.1 Soil sampling and storage

Site 1: The soils of Kenilworth Experimental Farm have been repeatedly characterized (Chimungu, 2009; Tesfuhuney, 2012). It was reported to be relatively homogenous with depth. Hence, only disturbed samples were collected over an area of 645 m^2 (43 m x 15 m). Samples were taken at 0.3 m intervals to 1.5 m depth from 11 points on each of four plots in correspondence to the field design for the first field trial (discussed in Chapter 4). A total of 220 samples were analyzed to classify the physical and chemical properties within the selected experimental area. Samples were collected with a hand auger, then sealed in plastic bags and carefully transported to the Soil Science Analytical Laboratory at the University of the Free State.

Site 2: Classification of soils on Paradys Experimental Farm has also been conducted previously (Fraenkel, 2008; Mavimbela & Van Rensburg, 2013) and it was reported that the soil is generally heterogeneous. For the present study, morphological characteristics were described *in situ* at fresh profile pits within a 1.96 ha area of Paradys Experimental Farm. Profile pits were dug 1 m deep on 12 plots selected following the field design for the second and third field trials (discussed in Chapter 5). Disturbed samples were collected from the A-, B- and C-horizons on each of these 12 plots. Also, undisturbed soil samples were collected by core method (Non-Affiliated Soil Analysis Work Committee, 1990).

Three different undisturbed core samples were collected horizontally at each horizon, using a PVC ring of a known weight (97.63 g), diameter (10.5 cm) and height (7.8 cm). The PVC rings were fixed into a metallic core sampler and driven horizontally into the soil using a manual hydraulic jack (Model: SS-Jacko-Hyd-08-12) (Figure 3.4). The two ends of the core samples were trimmed, sealed and tightly taped to prevent water loss. Samples were properly packed and carefully transported to the laboratory to prevent cracking.

Both disturbed and undisturbed soil samples from the field were weighed immediately and oven dried at 105ºC. Completely dried samples were ensured by repeated drying until a constant weight was obtained as described by Topp & Ferre (2002). Oven-dried disturbed samples from Site 1 were analyzed for gravimetric water content (GWC), particle size distribution, resistivity of the saturated soil, electrical conductivity of saturated paste extracts (EC_e) and water soluble cations (Ca^{2+}, Mg^{2+}, K^+ and Na^+). Samples from Site 2 were also analyzed for GWC, particle size, EC_e and water soluble cations. Undisturbed samples were used to determine soil bulk density.

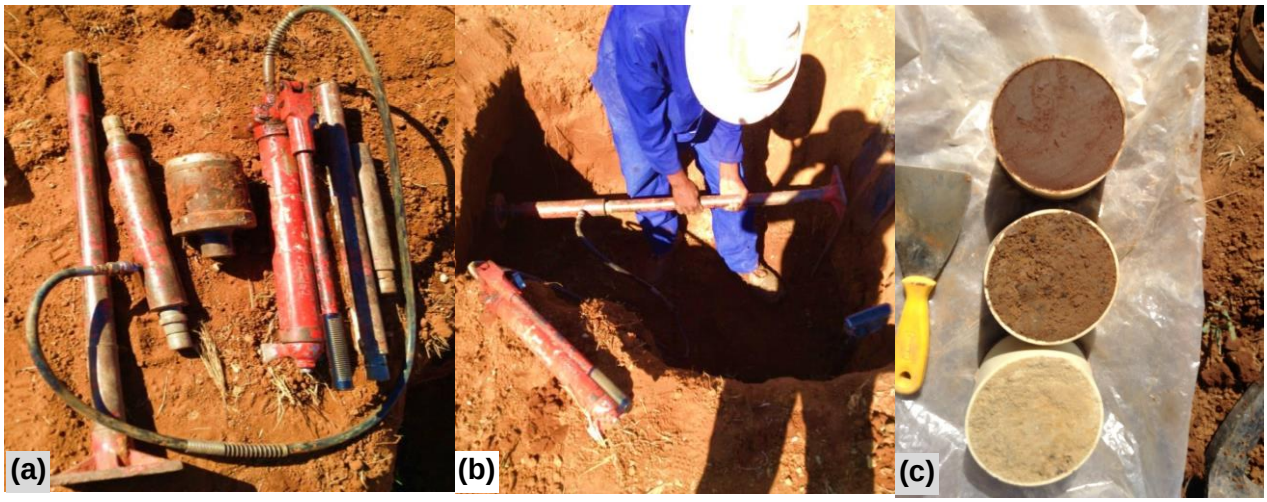

Figure 3.4 Field pictures showing the (a) Mechanical hydraulic-jack, (b) core sampling horizontally in the soil profile pit, and (c) the resulting soil core.

3.3.2 Measurements and laboratory analysis

Gravimetric water content

The weight of the plastic bag was subtracted from the disturbed samples and gravimetric soil water content (θg) was then expressed by weight as the ratio of the mass of water to the dry weight of the soil sample (Equation 3.1). The measurement was reported in percentage.

$$\theta g = \frac{M_W - M_d}{M_d} \times 100 \qquad 3.1$$

where, θg = Gravimetric water content,

M_w = Mass of wet samples and

M_d = Mass of oven-dried samples

The oven dried disturbed samples were then ground and passed through a 2 mm mesh sieve before used for further analysis.

Soil bulk density

Soil bulk density (ρ_d) was determined on dry weight basis. The weight of the PVC ring was first subtracted from the core samples. Bulk density of each core was calculated as the ratio of the mass of the dried core sample to its total volume. Hence, ρ_d was expressed in Mg m^{-3} to the nearest 0.01 Mg m^{-3} using Equation 3.2.

$$\rho_d = \frac{M_S}{V_S} \qquad 3.2$$

where, M_S = Mass of wet soil

V_s = Volume of core soil (Volume of pipe V_P)

$V_P = \pi \times \left(\frac{d}{2}\right)^2 \times h$

d = Diameter

h = Height

Volumetric water content

Volumetric soil water content (θ_V, $m^3\ m^{-3}$) of each sample was then calculated from the measured θg and ρ_d using Equation 3.3 and is expressed as the volume of water in a volume of undisturbed soil. This is regarded as the standard measure of soil water content.

$$\theta_V = \frac{\theta g \times \rho_d}{\rho_W} \qquad 3.3$$

where, θg = Gravimetric water content

ρ_d = Bulk density

ρ_W = Density of water with value of 1.0 Mg m^{-3}

Particle size analysis

Particle size distribution (sand, silt and clay) of a 30 g oven-dried sample was determined for each of the samples collected, using the pipette method as described by the Non-Affiliated Soil Analysis Work Committee (1990). The weighed samples were dispersed by adding 50 ml Calgon and stirred to separate particles (Figure 3.5b). After 5 minutes, the clay-plus-silt fraction was transferred, via a 53 µm aperture sieve, into a 1000 cm^3 cylinder and covered. Soil fractions with a size greater than 0.05 mm were transferred to a glass beaker and then oven-dried. To quantify the sand fractions, dried samples were shaken for 5 minutes through a set of sieves using a mechanical shaker (Figure 3.5c) according to the USDA standard.

The clay-plus-silt suspension in the cylinder was then stirred using a long metal stirring rod. The suspension was pipetted three times using an automatic pipette controller (Figure 3.5a). The first pipetted sample included all particle sizes present in the cylinder and was drawn at 0.1 m (10 cm) immediately after stirring the suspension. The second extraction was made at 0.1 m depth after 4 minutes for fine silts and clay, while the third extraction was made at 0.07 m (7 cm) after 5 hours for clay. The pipetted suspensions were oven-dried and weighed for percentage coarse silts, fine silts and clay. To represent the amount of each textural class in a sample, the percentage values of each of the classes were calculated. All size fractions were expressed as a percentage of the total mass of the sample.

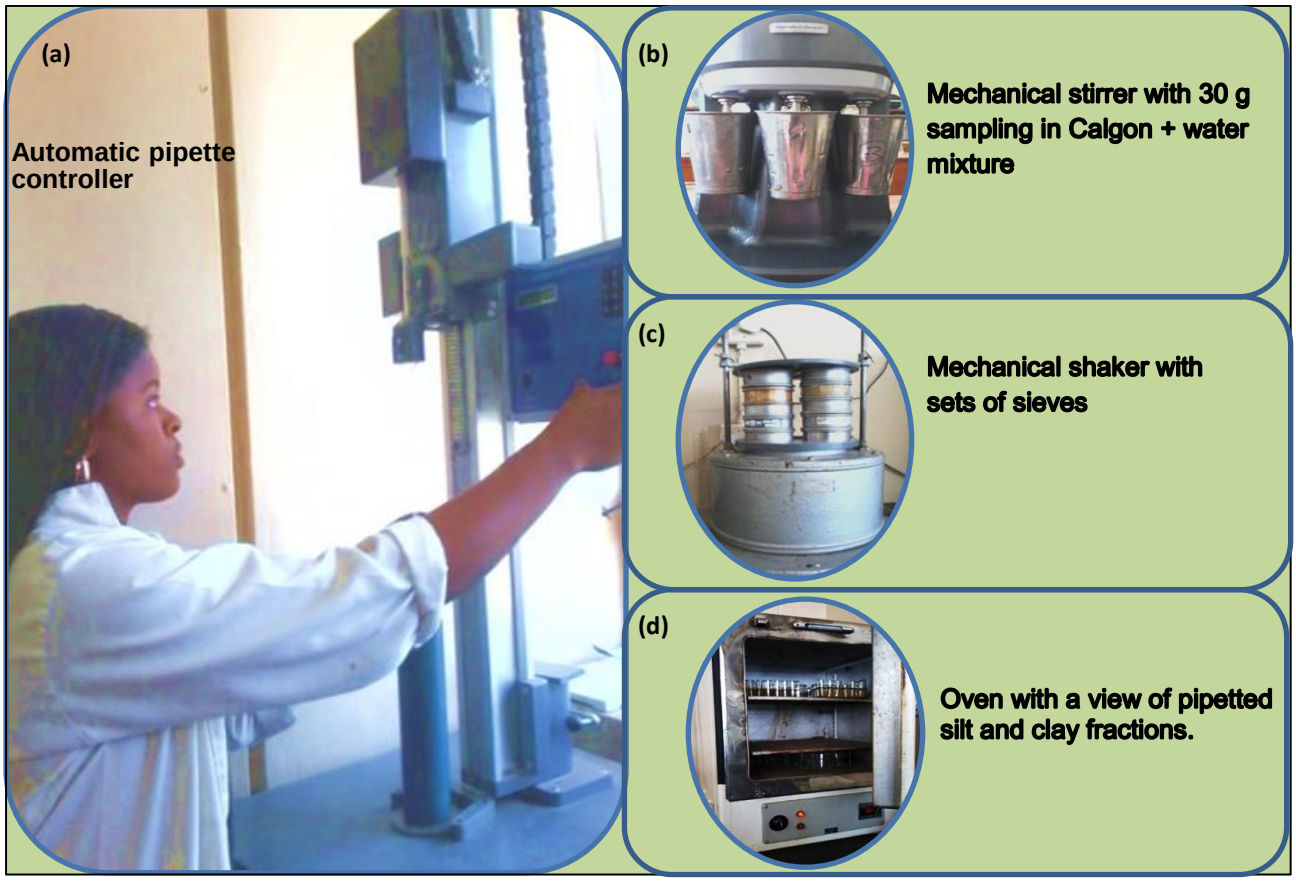

Figure 3.5 Illustrating (a) an automatic pipette controller, (b) stirrer, (c) shaker with sieves, and (d) a drying oven for the determination of soil textural classes.

Electrical conductivity of saturated paste extracts (EC_e)

Soil saturated paste is a mixture of soil and water in such a ratio that all the voids between soil particles are filled up with water without any excess water accumulating on the surface. Paste extract is the solution extracted under suction from a saturated paste. The EC of a solution is the summation of all contributing ions per unit volume of the solution and the velocity at which these ions move under the influence of an electrical current. Although the saturated paste extract method is labour intensive and requires soil sampling and laboratory analysis, it is commonly accepted as the most accurate measure of soil salinity (McNeill, 1992). The characteristics of a good saturated paste include a shiny surface, a lightly flowing of the paste when the container is tilted that does not cling to a spatula, except for clayey soils. Figure 3.6 shows the Laboratory activities during EC_e extractions.

A total of 250 g of each dry sample was mixed with de-ionized water to saturated paste with minimum stirring (Figure 3.6a). The soil paste was well covered overnight for the salts to properly dissolve. A set of Büchner funnels with highly retentive filter paper were mounted airtight onto Büchner flasks and connected to a suction pressure pipe (Figure 3.6b).

Figure 3.6 Laboratory preparations for EC_e measurement: (a) Saturating the soil samples, (b) setting up the Büchner funnels and flasks to the suction pipes, and (c) the Metrohm Module-856 conductivity meter for EC_e determination.

The pastes were transferred to the funnels to obtain the extract by vacuum into glass tubes. Extracts were re-filtered to remove extra soil debris. EC_e of the extracts was determined using the Metrohm Module-856 conductivity meter (Figure 3.6c). The conductivity meter was first calibrated to a temperature of 25°C using standard KCl solutions of 0.843 mS m^{-1} and 1.43 mS m^{-1} (Rhoades, 1982). Results were also expressed in milliSiemens per meter (mS m^{-1}). Note that the electrical conductivity of this extract is the laboratory equivalent of the EC_a measured in the field with EM38 instruments (U.S. Salinity Laboratory Staff, 1954).

Calculation of soil apparent electrical conductivity (EC_a)

Field measured EC_a is the product of static and dynamic factors such as soil salinity, clay content, bulk density and water content and these factors are considered during the interpretation of field measured EC_a. In the present study, EC_a was calculated from the laboratory measured soil properties (EC_e, %clay, ρ_d and θ_V) using the dual pathway parallel conductance (DPPC) model (Equations 2.7 to 2.13) developed by Rhoades *et al*. (1989b) as discussed in Chapter 2.

Electrical resistance of soil paste

Resistivity refers to the capability of a soil to prevent the flow of electrical current through it. Electrical resistance of a saturated paste is as a result of salt concentration in the soil. This is the inverse of the conductivity of a soil and is measured in ohms. Resistivity changes with a change in the volume of soil materials and is defined as the voltage, V, measured across a unit cube's length divided by the current, I, flowing through the unit cube's cross-sectional area (R=V/I).

A saturated soil paste was prepared from each soil sample. The paste was transferred into an electrode cup and placed on a bridge resistance board. Resistivity of the saturated soil paste was then determined with a Metrohm AG conductivity meter E382 (Figure 3.7), following the standard procedure according to the U.S. Salinity Laboratory Staff (1954).

Figure 3.7 Using soil saturated pastes to determine soil resistivity.

Water soluble cations of paste extract

This is the charged particles of the saturated soil paste extracts that are also capable of conducting electricity, and is expressed in milli-equivalent of cations per liter (me ℓ^{-1}) or centi-mol of cations per kilogram (cmol kg^{-1}). Cations were determined from the paste extracts, diluted 10 times with water deionized by reverse osmosis (EC ≤ 0.01 dS m^{-1}). The exchangeable cations, Ca^{2+}, Mg^{2+}, K^{+} and Na^{+}, were determined from the dilution using an Atomic Absorption Meter.

3.4 Results

3.4.1 Pedological characteristics: Kenilworth (Site 1)

At Kenilworth, the focus was on description of the physical and chemical soil properties corresponding to the current study. Soils were not classified in detail, since this has been done recently by other researchers. Soils were classified as the Bainsvlei soil form, belonging to the *Amalia* family. This soil type is regarded as a high potential soil for dry-land agriculture because of the depth for root growth and the presence of a soft plinthic layer at about 1500 mm depth.

Profile attributes of the Bainsvlei form

Table 3.1 shows the profile characteristics of the Bainsvlei soil form (*Amalia* 3200), while Table 3.2 presents the physical and chemical soil properties. The soil comprises of an orthic A-horizon, taken as Ap as it is ploughed over a depth of 250 mm and is of single grain structure, classified as a fine loamy sand with 7% clay content. The nature of this Ap and the underlying B-horizon shows that the soil has larger pore spaces that allow fast infiltration of water, encouraging rainfall infiltration.

Table 3.1 Morphological characteristics of the Bainsvlei form of the *Amalia* family (after Chimungu, 2009)

	Horizon					
Characteristic	Ap	B1	B2	B3	B4	B5
Depth (mm)	0-250	250-420	420-700	700-1200	1200-1450	1450-1850
Diagnostic horizon	Orthic A	Red apedal B	Red apedal B	Red apedal B	Yellow brown aeolian sand	Soft plinthic B
Colour (dry)	Reddish brown (5YR4/4)	Red (2.5YR4/6)	Red (2.5YR4/6)	Reddish brown (5YR4/4)	Strong brown (7.5YR5/6)	Strong brown (7.5YR4/6)
Structure	Massive apedal	Massive apedal	Massive apedal	Massive apedal	Massive apedal	Weak sub-angular blocky structure
Transition	Gradual smooth	Gradual smooth	Gradual wavy	Clear wavy	Clear wavy	Gradual smooth
Consistency	Friable	Friable	Friable	Slightly firm	Friable	Friable
Textural classes	Fine loamy sand	Fine sandy loam	Fine sandy loam	Fine sandy clay loam	Fine sand	Fine sandy clay loam

The B-horizon is divided into five distinct layers, and for the most part the horizon is massive apedal that is weakly structured. The B1- to B2-horizons are red apedal, with a fine sandy loam texture and a clay content of 16% and 17%, respectively. The B3-horizon is also red apedal with slightly higher clay content (21%) than the overlying horizons. It has a textural class of fine sandy clay loam. The B4-horizon is regarded as yellow brown aeolian sand with a fine sandy texture with 14% clay content, while B5 is a soft plinthic layer classified as a fine sandy clay loam soil with 22% clay content. The presence of the soft plinthic layer within 1500 mm soil depth causes water to accumulate in this layer during high rainfall periods. The depth of this soft plinthic layer and the ability to store water encourages effective root development and plant growth.

The topsoil of Bainsvlei is granular when dry and friable when it is wet. As the sand fraction decreases, clay and gravimetric water content slightly increases with depth. From Table 3.2, bulk density was almost the same for the depths with values ranging from 1.66 Mg m^{-3} to

1.68 Mg m^{-3}. Apart from the Ap-horizon with 7%, clay content was between 16% and 22% within the depths. EC_e decreased from 26 mS m^{-1} to 18 mS m^{-1} with depth, while the calculated EC_a increased with depth from 17 mS m^{-1} to 31 mS m^{-1}.

Table 3.2 Summary of physical and chemical properties of the Bainsvlei form

		Horizon					
	Soil property	Ap	B1	B2	B3	B4	B5
Physical properties	Coarse sand (2 – 0.5 mm) (%)	0.4	0.4	0.5	0.4	0.5	0.6
	Medium sand (0.5 – 0.25 mm) (%)	5.6	5.5	5.4	5.2	5.3	6.0
	Fine sand (0.25 – 0.106 mm) (%)	60.7	55.3	55	52.2	54.2	48.3
	Very fine sand (0.106 – 0.53) (%)	18.3	16.4	15.3	15.4	15.8	17
	Coarse silt (%)	4.2	3.5	3.5	3.5	3.6	4.0
	Fine silt (%)	1.9	2.3	2.3	2.3	2.2	2.0
	Clay (%)	6.9	16	17.3	21.1	14.3	22.1
	Gravimetric water content (%)	3.8	8.4	7.5	8.8	8.4	9.8
	Bulk density (Mg m^{-3})	1.66	1.68	1.66	1.67	1.68	1.67
Chemical properties	Resistivity (ohms)	3806	2376	2751	2892	2393	2802
	EC_e (mS m^{-1})	25.9	21.6	19.2	18.4	19.1	18.1
	Calculated EC_a (mS m^{-1})	16.8	30.4	29.5	27.4	30.4	31.1
	Ca (me ℓ^{-1})	1.3	1.1	1.0	1.0	1.0	1.0
	Mg (me ℓ^{-1})	0.5	0.5	0.4	0.4	0.5	0.5
	K (me ℓ^{-1})	0.3	0.2	0.1	0.1	0.1	0.1
	Na (me ℓ^{-1})	0.3	0.3	0.4	0.3	0.3	0.4
	Total cations (me ℓ^{-1})	2.4	2.1	1.9	1.9	1.9	2.0

3.4.2 Pedological characteristics: Paradys (Site 2)

Fraenkel (2008) reported the dominant soil forms on Paradys Experimental Farm to be Tukulu, Sepane and Bloemdal, while Mavimbela & Van Rensburg (2013) also identified Swartland on this farm. The soils are regarded as marginal for dry-land agriculture. This is because of its shallow depth, the presence of cutans that hamper root development and drainage, the mechanical strength of the B-horizon and an underlying prismatic, smectite rich, hydromorphic layer that restricts vertical water flow (Fraenkel, 2008). Fresh profile pits were used to identify the above soil forms within the selected experimental area. All the mentioned soil forms, Sepane, Swartland, Tukulu and Bloemdal, were identified within the mapped out area. Of the 12 profile pits that were described on Paradys Experimental Farm, three were Sepane, two were Swartland, five were Tukulu and two were Bloemdal. The profiles were classified according to the Soil Classification Taxonomic System for South Africa (Soil Classification Working Group, 1991).

Profile attributes of the Sepane form

The Sepane soil on Paradys belongs to the *Katdoorn* (1210) family (Figure 3.8). Table 3.3 presents the morphological characteristics of this soil, while Table 3.4 shows the physical and chemical properties of each horizon. The soil profile has an orthic Ap-horizon with a massive apedal structure over a depth of 200 mm. This horizon has a fine sandy loam texture with 14% clay. Transition to the B-horizon is abrupt at all times. The B-horizon is pedocutanic with strong and well-developed angular blocky peds covering a maximum depth of 350 mm. The horizon has a clay texture with a clay content of 51% and smoothly transitions to the C-horizon. The C-horizon is unconsolidated material that shows signs of wetness within a depth of 400 mm. This horizon has a well-developed medium prismatic structure with an abundance of red, yellow, grey and black mottles. The horizon is texturally classified as sandy clay loam with 31% clay.

Table 3.3 Morphological characteristics of the Sepane form of the *Katdoorn* Family

	Horizons		
Characteristics	Ap	B	C
Maximum depth (mm)	200	350	400
Diagnostic horizons	Orthic A	Pedocutanic B	Unconsolidated material with signs of wetness
Colour (dry)	Yellowish red (5YR4/6)	Strong brown (7.5YR4/6)	Light yellowish brown (2.5Y6/4)
Structure	Massive apedal	Strong and well developed blocky peds	Well-developed medium prismatic peds
Consistency	Loose	Very hard	Slightly hard
Transition	Abrupt	Smooth	--------
Textural class	Fine sandy loam	Clay	Fine sandy clay loam

From Table 3.4, bulk density slightly decreased from 1.68 Mg m^{-3} to 1.60 Mg m^{-3}. The Ap- and B-horizon recorded EC_e greater than 100 mS m^{-1} however, EC_e decreased with depth. The calculated EC_a increased to 122 mS m^{-1} at the B-horizon and decreased to 72 mS m^{-1} at the C-horizon. This is an indication of the presence of the cutans at the B-horizon.

Table 3.4 Summary of physical and chemical properties of the Sepane soil form

	Soil property	Horizons		
		Ap	B	C
Physical properties	Coarse sand (2 – 0.5 mm) (%)	4.2	2.8	8.8
	Medium sand (0.5 – 0.25) (%)	5.9	3.6	5.5
	Fine sand (0.25 – 0.106 mm) (%)	38.6	18.3	24.0
	Very fine sand (0.106 – 0.53 mm) (%)	24.3	12.5	14.8
	Coarse silt (%)	8.5	5.4	8.9
	Fine silt (%)	3.7	6.1	7.0
	Clay (%)	14.4	51.2	31.0
	Gravimetric water content (%)	12.0	16.0	13.0
	Bulk density (Mg m^{-3})	1.68	1.60	1.64
Chemical properties	EC_e (mS m^{-1})	145.5	104.1	57.2
	Calculated EC_a (mS m^{-1})	54.9	121.8	72.1
	Ca (me ℓ^{-1})	5.7	3.0	2.0
	Mg (me ℓ^{-1})	4.1	2.4	2.2
	K (me ℓ^{-1})	2.4	0.4	0.3
	Na (me ℓ^{-1})	3.1	2.4	1.4
	Total cations (me ℓ^{-1})	15.3	8.2	5.9

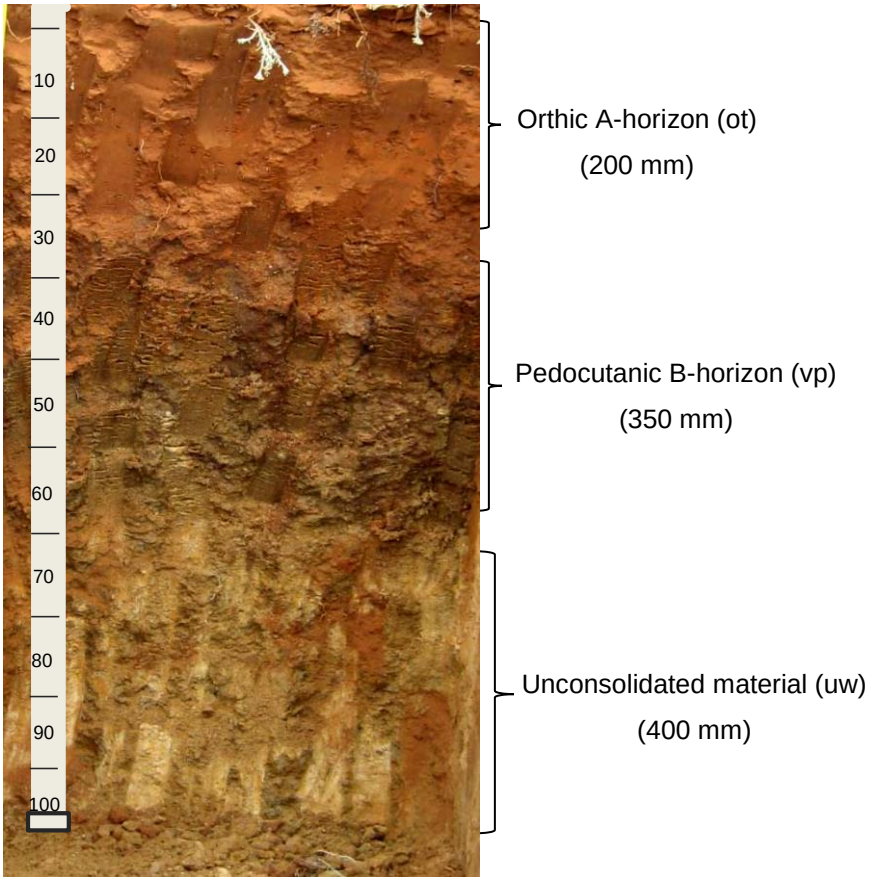

Figure 3.8 Profile view of Sepane on Paradys Experimental Farm.

Profile attributes of the Swartland form

The Swartland soil on Paradys belongs to the *Amandel* (1122) family (Figure 3.9). Table 3.5 provides the morphological characteristics of the Swartland soil form, while Table 3.6 presents the physical and chemical properties of each horizon.

Table 3.5 Morphological characteristics of the Swartland form of the *Amandel* family

	Horizons		
Characteristic	Ap	B	C
Maximum depth (mm)	200	300	250
Diagnostic horizons	Orthic A	Pedocutanic B	Saprolite
Colour (dry)	Yellowish red (5YR4/6)	Strong brown (7.5YR5/6)	Pale brown (2.5Y7/4)
Structure	Massive apedal	Course and sub-angular blocky peds	Weakly weathered peds and saprolite rocks
Consistency	Loose	Hard	Slightly hard
Transition	Smooth	---	---
Textural class	Fine sandy loam	Fine sandy clay	Fine sandy clay loam

Table 3.6 Summary of physical and chemical properties of the Swartland form

		Horizons		
	Soil property	Ap	B	C
Physical properties	Coarse sand (2 – 0.5 mm) (%)	8.6	6.2	6.4
	Medium sand (0.5 – 0.25) (%)	7.9	5.1	7.1
	Fine sand (0.25 – 0.106 mm) (%)	39.2	20.8	26.4
	Very fine sand (0.106 – 0.53 mm) (%)	22.4	13.6	15.3
	Coarse silt (%)	6.2	6.5	5.3
	Fine silt (%)	3.3	3.5	8.6
	Clay (%)	12.6	44.2	30.9
	Gravimetric water content (%)	10.0	17.0	10.0
	Bulk density (Mg m^{-3})	1.70	1.56	1.63
Chemical properties	EC_e (mS m^{-1})	156.2	101.1	56.4
	Calculated EC_a (mS m^{-1})	51.5	119.9	72.1
	Ca (me ℓ^{-1})	3.9	2.3	2.4
	Mg (me ℓ^{-1})	3.4	2.1	1.7
	K (me ℓ^{-1})	1.5	0.2	0.3
	Na (me ℓ^{-1})	3.0	2.1	1.6
	Total cations (me ℓ^{-1})	11.8	6.8	6.1

The soil profile has an orthic Ap-horizon that is massively structured over a depth of 200 mm. The soil has a fine sandy loam texture with 13% clay. Transition to the B-horizon is smooth. The B-horizon is pedocutanic with sub-angular blocky peds covering a maximum depth of 300 mm. This horizon has a sandy clay texture with a clay content of 44%. The C-horizon is saprolite and covers a depth of 250 mm. This horizon ranges from weakly weathered peds to saprolite rocks. The horizon is of sandy clay loam texture with a clay content of 31%. Soil conductivity ranged from 60 mS m^{-1} to 127 mS m^{-1}. From Table 3.6, bulk density decreased from 1.70 Mg m^{-3} at the A-horizon to 1.56 Mg m^{-3} at B and 1.63 Mg m^{-3} at the C-horizon. Likewise, in Sepane EC_e decreased with depth from 156 mS m^{-1} to 56 mS m^{-1}. The calculated EC_a increased from 52 mS m^{-1} to 122 mS m^{-1} at the B-horizon and decreased to 72 mS m^{-1} at the C-horizon

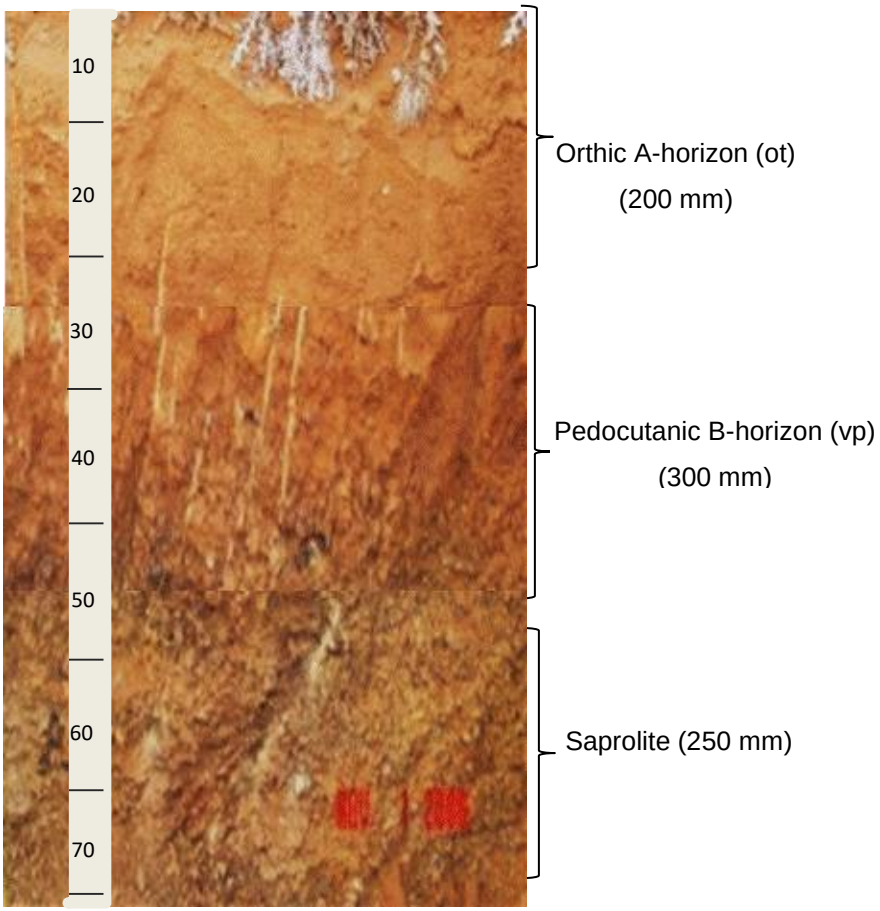

Figure 3.9 Profile view of Swartland on Paradys Experimental Farm (Mavimbela & Van Rensburg, 2013).

Profile attributes of the Tukulu form

The Tukulu soil on Paradys belongs to the *Dikeni* (1220) family (Figure 3.10). The morphological characteristics are presented in Table 3.7, and physical and chemical properties are given in Table 3.8. This soil form comprises of Ap-, B- and C-horizons.

Table 3.7 Morphological characteristics of the Tukulu soil form of the *Dikeni* family

	Horizons		
Characteristic	Ap	B	C
Maximum depth (mm)	210	410	250
Diagnostic horizons	Orthic A	Neocutanic B	Unspecified material with signs of wetness
Colour (dry)	Yellowish red (5YR4/6)	Brown (7.5YR5/4)	Light yellowish brown (2.5Y6/4)
Structure	Massive apedal	Weak developed sub angular blocky peds	Medium to strong developed prismatic peds
Consistency	Loose	Hard	Hard
Transition	Clear flat	Abrupt flat	Abrupt flat
Textural class	Fine sandy loam	Find sandy clay	Fine sandy clay

Table 3.8 Summary of physical and chemical properties of the Tukulu soil form

		Horizons		
	Soil property	Ap	B	C
Physical properties	Coarse sand (2 – 0.5 mm) (%)	7.9	6.0	5.7
	Medium sand (0.5 – 0.25) (%)	7.1	5.3	5.4
	Fine sand (0.25 – 0.106 mm) (%)	40.8	24.9	21.3
	Very fine sand (0.106 – 0.53 mm) (%)	22.2	17.2	13.1
	Coarse silt (%)	6.4	6.5	7.1
	Fine silt (%)	4.2	4.2	6.7
	Clay (%)	12.5	36.1	41.0
	Gravimetric water content (%)	11.0	16.0	13.0
	Bulk density (Mg m^{-3})	1.67	1.58	1.64
Chemical properties	EC_e (mS m^{-1})	92.6	66.6	56.2
	Calculated E_a (mS m^{-1})	44.3	86.4	85.0
	Ca (me ℓ^{-1})	4.6	2.8	2.5
	Mg (me ℓ^{-1})	3.1	2.3	1.7
	K (me ℓ^{-1})	1.3	0.3	0.2
	Na (me ℓ^{-1})	2.5	2.1	1.4
	Total cations (me ℓ^{-1})	11.5	7.6	5.7

The orthic Ap-horizon covers a depth of 210 mm with a massive apedal structure and an average clay content of 13%. The underlying B-horizon is neocutanic, covering a maximum depth of 410 mm. This horizon has a weakly developed sub-angular blocky structure with medium peds and was classified as sandy clay with a 36% clay content. The C-horizon

comprises of unspecified material with signs of wetness over 250 mm soil depth. The structure of the C-horizon is medium to strongly developed prismatic peds. This horizon was classified as a sandy clay soil with a clay content of 41%. Soil chemical properties all decrease with depth, with EC_e ranging from 113 mS m^{-1} to 54 mS m^{-1}. From Table 3.8, bulk density decreased from 1.67 Mg m^{-3} at the A-horizon to 1.58 Mg m^{-3} at B and increased to 1.64 Mg m^{-3} at the C-horizon. EC_e was 93 mS m^{-1} at A-horizon but decreased with depth to 56 mS m^{-1}. The calculated EC_a increased from 44 mS m^{-1} to a relatively uniform value of 85 mS m^{-1} at the B- and C-horizons.

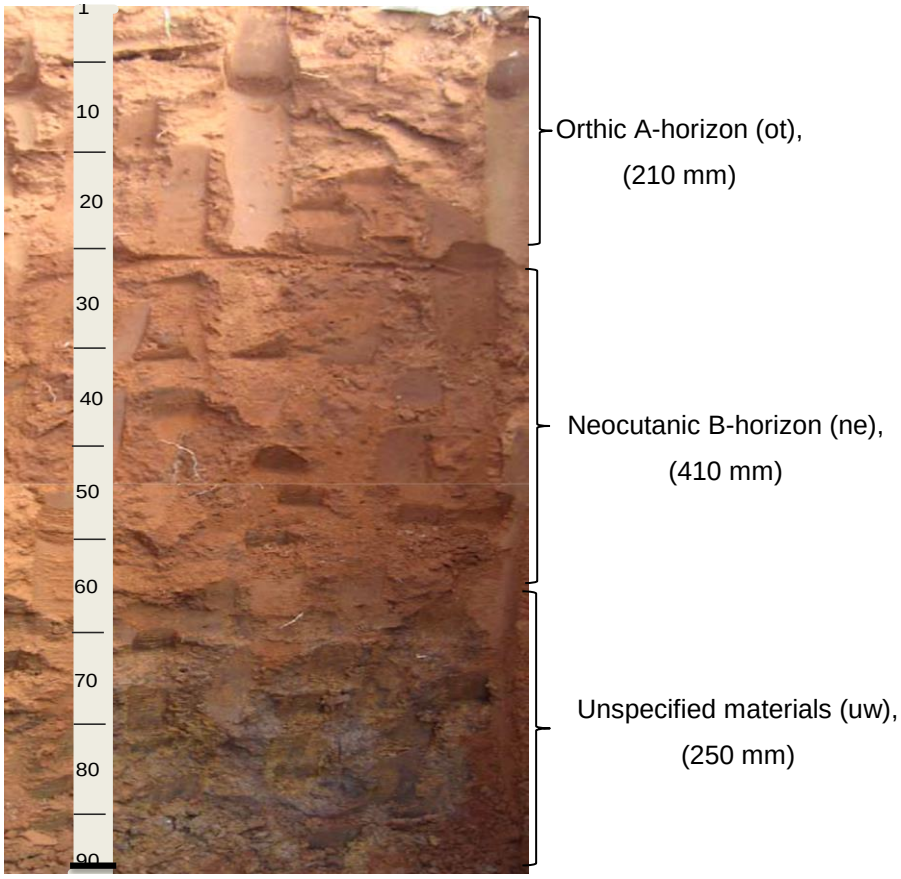

Figure 3.10 Profile view of Tukulu on Paradys Experimental Farm.

Profile attributes of the Bloemdal form

The Bloemdal soil form belongs to the *Roodeplaat* (3200) family (Figure 3.11). Table 3.9 presents the morphological characteristics of the Ap-, B- and C-horizons, while the physical and chemical properties can be seen in Table 3.10. The Ap-horizon has a massive apedal structure covering over a maximum depth of 150 mm. The horizon is of sandy loam texture with an average clay content of 16%. The red apedal B-horizon that covers to a maximum depth of 400 mm has a medium developed blocky structure. The soil is sandy clay loam with 28% clay.

Table 3.9 Morphological characteristics of the Bloemdal soil form of the *Roodeplaat* family

	Horizons		
Characteristic	Ap	B	C
Maximum depth (mm)	150	400	300
Diagnostic horizons	Orthic A	Red apedal B	Unspecified material with signs of wetness
Colour (dry)	Yellowish red (5YR4/6)	Red (2.5YR4/8)	Brownish yellow (10Y6/6)
Structure	Massive apedal	Massive apedal	Medium developed medium prismatic peds
Consistency	Loose	Loose	Hard
Transition	Smooth	Smooth	Flat
Textural class	Fine sandy loam	Fine sand clay	Fine sandy clay

Table 3.10 Summary of physical and chemical properties of the Bloemdal soil form

		Horizons		
	Soil property	Ap	B	C
Physical properties	Coarse sand (2 – 0.5 mm) (%)	7.2	5.5	4.2
	Medium sand (0.5 – 0.25) (%)	5.5	5.2	4.1
	Fine sand (0.25 – 0.106 mm) (%)	38.5	31.2	23.6
	Very fine sand (0.106 – 0.53 mm) (%)	23.1	18.9	14.4
	Coarse silt (%)	6.1	7.6	4.6
	Fine silt (%)	4.0	4.2	7.0
	Clay (%)	16.4	27.5	42.4
	Gravimetric water content (%)	12.0	16.0	13.0
	Bulk density (Mg m^{-3})	1.65	1.58	1.63
Chemical properties	EC_e (mS m^{-1})	73.2	31.0	38.9
	Calculated EC_a (mS m^{-1})	41.8	64.9	85.5
	Ca (me ℓ^{-1})	2.81	1.26	2.10
	Mg (me ℓ^{-1})	1.54	0.53	0.89
	K (me ℓ^{-1})	1.20	0.22	0.18
	Na (me ℓ^{-1})	0.95	0.81	0.54
	Total cations (me ℓ^{-1})	6.50	2.82	3.72

The C-horizon is occupied by an unspecified material that shows signs of wetness and covers a maximum depth of 300 mm. This horizon has a well-developed prismatic structure with clay content of 42%. The soil is of sandy clay texture. From Table 3.10, bulk density decreased from 1.65 Mg m^{-3} at the A-horizon to 1.58 Mg m^{-3} at the B-horizon and increased to 1.63 Mg m^{-3} at the C-horizon. EC_e was 73 mS m^{-1} at A-horizon but decreased with depth to 31 mS m^{-1} with a

small increase at C-horizon. The calculated EC_a increased from 42 mS m^{-1} to a value of 86 mS m^{-1} at the C-horizons.

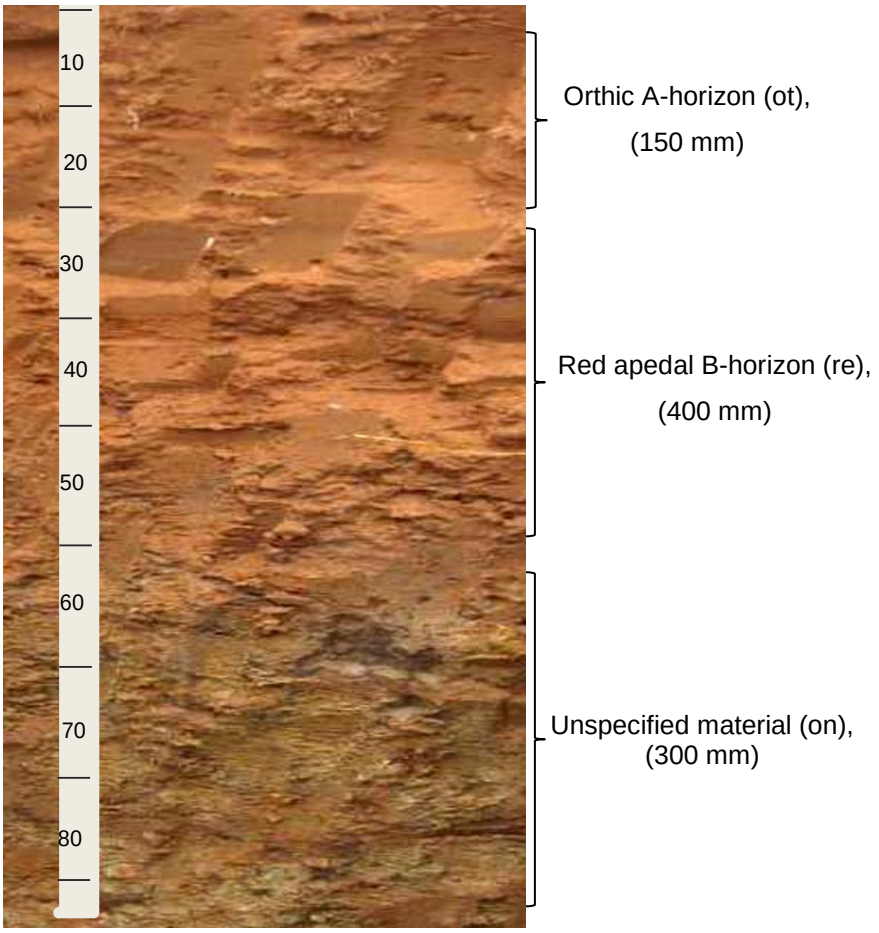

Figure 3.11 Profile view of the Bloemdal soil at Paradys Experimental Farm

3.5 Discussion

Field observations and laboratory analyses as reported in Tables 3.1 to 3.10 were able to characterize individual soil forms of both Kenilworth and Paradys Experimental Farms and their corresponding soil physical and chemical properties. Using Rhoades *et al*. (1989b) model equations, as presented in Corwin & Lesch (2003), this study was able to calculate the possible EC_a values to be expected within the two Experimental sites.

Kenilworth farm is classified as Bainsvlei and has an even spatial distribution of soil properties that are relatively uniform with depth. The ploughed Ap-horizon lead to the granular structure of the top soil layer thereby, allowing water to flow easily through this layer and moving clay contents down the profile. The usefulness of this soil form is not only on its deep profile depth, but also on the presence of the soft plinthic layer that stores much water for plant intake during

drought. The position of this soil form in the landscape explains that, it is flat; therefore, it does not encourage water run-off during rainfall.

On the other hand, Paradys Experimental Farm has uneven distribution of soil properties that is shown in the four different soil forms (Sepane, Swartland, Tukulu and Bloemdal) within the area. All the soil forms had a generic orthic A-horizon of sandy loam texture and the horizon is regarded as Ap because the top soils were also ploughed. The structure of the B-horizons and the presence of the cutans are what characterized these soil forms. Clay content decreases with depth except for Sepane and Swartland with higher values at the B-horizon. The values recorded at present for clay content, is slightly higher compared to that reported in previous studies (Fraenkel, 2008; Bothma, 2009; Mavimbela & Van Rensburg, 2011).

Several factors contributed to the formation of these soil forms in Paradys Experimental Farm. Firstly, is the parent material (Dolerite, Beaufort Sandstone and Shale) which are very high in clay content. These are materials of montmorillonite and illite, which can cause a soil to swell and shrink. The colluvial dolerite is capable of contributing up to 40% of the soil clay content; while shale and sandstone contribute more than 45% to the clay content (Fraenkel, 2008). Secondly is the aeolian activity, which is the movement of fine-grained sand particles by the turbulent action of wind. Thirdly, perturbation, bioturbation and ploughing activities resulting in the displacement of the windblown sand deposits with depth, thereby, moving the clay content down to the underlying soil horizons. These activities cause the soil to exhibit a prominent duplex character, mostly in Sepane soil form and this often results in slow and limited water drainage down the soil profile. Not only is water infiltration slow, but plant rooting is also difficult, especially in the dry periods. This is because rooting by plants is often suppressed by the mechanical strength of the soil, which is as a result of cementation from clay and water mixture.

The depth range of these soil forms were 900 mm, 750 mm, 870 mm and 800 mm for Sepane, Swartland, Tukulu and Bloemdal, respectively. Both Swartland and Tukulu soil forms were found at the up-slope unit of the landscape. This explains the stone concentration found within the surface. Bloemdal soils are within the slope parts of the landscape and are formed from windblown sands and water eroded soils, while Sepane soil forms were found in the lower lying area, receiving materials flowing down the slope. The shallow depths of these soil forms will most probably influence EC_a measurements due to the differences in the B-horizon that are within the depth range of EM38-MK2.

According to the United States Salinity Staff (1969) description for salinity, soils with EC_e <400 mS m^{-1} are non-saline. Therefore, the two sites described in this study are generally non-saline soils. For Bainsvlei, soil salinity and water-soluble cations were extremely low and

decreased with depth. The calculated EC_a values were also low but increased with depth. In the following order: Sepane, Swartland, Tukulu and Bloemdal, the result of the chemical properties explained that soil salinity (EC_e) and water-soluble cations (Ca, Mg, K and Na) were more pronounced in the A-horizon and decreased with depth. On the contrary, the calculated EC_a from Rhoades' model produced lower values at the A-horizon, and increased at the B-horizon, with a slight decrease at the C-horizon. For Sepane, calculated EC_a values were 55 mS m^{-1}, 122 mS $m^{-1}$and 72 mS m^{-1}; while for Swartland, values were 52 mS m^{-1}, 120 mS m^{-1} and 72 mS m^{-1} at A-, B- and C-horizon, respectively. For Tukulu, EC_a values were 44 mS m^{-1}, 86 mS m^{-1} and 85 mS m^{-1}; and for Bloemdal, values were 42, 65 and 86 at A-, B- and C-horizon, respectively.

These calculated EC_a values were in line with clay and water distribution within the horizons of these soil forms. Therefore, this explained that soil salinity was not the cause of EC_a variation at these soil forms, rather the main causes of EC_a variation are soil clay and water content because of the low EC. This implies that if the EM38-MK2 is used on these soils, areas with a higher clay content will show higher EC_a readings as well. In addition, if there is considerable soil water variability over these sites, the EC_a readings should reflect that as well. In using the EM38-MK2 for *in-situ* measurements for the next experiments, it can be expected that the EC_a values from the instrument would relate to the calculated values.

3.6 Conclusion

This chapter provided descriptions of both field and laboratory characteristics of Kenilworth and Paradys Experimental Farms where trials in Chapters 4 and 5 were performed. The soils of Kenilworth Experimental Farm were relatively homogeneous with deeper soil depths, lower conductivity and can be regarded as suitable for dry-land agriculture. The soils of Paradys Experimental Farm are heterogeneous with a shallow depth, and are regarded as less suitable for dry-land agriculture. Conductive soil properties, such as EC_e, clay content, calculated EC_a and water-soluble cations, were more pronounced compared to Kenilworth. Soils on both sites could be regarded as non-saline, this implies that the most contributing factors of the field EC_a measure are soil water content and clay content.

To examine the effect of interferences on EC_a measurement with the EM38-MK2 in Chapter 4, a homogenous soil was required. Therefore the soil of Kenilworth was suitable to best show the EM38-MK2 response to treatments rather than to soil property variations. In Chapter 5, it was attempted to evaluate the use of the EM38-MK2 to spatially characterize soil water content over a heterogeneous field. Soils of Paradys were suitable for this purpose.

CHAPTER 4. INFLUENCE OF SOIL WATER INSTRUMENTS AND TRENCHES ON ELECTRICAL CONDUCTIVITY MEASURED WITH THE EM38-MK2

4.1 Introduction

Apparent electrical conductivity (EC_a) is a way of characterizing spatial variability of soil properties in agriculture (Corwin *et al*., 2003b; Corwin & Lesch, 2005b, c; Sudduth *et al*., 2005; Kweon, 2012). The EM38-MK2 device offers instantaneous EC_a readings and integrates several soil properties (Salinity, Water content, Clay, Soluble cations and temperature), over a large soil volume.

The EM38-MK2 can account for spatial variation of these soil properties, but through site-specific calibration (Corwin & Lesch, 2003; Heiniger *et al*., 2003; Hossian *et al*., 2010; Gangrade, 2012). Apart from the standard gravimetric method, calibration of this EM device for soil water content can also be performed using other indirect methods, such as capacitance probes or a neutron water meter (NWM). The capacitance probe comprises of copper with rings of sensors, while NWM uses an access tube (such as, galvanized steel and aluminium tubes) and both instruments need to be installed in the field for long-term use.

However, it has been reported that EM devices are sensitive to metallic objects within the survey area (McNeill, 1996; Geonics, 2003). The sensitivity of EM38 for detecting metallic objects has been examined by Bevan (1998). Excluding the effect of soil properties, results showed that EM38 device could detect both large and small metal objects in the soil. This implies that the presence of metals within a survey area can affect EC_a measurement. Thus when using other indirect soil water instruments containing metals for calibration of the EM38-MK2, it would be ideal to study these instruments for any possible interference in EC_a readings. This is because EM38-MK2 will more accurately explain soil water variation if EC_a measurements were taken close to soil water measuring points. Metals in soil water instruments at these points could lead to EC_a measurement inaccuracy. Moving away from these points can also influence the relationship between EC_a and soil water content.

EC_a was able to explain over 93% soil water variation, where field calibration of EM38 device was performed with both EC_a and soil water estimated from TDR and NWM are collected at the same reference point (Kachanoski *et al*., 1988; Stanley *et al*., 2014). When EC_a was taken 2 m away from soil water measuring points, the relationship between EC_a and soil water estimated from NWM was reduced to 0.80 (Kachanoski *et al*., 1990), while in another study, at 10 m away, even weaker relationships of 0.58 were recorded (Sheet & Hendrickx, 1995). Grisso *et*

al. (2009) suggested keeping a distance of about 1.2 to 1.5 m between the EM38 and any metal object, but did not specify what type of metals were used

In a study by Clay (2005), it was explained that EM38 instruments can also detect pit features, ditches and earthworks through EC_a measurements. Following observations in a current preliminary study, it was suspected that profile pits, often used on research farms, may cut off current flow from the EM38-MK2 and interfere with EC_a measurement.

Though Stanley *et al*. (2014) examined EM38 response to polyethylene, polyvinylchloride and aluminium access tubes, and their insertion holes, this study wants to examine whether obstructions such as: NWM galvanized-steel access tubes, DFM capacitance probes and profile pits within the EM38-MK2 survey area would influence EC_a measurement. The first objective was to determine at what distance to place the EM38-MK2 from these obstructions during field surveys, since EC_a readings should preferably be taken as close as possible to soil water measurement points. A second objective was to examine the stability of EC_a readings after the EM38-MK2 encountered the various interferences, in order to determine whether instrument re-zeroing would be required.

4.2 Materials and methods

This study was conducted at Kenilworth Experimental Farm (latitude 29°01'47.6"S, longitude 26°08'58.3"E and altitude 1366 m). A detailed site description is presented in Chapter 3. The climate of the area is characterized by a high evaporative demand with relatively low and erratic rainfall. Soils are fine sandy loam textured and are classified as the Bainsvlei form belonging to *Amalia* family. This soil is known to have a high water infiltration rate and is suitable for dry-land agriculture in the Free State Province. This site was chosen specifically because it has more homogenous soils, hence it should best show the EM38-MK2 response to treatments rather than to soil property variations.

4.2.1 Experimental layout and measurements

The experiment was conducted within a 645 m² (43 m x 15 m) field area. Four transects, 21 m each, was marked in two parallel lanes (Figure 4.1). From one end of each transect, a measuring tape was used to mark 1 m intervals with a center point (0 m), with 10 distance points on either side (totalling 21 measuring points per transect). The center point is where all treatments were applied and can be regarded as the point of influence. Four interference treatments were evaluated: (i) a control with no interference, (ii) DFM capacitance probes, (iii) NWM galvanized steel access tubes, and (iv) trenches (profile pits).

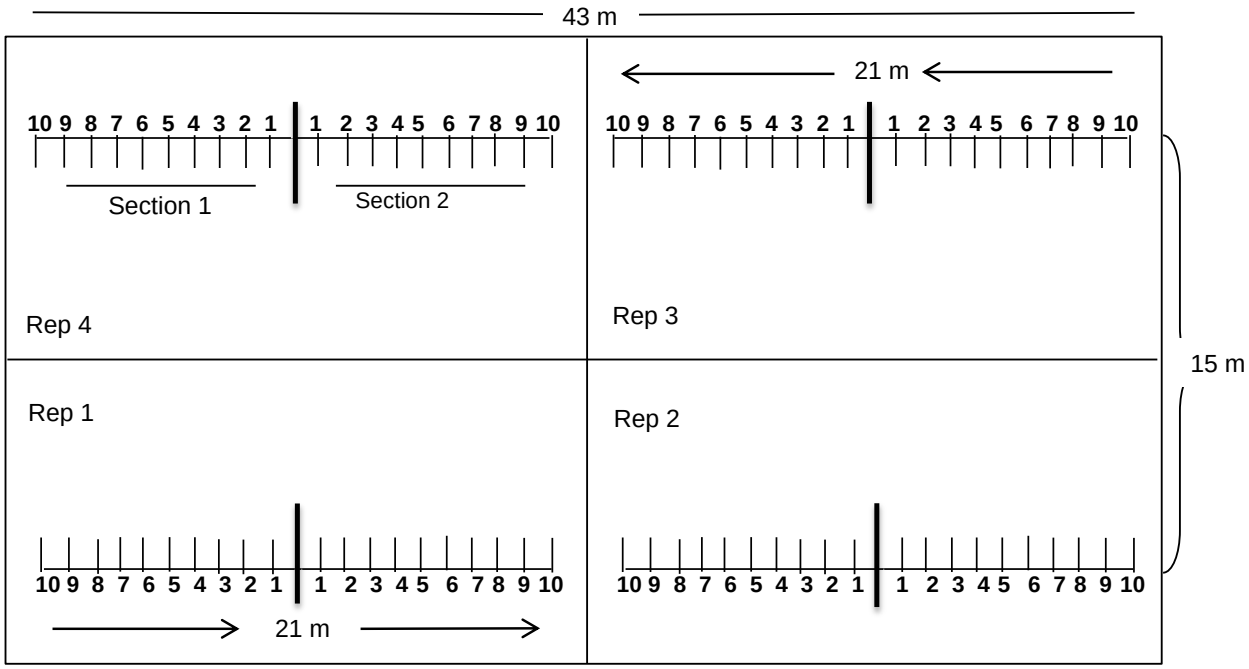

Figure 4.1 The schematic diagram showing the field layout for Experiment 1, with four replications (Rep 1 to 4), 1 m interval measuring points and a center point of influence (thick vertical lines at the center of each transect).

Treatments were applied on consecutive days to the same four plots all at the center point (Figures 4.2a, b and c). The control readings were taken first since it does not require any material or soil disturbance. Next, three DFM probes were installed 0.3 m apart from each other at the center of each transect (Figure 4.2b). This 0.3 m spacing was to ensure that the whole length of the EM38-MK2, i.e. both receiver coils, have equal contact with the source of interference. The DFM-capacitance probes used in this experiment were 1.2 m long with sensors located at 0.2 m intervals. After this, three NWM galvanized steel access tubes were installed in the positions where DFM probes were. The length and internal diameter of the access tubes were 1.5 m and 0.07 m, respectively. Likewise, a trench was made at the center of each transect, 1 m wide and 1.5 m deep, in correspondence with the EM38-MK2 measurement depth (Figures 4.2c).

The EM38-MK2 operating instructions were followed according to the manufacturer's manual (Geonics, 2003) before starting with measurements for each treatment. This included a battery test, initial in-phase nulling, instrument zero and final in-phase nulling. In this study, the EM38-MK2 was not zeroed after encountering the treatments applied, in order to examine the instrument's response before and after the influence of the treatments. However, the EM-device was re-zeroed between transect measurements.

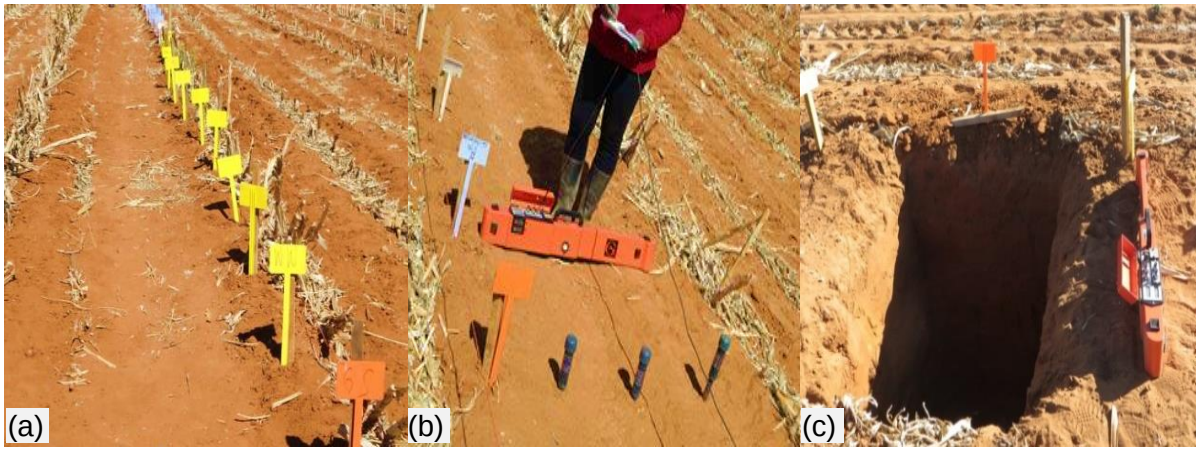

Figure 4.2 Layout showing (a) the measurement transect with the distance points marked using sign posts, (b) the EM38-MK2 at 1 m to the DFM capacitance probes and (c) at close distance to the trench.

Measurements were made by placing the EM38-MK2 at every 1 m interval, from 10 m towards the point of influence (0 point) and then passed further to 10 m away from the point of influence without zeroing the instrument. Both IP (in-phase) and QP (quad-phase or ground conductivity) readings, were manually recorded on both horizontal (shallow depth, 0.75 m) and vertical (deeper depth, 1.5 m) dipole orientation. The IP readings, a self-generated signal resulting from magnetic susceptibility of the soil, were used to explain how the EM38-MK2 reacts towards the interferences. The instrument should read IP values below ±10 ppm otherwise there is interference. The QP readings, expressed as EC_a (mS m^{-1}), was also used to examine the effect of each treatment.

4.2.2 Soil sampling

Soil samples were collected immediately after the experiment to assess soil properties that might contribute to the EC_a measured at each point. If the soil between the points were homogenous, then any substantial deviation in measurement could be contributed to interference from the treatments at the center of each transect. Using a hand auger, samples were collected from five different depth intervals (0 to 0.3 m, 0.3 to 0.6 m, 0.6 to 0.9 m, 0.9 to 1.2 m, and 1.2 to 1.5 m) at the 11 measuring points on each plot, giving a total of 220 samples for the experiment. These samples were collected in plastic bags and weighed immediately before oven drying.

At the Division of Soil Science Analytical Laboratory, University of the Free State, the oven-dried samples were analyzed according to the Non-Affiliated Soil Analysis Work Committee (1990). Samples were analyzed for gravimetric water content (GWC) using the oven dry method, particle size distribution using the pipette method, electrical conductivity (EC_e, mS

m^{-1}) using the soil saturated paste extraction method, and water-soluble cations (Na^+, K^+, Ca^{2+} and Mg^{2+}) generated from the paste extract. Laboratory procedures have been detailed in Chapter 3 (Section 3.2.3).

4.2.3 Statistical analysis

The IP readings were used as a first indication of interference during EM38-MK2 measurements. No statistical test was performed on the IP data, however, graphs of IP values were developed using a broken y-axis to accommodate all values, as described by Blakeston (2015). Recorded EC_a data were first standardized to an equivalent conductivity of EC_{25} at a reference temperature of 25ºC using Equation 2.4 and the exponential model (Corwin & Lesch, 2005a), in Table 2.2 (Chapter 2). Means and standard deviations were calculated in Microsoft Excel for every measurement point to develop a graph for each interfering treatments. EC_a data were then arranged into two groups based on measurements taken before and after interference for each treatment. The equality of variance was tested between the two groups. For each treatment, a *t*-test was used to compare the means of these two groups using the SAS (Statistical Analysis System Institute Inc., 1999) software program. In the cases where there was unequal variance between EC_a data collected before and after the point of influence, the Cochran method for unequal variance was used in the *t*-test to check for any significant difference. If both groups had equal variance, the pooled method was used.

4.3 Results

4.3.1 Soil homogeneity

For all soil properties tested (particle sizes, EC_e, GWC, resistivity and water-soluble cations), there was a common population variance over the distance points. Table 4.1 is a summarized statistics of the homogeneity test. Results showed that there was considerable variability of these soil properties over the depth. The result shows that the soils within the experimental area at Kenilworth are spatially homogenous in soil properties for every depth.

Since the measured properties were homogenous over distance points, the EC_a readings on transects were expected to have a uniform trend except where there was interference from the imposed treatments. This is an advantage to this study since the aim was to examine if EM38-MK2 would respond to proposed soil water probes and trenches.

Table 4.1 Summarized statistics showing the homogeneity of measured soil properties over the distance points (m), n = 44 per depth

Soil depths (m)	Soil properties	Total sand (%)	Total silt (%)	Clay (%)	GWC (%)	Total cations (me ℓ^{-1})	ECe (mS m^{-1})	Resistivity (ohm)
0 to 0.3	Mean	86.2	6.14	6.94	3.87	2.41	0.26	3806
	F-values	1.90	0.37	0.76	2.25	1.09	1.36	0.76
	p>F	0.08	0.95	0.66	0.04	0.40	0.24	0.66
0.3 to 0.6	Mean	75.8	5.85	16.97	8.49	2.12	0.22	2376
	F-values	0.88	0.41	1.04	1.73	0.72	1.36	1.05
	p>F	0.56	0.93	0.44	0.12	0.70	0.24	0.42
0.6 to 0.9	Mean	77.4	5.64	15.79	7.55	1.88	0.19	2751
	F-values	0.37	0.67	1.87	0.93	0.81	0.65	0.33
	p>F	0.95	0.74	0.09	0.52	0.62	0.76	0.97
0.9 to 1.2	Mean	80.4	5.71	13.27	7.27	1.84	0.18	2892
	F-values	1.07	0.99	0.29	0.42	1.11	1.40	0.48
	p>F	0.41	0.47	0.98	0.92	0.38	0.22	0.89
1.2 to 1.5	Mean	77.4	5.90	14.64	8.59	1.92	0.19	2392
	F-values	0.27	1.27	0.84	0.09	0.21	0.18	0.67
	p>F	0.98	0.29	0.59	1.00	0.99	1.00	0.75

4.3.2 Magnetic susceptibility (IP readings)

The trend in IP readings for vertical (V) and horizontal (H) dipole modes is presented in Figure 4.3a and b, respectively. The control and trenches gave consistent IP readings that were below ±10 ppm at all distance points. The IP values recorded for DFM probes and steel NWM access tubes had the same trend in both measurement modes, starting with low a IP, followed by a sharp effect on the readings as the EM38-MK2 was placed closer than 1 m to the point of influence. At the point of influence (0 m), the mean IP readings for DFM probes were -33 ppm and -62 ppm, while for access tubes -210 ppm and -506 ppm were recorded in V-mode and H-mode, respectively. The result indicates that trenches had no influence on IP readings even at close distance, while the huge IP readings for DFM probes and access tubes are an indication that they were detected by the EM38-MK2, but only at a distance closer than 1 m. This implies that EC_a readings at points closer than 1 m to the probes and access tubes will be influenced.

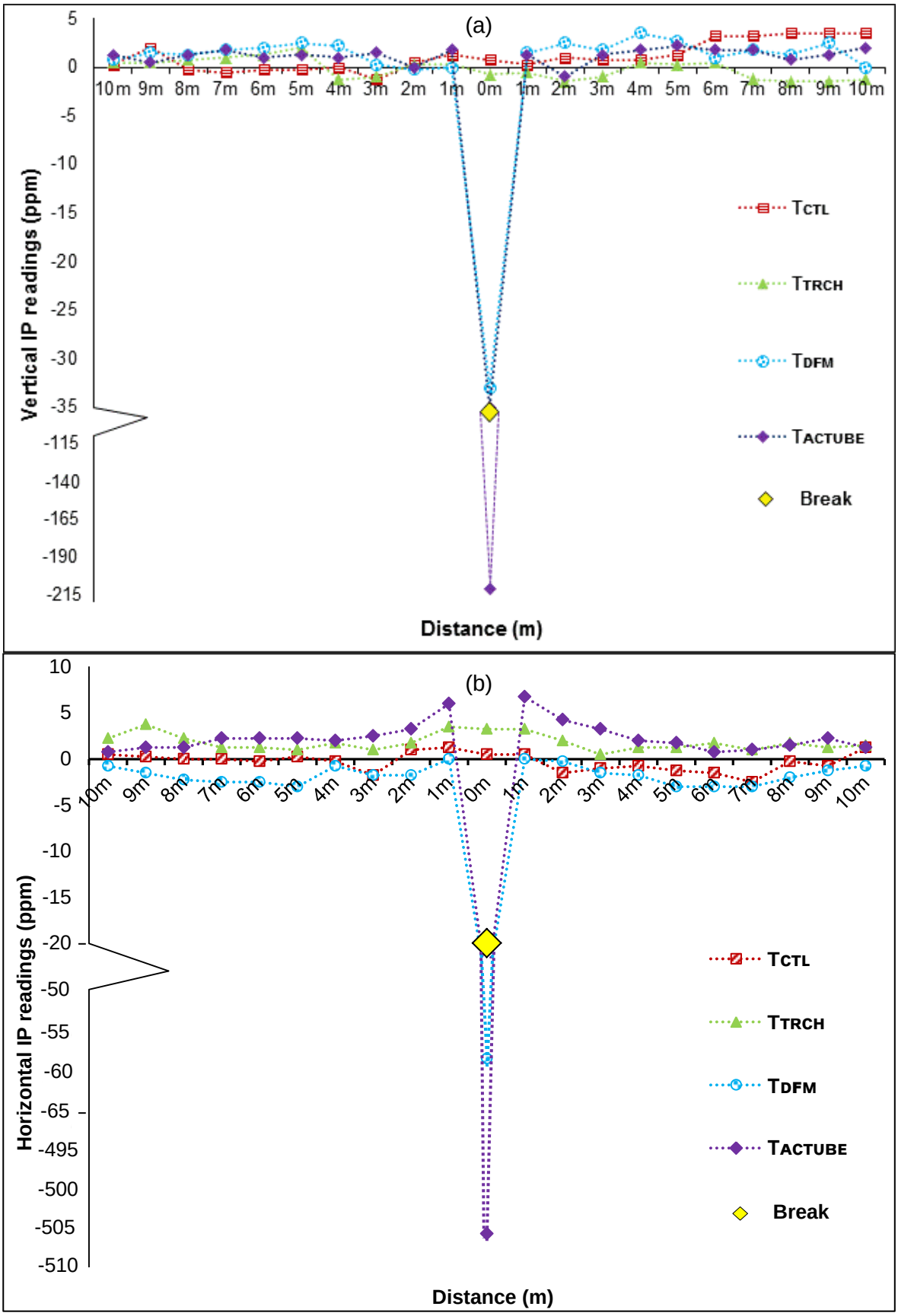

Figure 4.3 Average IP readings of the EM38-MK2 in the (a) horizontal (b) vertical mode taken along a survey transect without interference (T_{CTL}), and with interference from a trench (T_{TRCH}), DFM probes (T_{DFM}) and steel NWM access tubes (T_{ACTUBE}).

4.3.3 Apparent electrical conductivity

Effect of trenches on EC_a readings

Figure 4.4 shows the EM38-MK2 response toward trenches. The measured EC_a ranges from 15 mS m^{-1} to 19 mS m^{-1} and 7 mS m^{-1} to 10 mS m^{-1} in V-mode and H-mode, respectively. With the instrument right next to the trenches, there was a slight reduction in EC_a readings only in the V-mode. Statistically, the group EC_a values before and after the trenches have equal variance for V-mode readings. The means was not significantly different, because the calculated *t*-value is smaller than the critical value (t = 0.24, p = 0.8129). While in the H-mode, there was unequal variance for the two groups, but the means were not significantly different (t = -1.30, p = 0.2027). This indicates that trenches did not interfere with the current flowing from the EM38-MK2.

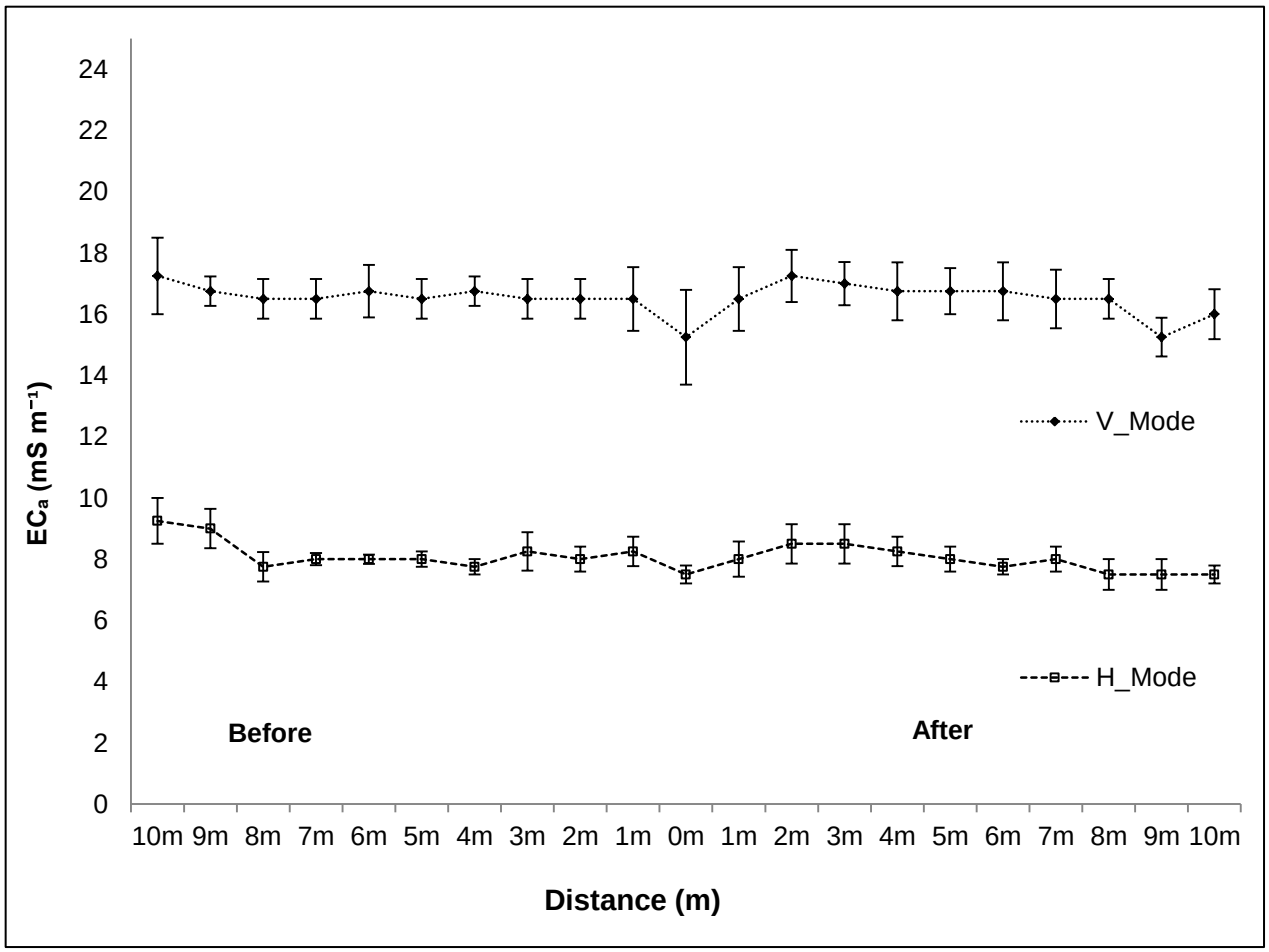

Figure 4.4 Measured EC_a on both vertical (V-mode) and horizontal (H-mode) dipole mode before and after encountering the trenches

Effect of DFM capacitance probes on EC_a readings

Figure 4.5 presents the EM38-MK2 response as the instrument was moved towards and over the inserted DFM probes. The EC_a values measured moving towards the probes ranged from 13 mS m^{-1} to 24 mS m^{-1} and 7 mS m^{-1} to 12 mS m^{-1} in V-mode and H-mode, respectively. Only at the point of influence (closer than 1 m), there was a strong effect on the readings (Figure 4.5). The instrument recorded a mean EC_a value of -44 mS m^{-1} in the V-mode and -80 mS m^{-1} in the H-mode. Note, however that the standard deviation of these means were 72 mS m^{-1} and 14 mS m^{-1} in the V-mode and H-mode, respectively. This indicates an inconsistent response of the EM38-MK2 to the DFM probes.

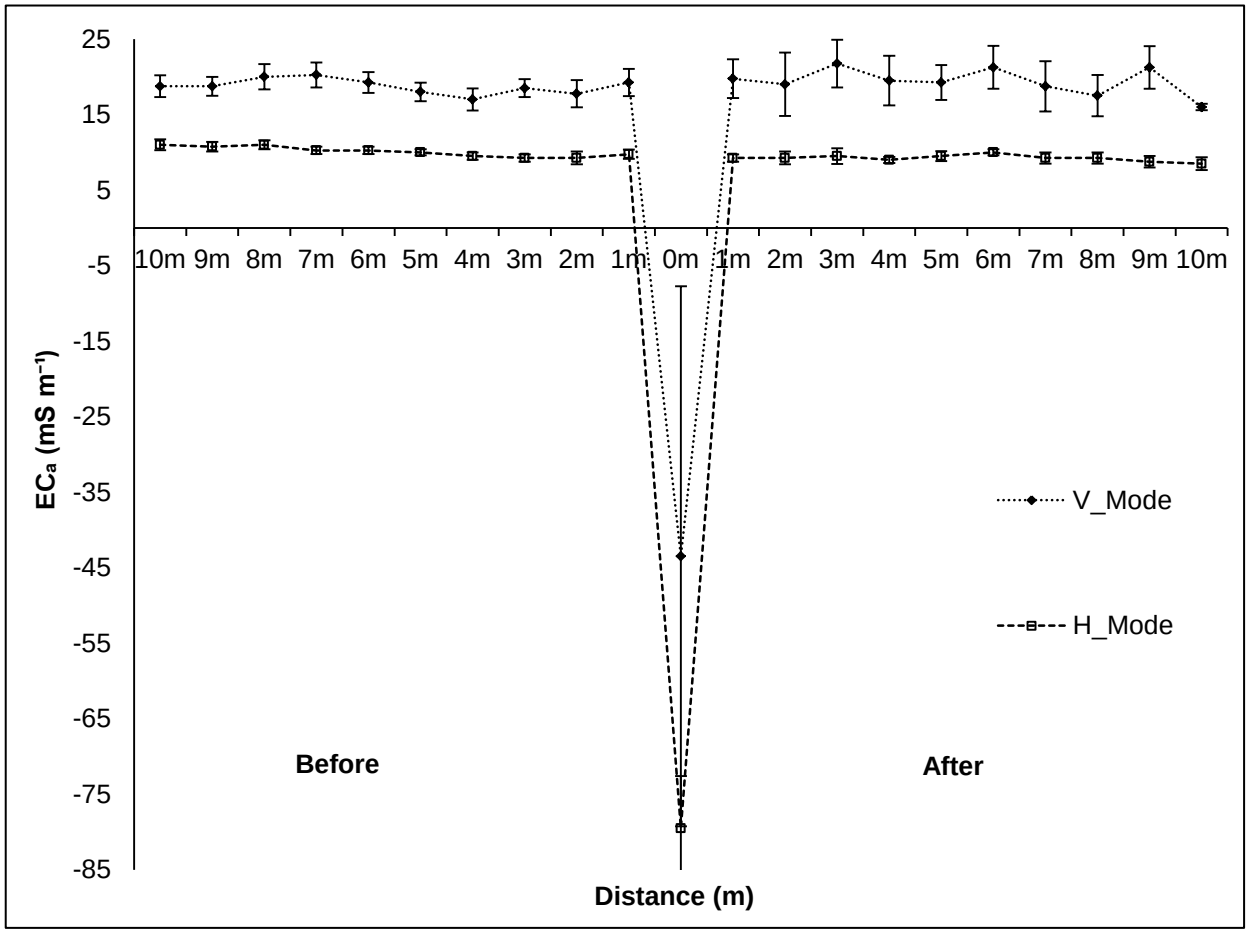

Figure 4.5 Measured EC_a on both vertical (V-mode) and horizontal (H-mode) dipole mode before and after encountering DFM-probes

After the EM38-MK2 encountered DFM probes, EC_a readings were relatively variable in the V-mode. Statistically, the EC_a group means before and after encountering DFM probes had unequal variance. The CV for EC_a readings was 15% before encountering DFM probes and 28% thereafter (Appendix 4.1). However, the means before and after the point of influence were not significantly different (t = 0.68, p = 0.5029).

In the H-mode, the two groups had equal variance but the means were significantly different (t = -3.07, p = 0.0029). The mean EC_a values after an encounter with the DFM probes were 9% (0.88 mS m^{-1}) smaller (Appendix 4.2).

Effect of NWM steel access tubes on EC_a readings

Figure 4.6 shows the EM38-MK2 response as the instrument was moved towards the inserted steel tubes. A steady reading was recorded from 10 m to 1 m distance points with EC_a values ranging from 14 mS m^{-1} to 22 mS m^{-1} and 7 mS m^{-1} to 13 mS m^{-1} in the V-mode and H-mode, respectively. At the point of influence, the steel tubes caused the EM38-MK2 to produce a very strong response with mean values of -30 mS m^{-1} for V-mode, and -1541 mS m^{-1} for H-mode. The response was extremely inconsistent with a standard deviation of 103 mS m^{-1} and 655 mS m^{-1} in the V-mode and H-mode, respectively.

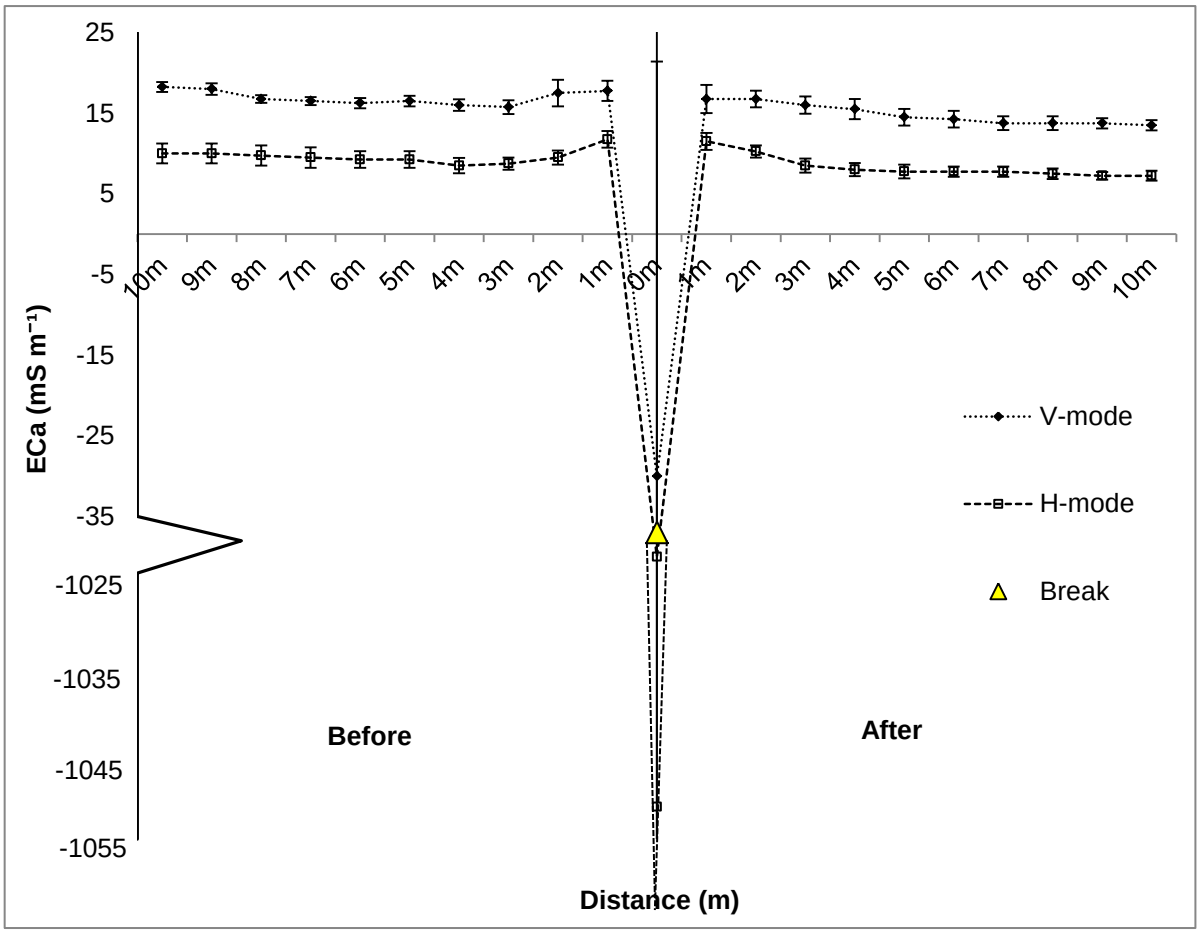

Figure 4.6 Measured EC_a on both vertical (V-mode) and horizontal (H-mode) dipole mode before and after encountering the steel NWM access tubes

Statistically, the measured EC_a values before and after the steel tubes have equal variance in the V-mode but, the t-test in Appendix 4.2 confirms that the means of these two groups were significantly different (t = -4.61, p = <0.001). The EC_a values recorded after the EM38-MK2

encountered the steel tubes were 2.1 mS m^{-1} smaller than the EC_a measured before the steel tubes. In the H-mode, the two groups also had equal variance, but the means were significantly different (t = -2.88, p = 0.0052). The mean after an encounter with the steel tubes were smaller by 13% (1.3 mS m^{-1}).

4.4 Discussion

Generally, the reaction of the EM38-MK2 each time it encounters an influence depends on the current flowing from the instrument and the electrical force coming from the conductive objects. From the results, it was observed that the trenches did not influence the EC_a reading with EM38-MK2, while the DFM capacitance probes and galvanized steel access tubes that contain metal had a pronounced effect. These metal containing interferences elicited a strong response when the EM-device was moved closer than 1 m proximity. This is similar to results reported by Stanley *et al*. (2014) where effects on EC_a was observed within 0.5 m distance to aluminium NWM access tubes.

In this study, the presence of steel tubes resulted in more pronounced and more erratic EC_a readings compared to the DFM probes. This is probably due to the fact that DFM probes contain only small rings of copper over the probe length, compared to the steel access tubes that comprises much more metal (1.5 m length). This is in accordance with findings by Bevan (1998) who reported a strong response when large metal objects was passed under the coils of the EM38 and a weak response with smaller pieces of metal. The response from the metals gave a negative values and this was also confirmed in the present study; when EM38-MK2 was in close proximity to DFM capacitance probes and steel NWM access tubes, readings could be a huge number that were either positive or negative.

Sheet & Hendrickx (1995) and Bevan (1998) stated that an EM-device in the H-mode had a greater relative sensitivity to conductive materials near the ground surface. This effect was also clearly visible in the current study, where a larger EC_a response to DFM probes and steel tubes was obtained in the H-mode compared to the V-mode.

More importantly, after the EM38-MK2 encountered the DFM probes and steel tubes, there was a significantly measurable effect on the EC_a readings. The EC_a was either less stable (DFM in the V-mode) or lower (DFM in the H-mode and steel tubes in the V- and H-modes). The instability that was observed in the V-mode after an encounter with DFM probes was relatively small. The standard deviation of the EC_a readings before and after the probes differed with only 4.3 mS m^{-1} (Std Err = 0.96 mS m^{-1}) (Appendix 4.2). The decrease in the mean EC_a values after encountering DFM (H-mode) and steel tubes (V- and H-modes) were all relatively small

(< 2 mS m^{-1}). On a practical level, these small differences would probably not have a meaningful effect. Other researchers did not report on the extent of this effect as reported in this study. The manufacturer suggested to evaluate field objects as presented in this study and stated that, if the two readings before and after the objects differ by more than 10%, a significant disturbance is being felt. It was recommended to either remove or take EC_a measurements at a located further away from the object (Geonics, 2003). Moving away from a reference points might not favour the use of other indirect soil measuring instruments considering a two-step process in calibrating EM38-MK2 for soil water studies. The ideal step would be to re-zero the EM-device if it accidentally detected any form of metals within its line of measurement. However, this can be quite time consuming because the operator is required to return to the same location of first EM-device zeroing each time. Although statistically significant, the extent to which EC_a values were affected in this study was very small and not practically relevant. From an operational point of view, the slight increase in accuracy obtained by re-zeroing would likely not be worth the effort.

4.5 Conclusion

The experiment was conducted on a homogenous soil, therefore results would clearly indicate the effect of the applied interferences, i.e. the presence of trenches, DFM capacitance probes and NWM galvanized-steel access tubes, on the response of the EM38-MK2. The IP readings were able to identify differences in EM38-MK2 response to the treatments (applied influences), and a change in IP values leads to a consecutive increase in EC_a readings. This study did not find any influence from the trenches on any EM38-MK2 measurement modes. The DFM probes and NWM steel access tubes influenced the EC_a readings but only closer than 1 m to the probes. The effect from the steel tubes was more pronounced compared to that from the DFM probes at close proximity with the EM38 device. The EC_a V-mode readings after the DFM probes became inconsistent, while a reduction was obtained in the H-mode and in both modes of EC_a readings after the steel tubes as well. The influence imposed on EC_a values due to the presence of DFM probes and NWM steel access tubes although statistically significant, were so small that, it would probably not warrant re-zeroing the EM38-MK2 during a field survey.

In conclusion, one must avoid field instruments that contain any form of metals during a field survey by using EM38-MK2 not closer than 1 m to such instruments as DFM probes or NWM steel access tubes. If by any mistake, the EM38-MK2 encountered any of these probes buried in the ground, it should not be necessary to go back and re-zero this EM-device during a field survey. However, it is a good idea to monitor the stability of the EC_a readings during field survey.

CHAPTER 5. CALIBRATION OF EM38-MK2 USING DFM CAPACITANCE PROBES FOR SPATIAL CHARACTERIZATION OF SOIL WATER CONTENT

5.1 Introduction

The accurate, direct and standard way to quantify water within a soil is through the gravimetric method. Soil water content can also be estimated indirectly with the EM38-MK2 from the measured apparent electrical conductivity (EC_a). This requires site specific calibration of the EM38-MK2 using same-day measured EC_a and soil water content determined by the standard volumetric method (Munoz-Carpena *et al.*, 2004), which should be performed each time the instrument is used. This is done to develop an equation that can be used in generating soil water content from EC_a values when the instrument is used on the same site or soil type. However, frequent soil sampling is labour intensive and time consuming, hence the need for other intermediate calibration methods that can be used continuously to calibrate the EM38-MK2.

Studies have successfully used several indirect methods to calibrate EM38 instruments. On a non-saline soil with low conductivity, EC_a calibrated with soil water estimated from time-domain reflectometry (TDR) was able to explain 96% of spatial variation in soil water content within a depth of 0 to 0.5 m (Kachanoski *et al*., 1988). In another study Kachanoski *et al*. (1990) also showed that calibrated EC_a (EM38) with water content estimated from a neutron water meter (NWM) can explain up to 75% of variation in water content. Reedy & Scanlon (2003) used an EM38 device at the exact location of NWM measurements and reported that EC_a explained 80% of the averaged vertical soil water variation over 1.5 m soil depth and 90% of the averaged spatial soil water variation. Stanley *et al*. (2014) adopted the same method to calibrate EM38 response to soil water content, but used polyethylene NWM access tubes and operated EM38 directly over the same soil where the NWM were used and recorded strong relationship explaining 94% of water content over 0.4 to 0.6 m soil depth. Also, Lavoué *et al*. (2010) successfully used electrical resistivity tomography (ERT) to relate EC_a measured with the EM38 for soil water variability.

The present study wanted to explore the use of DFM capacitance probes (DFM Software Solutions, South Africa) in calibrating the EM38-MK2 for soil water estimation. The accuracy of using capacitance probes for soil water estimation has been reported in several studies (Atkins *et al.*, 1998; Zerizghy, 2013). DFM capacitance probes are indirect, point measurement instruments that need to be installed only once into the soil to continuously measure soil water

and soil temperature simultaneously. This instrument can also keep a backup of its data for up to six months.

There is limited literature available on the use of the EM38-MK2 for soil water assessment in Africa, including spatial characterization of soil water on rangelands. The first aim of this study was to calibrate DFM capacitance probes for soil water estimation. Secondly is to conduct field calibration of the EM38-MK2 for soil water estimation by using calibrated DFM probes readings. Thirdly is to produce a general calibration equation that can be used to characterize soil water content on a heterogeneous site comprising of four different soil forms.

5.2 Materials and methods

5.2.1 Description of experimental site

The experiment was conducted at Paradys Experimental Farm (latitude 29º13.375'S, longitude 026º12.527'E and altitude 1422 m) as was described in Chapter 3 (Figure 3.1c). The farm is known for its dry-grassland climate, with a surface area that encourages runoff during high intensity rain. The soil forms within this site are regarded as marginal for dry-land agriculture due to its shallow depth, mechanical strength of the B-horizon, and the presence of cutans that impede root development and drainage. The farm is used for rain-fed and irrigated forage production for animal grazing.

5.2.2 Experimental layout

The experiment was designed in order to calibrate both DFM probes and EM38-MK2 under wet and dry conditions for soil water estimation. An area of 1.96 ha (140 m x 140 m) of the field was mapped out. Subsequently, a systematic sampling procedure (20 m x 20 m) was used to produce a grid sampling design of 64 points (Figure 5.1a). Hereafter, the EM38-MK2 was used to take geo-referenced measurements of EC_a in the horizontal dipole orientation at each of the 64 grid points. Data was automatically recorded via Bluetooth using a data logger and GPS receiver and then transferred to a computer system. The EC_a data were then analyzed with the ESAP software package specifically developed for EC_a measurements (Lesch, 2005). The response surface sampling design (RSSD) programed into this software (See Chapter 2, section 2.4.3), was used to design a sampling plan within the 64 grid points. The software generated 12 optimal sampling or reference points (i.e. the black dots in Figure 5.1a) based on EC_a variation. These reference points represent the best possible sampling sites (noted as plots in this study) where DFM and EM38-MK2 outputs were calibrated for soil water estimation. Among these plots, three were Sepane, two were Swartland, five were Tukulu and

two were Bloemdal soil forms according to the Soil Classification Taxonomic System for South Africa (Soil Classification Working Group, 1991). Each of these soil forms has its own characteristics and full profile descriptions of the individual soil forms have been presented in Chapter 3.

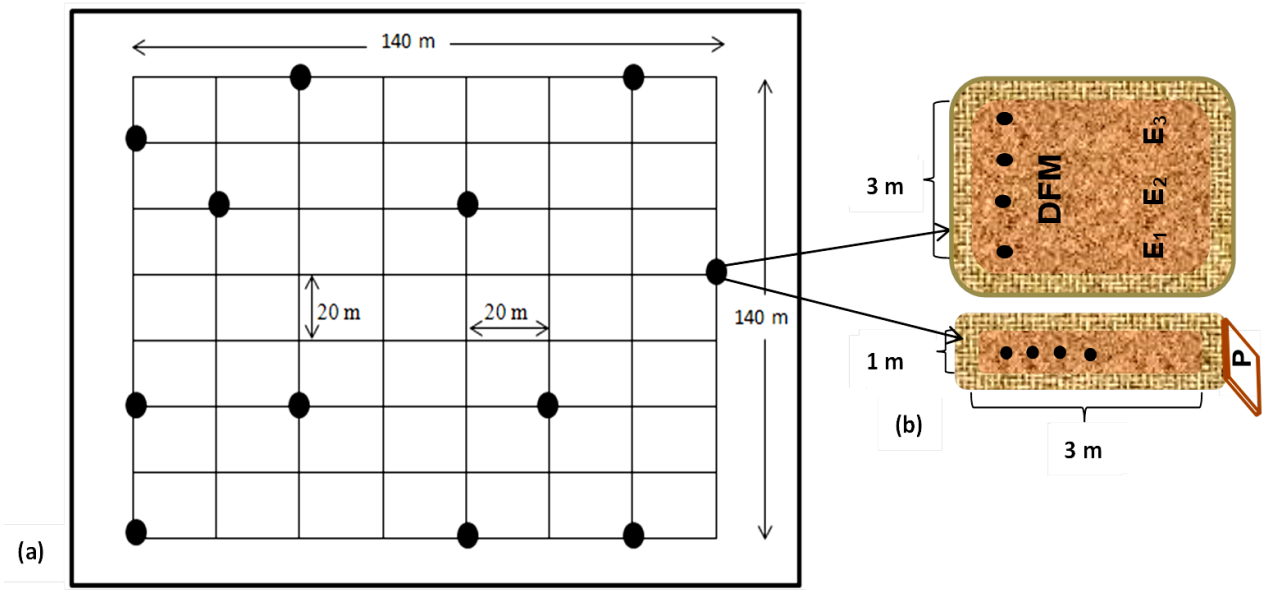

Figure 5.1 A schematic diagram of the field layout for Experiment 2, (a) with the black dots showing the 12 reference points. The individual plot (b) showing the DFM probes at the center, the EC_a measurment points (E_1 E_2 E_3), the profile pit to the right (P) and sampling points (black dots) are also included.

Furthermore, plots with an area of 3 m x 3 m (Figure 5.1b) were marked around each reference point. These plots were constructed by making ridges around the borders to prevent water runoff during soil wetting. A level surface was maintained for all plots to ensure equal water distribution. A separate 1 m x 3 m plot was also mapped outside the main plot with a profile pit dug at one end specifically for undisturbed (core) soil sampling for soil bulk density determination. The idea of this second plot was to avoid disrupting the main plots during core sampling. On the main plots, disturbed samples, EC_a measured with the EM38-MK2 and DFM probe readings were recorded all at the same time. A single DFM capacitance probe was installed 1 m from the edge of each main plot, using a drilling machine with an iron rod to ensure tight contact with the soil. The DFM probes were in lengths of 0.8 m with sensors positioned at 10, 20, 30, 40, 60 and 80 cm of the probe, and 1.0 m with sensors positioned at 10, 20, 40, 60, 80 and 100 cm of the probe. All the probes were set to take hourly readings. EM38-MK2 measurements were taken in the horizontal dipole mode with measuring depths of 0 to 0.375 m and 0 to 0.75 m at the 12 plots.

5.2.3 Calibration procedures

The DFM capacitance probes and EM38-MK2 were calibrated simultaneously during this study. Calibrations were performed *in situ* under wet and dry conditions. While the soils were dry, multiple EC_a readings were first logged by a double click on the instrument log button at 3 different points (E_1, E_2 & E_3). The EM38-MK2 was placed approximately 1 m from the DFM probes (Figure 5.1b) based on the conclusions in Chapter 4. Between the edge of the plots and the DFM probes, disturbed soil samples were taken on the main plots, as well as on the subplots. This was done using a soil auger at a corresponding depth to the three soil horizons. This set of data was used to determine the gravimetric water content. In each of the profile pits, three undisturbed core samples were collected horizontally for each soil horizons under dry and wet conditions, respectively. The core samples were used to determine soil bulk density. Gravimetric water content of the core soils were also recorded. The DFM probe data, including temperature values, for the whole duration of soil sampling were downloaded using a data logger. Next, a known amount of water was smoothly applied to both the main and sub-plots to saturation. After wetting, the plots were covered immediately to prevent evaporation (Figure 5.2). Sampling and data collection, as described above, were repeated within 12 hours after the first application of water had infiltrated the soil. Now the plots were left open to dry out for 5 days. After 5 days, the plots were wetted again and data collected as stipulated earlier. This cycle of wetting and drying was repeated three times. Therefore, all data were recorded four times: in the dry condition, after the first wetting, after the second wetting and after the third wetting.

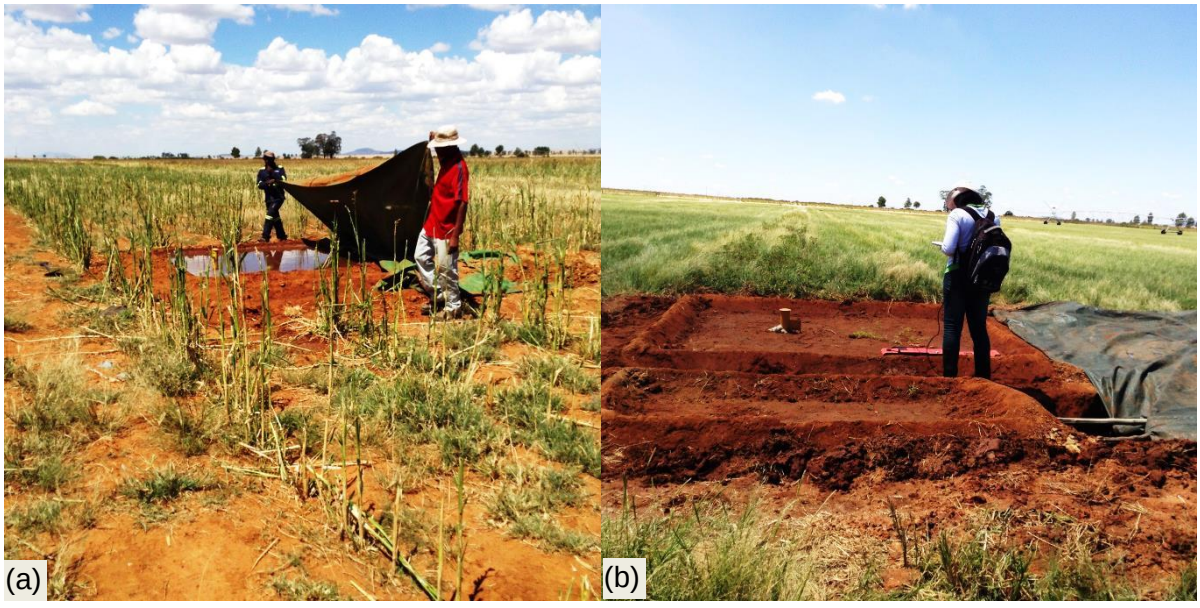

Figure 5.2 (a) Plot after first water application, being covered to avoid evaporation, and (b) plot showing EC_a data collection in the horizontal mode.

All the soil samples were weighed immediately, oven-dried at 105ºC and weighed again until a constant weight was obtained. The gravimetric water content (θg) was determined using Equation 3.1, while soil bulk density was calculated using Equation 3.2 (Chapter 3). Descriptive statistics comprising of range, mean and coefficient of variation were generated on the measured bulk density and gravimetric water content. The relationship between bulk density and gravimetric water content helps to quantify soil water content on volumetric basis (θv, $m^3\ m^{-3}$) which is regarded as the standard for soil water content.

Note that the DFM probe output is the scaled frequency (*SF*), based on the manufacturer's equation. Readings from the probes were sorted and corrected for temperature as described by Zerizghy (2013). Hourly readings, from the start until the end of sampling, were taken as repeated DFM readings for each soil condition.

All data sets recorded during this procedure was divided into *K*-fold, one data set was used for calibration and the other for validation. Recorded θ_V from 0 to 0.3 m and *SF* from sensors at 0.3 m were related to the EM measuring depth of 0.38 m. Recorded θ_V at the approximate depth of 0.4 m to 0.9 m and *SF* from sensors at 0.6 m and 0.8 m were related to the EM measuring depth of 0.75 m.

In order to accomplish the specific objectives of this chapter, three relationships were considered, i.e. relationship between (i) DFM *SF* and θ_V, (ii) and EC_a and θ_V for comparison, and (iii) EC_a and estimated water content from DFM *SF* (θ_{DFM}) (i). Calibrations were first performed for each depth per plot and on each of the four soil forms. For model evaluation, the coefficient of determination (r^2) was obtained to show the strength of the relationships between *SF* and θ_V, EC_a and θ_V, as well as EC_a and θ_{DFM}. Also, *p*-values were derived from regression statistics using Microsoft Excel to show the significance of the model functions.

5.2.4 Model validation

Models produced from the above mentioned relationships were validated using separate data sets as explained earlier. The degree to which the predicted soil water (*Pr*) values approach observed soil water explains the accuracy of the calibrated models. Due to non-normal distribution of field data, accuracy and model performance was tested using non-parametric statistical indices that use the median of the predicted and observed soil water differences. The relative median absolute error (RMdAE) recommended by Armstrong and Collopy (1992), was used to check for model accuracy (a model performed well if lower values were obtained). Relative modelling efficiency (REF) was used to compare the predicted values to the median of the observed values. Also, Spearman's rank correlation (r_S) (Equation 2.5), proposed by

Vachaud *et al.* (1985), was conducted to show the strength of the relationship between predicted and observed values. The closer r_S is to '1', the more stable the spatial pattern of soil water content, and if r_S = 1, there is no change in the rank of the observed values. The significance of the correlation was tested using the *p*-values that explain the equality of the estimated and observed values.

$$\mathrm{RMdAE} = \mathrm{median}_{\mathrm{i}=1,\ldots\mathrm{n}}|\mathrm{Obs}_\mathrm{i} - \mathrm{Pr}_\mathrm{i}|\frac{100}{\bar{\mathrm{O}}\mathrm{bs}} \qquad 5.1$$

$$\mathrm{REF} = \mathrm{median}_{\mathrm{i}=1,\ldots\mathrm{n}}\left(\frac{\mathrm{median}_{\mathrm{i}=1,\ldots\mathrm{n}}\,|\mathrm{Obs}_\mathrm{i} - \bar{\mathrm{O}}\mathrm{bs}| - \mathrm{median}_{\mathrm{i}=1,\ldots\mathrm{n}}\,|\mathrm{Obs}_\mathrm{i} - \mathrm{Pr}_\mathrm{i}|}{\mathrm{median}_{\mathrm{i}=1,\ldots\mathrm{n}}\,|\mathrm{Obs}_\mathrm{i} - \bar{\mathrm{O}}\mathrm{bs}|}\right) \qquad 5.2$$

$$\mathrm{r_s} = 1 - \frac{6\ \sum_{\mathrm{i}=1,\ldots\mathrm{n}}^{\mathrm{n}}(\mathrm{Obs}_\mathrm{i} - \mathrm{Pr}_\mathrm{i})^2}{\mathrm{n}(\mathrm{n}^2-1)}\ ; \qquad 5.3$$

Where, n = Number of observations
i = Observation location
Obs = Observed measure
$\bar{\mathrm{O}}\mathrm{bs}$ = Mean of the observed measure
$\mathrm{Pr_i}$ = Predicted values

To obtain a 1:1 slope and a "0" y-intercept, least square regression was performed to fit the predicted soil water values to a linear model that describes the observed water content. Data points that fall below the 1:1 line indicate underestimation of water content, whilst those that fall above the line indicate overestimation. Finally, a general calibration model was produced from the relationship between EC_a and θ_{DFM} that can be used to spatially characterize soil water content.

5.3 Results

5.3.1 Relationship between bulk density and gravimetric water content

As expected, dry soil bulk density decreased as more water was applied to the plots (Figure 5.3) because of the nature of various soil forms at this site. A good relationship between bulk density and gravimetric water content with r^2 of 0.86, 0.85 and 0.86, was observed at the A-, B- and C-horizons, respectively. When the plots were individually examined, the relationship was much stronger, with r^2 ranging between 0.90 and 0.97 (Appendix 5.1). A strong relationship between bulk density and gravimetric water content ensures that the volumetric

water content generated from these two measurements is accurate. The range, mean and coefficient of variation (CV) of the recorded bulk densities and soil water content from samples collected at the three horizons for each plot can be viewed in the Appendix 5 2.

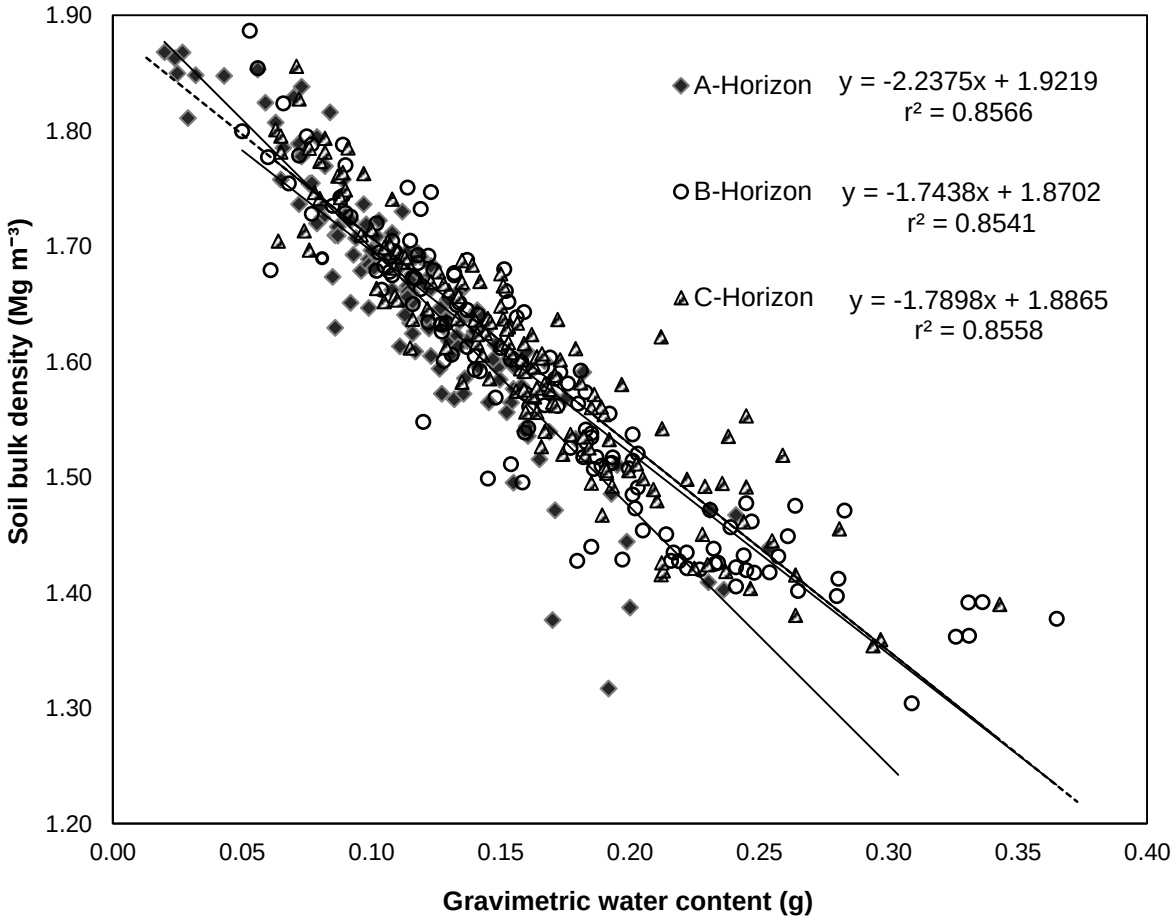

Figure 5.3 Relationship between soil bulk density and gravimetric soil water content for all plots.

The change in bulk density with change in water content was taken into account during field calibration of the instruments. Due to the stronger relationship for individual plots, *in situ* calibrations of DFM probes and EM38-MK2 were first performed for individual plots, then for each soil form and finally a general equation was developed for all 12 plots, to characterize soil water content.

5.3.2 Field calibration of DFM probes (*SF* vs θ_V)

The *SF* measured with DFM capacitance probes were successfully calibrated against θ_V (using the first dataset as explained in Section 5.2.3), under dry and wet soil conditions, at 0.38 m and 0.75 m soil depths. Table 5.1 presents the model equations developed from the relationship between *SF* and θ_V, at both soil depths, on all 12 plots. In all occasions, 2-degree polynomial,

power and exponential model functions were tested before selecting the model that best described the relationship at each depth for each individual plot.

Table 5.1 Model equations describing the relationship between scaled frequency (*SF*) and volumetric water content (θ_V), n=12 per plot

Depth (m)	Plot No.	Model Name	*SF* vs θ_V		
			Model Function	r^2	*p*-value
0.38	1	Poly.	$\theta_{DFM} = -0.0001(SF)^2 + 0.0149(SF) - 0.1599$	0.950	0.002
	2	Power	$\theta_{DFM} = 0.0004(SF)^{1.7462}$	0.940	<0.001
	3	Power	$\theta_{DFM} = 0.0013(SF)^{1.3448}$	0.980	0.003
	4	Poly.	$\theta_{DFM} = -0.0003(SF)^2 + 0.0322(SF) - 0.6037$	0.994	<.0001
	5	Poly.	$\theta_{DFM} = 8x10^{-05}(SF)^2 - 0.0022(SF) + 0.1803$	0.900	<0.001
	6	Poly.	$\theta_{DFM} = 0.0003(SF)^2 - 0.018(SF) + 0.392$	0.930	<0.001
	7	Poly.	$\theta_{DFM} = -0.0004(SF)^2 + 0.041(SF) - 0.7546$	0.960	<0.001
	8	Expon.	$\theta_{DFM} = 0.0775e^{0.0349(SF)}$	0.900	<0.001
	9	Poly.	$\theta_{DFM} = 0.0001(SF)^2 - 0.0052(SF) + 0.179$	0.841	0.002
	10	Poly.	$\theta_{DFM} = -0.0032(SF)^2 + 0.2707(SF) - 5.4045$	0.970	<0.001
	11	Expon.	$\theta_{DFM} = 0.0538e^{0.0331(SF)}$	0.930	<0.001
	12	Expon.	$\theta_{DFM} = 0.0019e^{0.1178(SF)}$	0.980	<0.001
0.75	1	Poly.	$\theta_{DFM} = 0.0002(SF)^2 - 0.0203(SF) + 0.7349$	0.883	<0.001
	2	Expon.	$\theta_{DFM} = 0.0268e^{0.0347(SF)}$	0.960	<0.001
	3	Poly.	$\theta_{DFM} = 3x10^{-05}(SF)^2 + 0.0043(SF) - 0.1054$	0.973	<0.001
	4	Poly.	$\theta_{DFM} = -8x10^{-05}(SF)^2 + 0.0122(SF) - 0.169$	0.970	<0.001
	5	Power	$\theta_{DFM} = 0.0003(SF)^{1.7236}$	0.960	<0.001
	6	Poly.	$\theta_{DFM} = 0.0005(SF)^2 - 0.0599(SF) + 1.8379$	0.842	<.0001
	7	Poly.	$\theta_{DFM} = -6x10^{-05}(SF)^2 + 0.0132(SF) - 0.2746$	0.934	<0.001
	8	Poly.	$\theta_{DFM} = 0.0002(SF)^2 - 0.0169(SF) + 0.5258$	0.980	<0.001
	9	Poly.	$\theta_{DFM} = -5x10^{-05}(SF)^2 + 0.0099(SF) - 0.1353$	0.960	<0.001
	10	Expon.	$\theta_{DFM} = 0.0978e^{0.0169(SF)}$	0.923	<0.001
	11	Poly.	$\theta_{DFM} = 5x10^{-05}(SF)^2 + 0.003(SF) - 0.0918$	0.954	<0.001
	12	Expon.	$\theta_{DFM} = 0.0111e^{0.056(SF)}$	0.920	<0.001

For all 12 plots, the *SF* related very well to θv with a linear function, but the relation was stronger when non-linear model functions were applied ($r^2 > 0.84$). The *p*-values indicated that all the model functions that described the relationship between *SF* and θ_V, were highly significant. Calibration performed for each soil form produced a good relationship with r^2 between 0.57 and 0.90 (Appendix 5.7), but this was not as strong as individual plot calibration in Table 5.1. The lower precision (r^2 values) for some of the soil forms (particularly Swartland) could probably be attributed to the variation in DFM readings due to heterogeneity of this soil, which introduced scatter to the relationship between *SF* readings and θv. Hence, calibration

performed for individual plots was used to predict water content (θ_{DFM}) for the calibration of EM38-MK2. All DFM calibration result tables and graphs for individual soil forms (Sepane, Swartland, Tukulu and Bloemdal) can be viewed from Appendix 5.7 to 5.10.

5.3.3 Validation of DFM-based models

Validation of DFM calibration models from Table 5.1, showed that the models could accurately estimate actual volumetric water content. Statistical indices (averages over the 12 plots) evaluating the performance of these models, explaining its efficiency and accuracy are presented in Figure 5.4. A comprehensive table of the statistics on individual performance of each model can be viewed in Appendix 5.3 and the regression trends in Appendix 5.4. These models were efficient enough to predict water content (REF > 0.30, except for plot 1 at 0.75 m) with high accuracy (RMdAE < 12 m^3 m^{-3}). There was strong correlation (r_S) between the predicted and observed water contents and this was significant for all plots.

Figure 5.4a and b also show the line of best fit between observed and predicted soil water values, basically lying on the 1:1 line for both soil depths. It can also be observed that the predicted water content was mostly within 20% deviation from the 1:1 line. On average, calibrated DFM probes spatially explained up to 96% of the observed soil water content at both soil depths (Figure 5.4). With such high values, DFM probes could provide reliable calibration of the EM2-MK2.

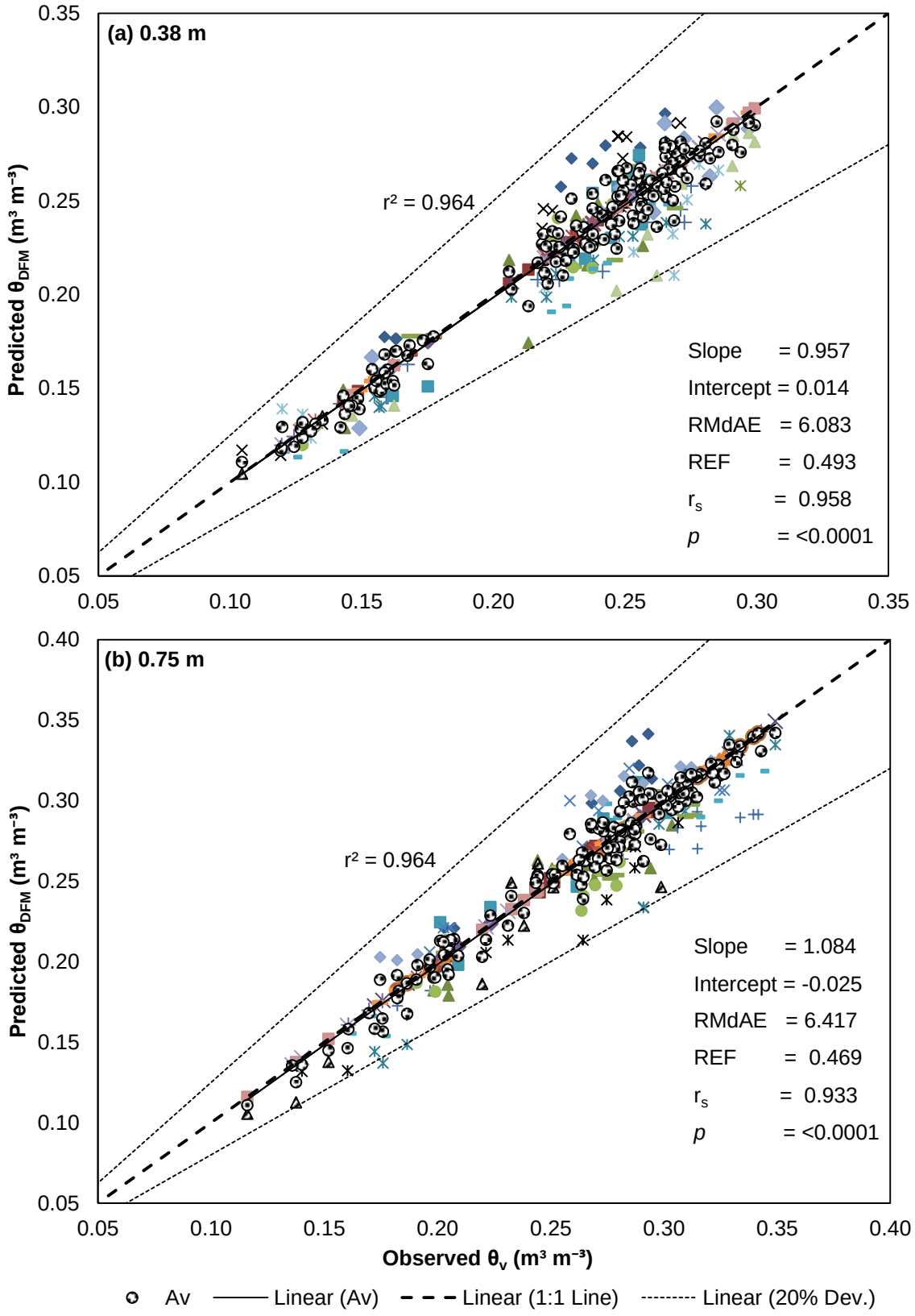

Figure 5.4 Validation results showing comparison of predicted (θ_{DFM}) and observed water content (θ_V) at (a) 0.38 m depth and (b) 0.75 m depth (RMdAE = relative median absolute error; REF = relative modelling efficiency; and r_s = Spearman's rank correlation).

5.3.4 Field calibration of EM38-MK2 with DFM probes (EC_a vs θ_{DFM})

The EC_a measured *in situ* with the EM38-MK2 under dry and wet soil conditions, was finally calibrated with soil water estimated from the calibrated DFM probes (θ_{DFM}). Field measured EC_a values at each depth and for every plot were plotted against corresponding estimated water content (θ_{DFM}). Both 2-degree polynomial and power model functions were tested in each occasion before selecting the model that best described the relationship between EC_a and θ_{DFM}. The graphs of the general equations for this relationship (data pooled over the 12 plots) at 0.38 m and 0.75 m depths, are presented in Figure 5.5. Model equations of this relationship for individual plots, at both soil depths, can be viewed in Appendix 5.5, while equations developed for each soil form are given in Appendix 5.11.

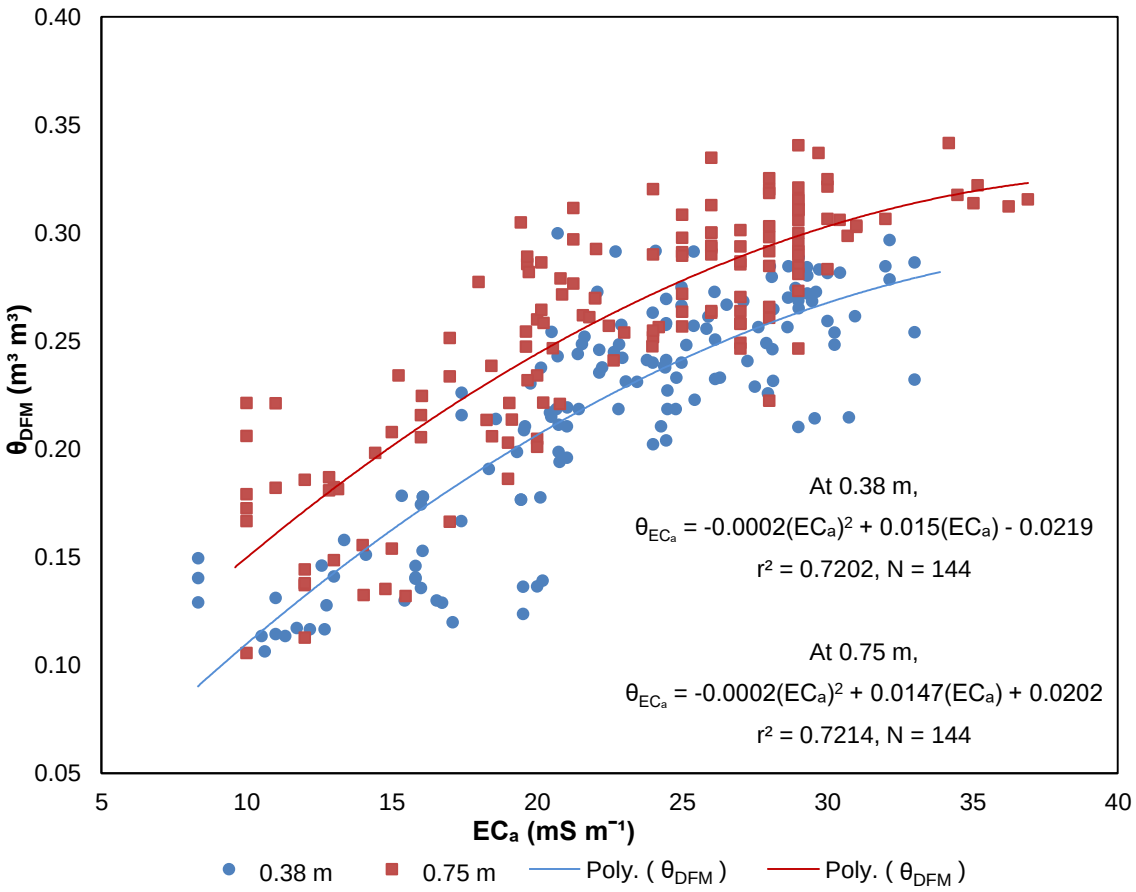

Figure 5.5 General calibration models developed from the relationship between field-measured EC_a and DFM probe predicted water content (θ_{DFM}) over all 12 plots, at 0.38 m and 0.75 m depths.

The general calibration models for both soil depths show the best relationship between EC_a and θ_{DFM} using a 2-degree polynomial function with an r^2 of 0.72 for both 0.38 m and 0.75 m depth. Calibration for individual plots produced a stronger relationship between EC_a and θ_{DFM}. The r^2 values were within the range of 0.81 and 0.97 for both soil depths (Appendix 5.5). The

p-values indicated that all these model functions that described the relationship between EC_a and θ_{DFM}, were statistically significant.

It is important to note at this point that the temperature effect on EC_a, measured with the EM38-MK2, was clearly visible in this study. In agreement with Jury *et al*. (1991), it was observed that EC_a variation due to temperature was greater at shallow depths. In the current study, temperature introduced an error of 0.22 to the model performance at 0.38 m depth, while an error of 0.08 was seen at 0.75 m depth. Temperature correction strengthened the relationship between EC_a and θ_V. On occasions where r^2 was 0.65 and 0.67, temperature corrected EC_a increased r^2 to 0.90 and 0.95, at 0.38 and 0.75 m depths respectively (data not shown). This effect was expected since data collection was mostly done on sunny days.

5.3.5 Validation of EC_a-based models

The calibration models in Section 5.3.4 were validated with the second data set and water content based on EC_a field measurements was accurately estimated. Statistical indices evaluating the general model efficiency and accuracy at both soil depths are presented in Figures 5.6a and b. With this general model for both depths, water content was slightly overestimated under dryer soil conditions, while there was a slight underestimation under very wet soil conditions. Overall, the predicted soil water content was mostly within 20% deviation from the 1:1 regression line. The models developed for 0.38 m and 0.75 m depths were both accurate as indicated by the relatively low RMdAE. Correlation (r_S) between the predicted and observed soil water content was strong and significant.

In comparison, the models for individual plots (Figure 5.7a and b) estimated water content more accurately than the general models, with RMdAE below 7 at both soil depths. The individual models were very efficient with REF of 0.63 and 0.47 on average, at 0.38 m and 0.75 m depths, respectively. A complete table of the statistical indices on individual plot model performance can be viewed from the Appendix 5.6, while for the soil forms are in Appendix 5.13 and 5.14. The correlation between predicted θ_{ECa} and observed θ_V for individual plots was stronger (at 0.38 m depth r_s increased from 0.74 to 0.81) and produced a better fit to the 1:1 regression line (Figure 5.7a), with less improvement at 0.75 depth (Figure 5.7b).

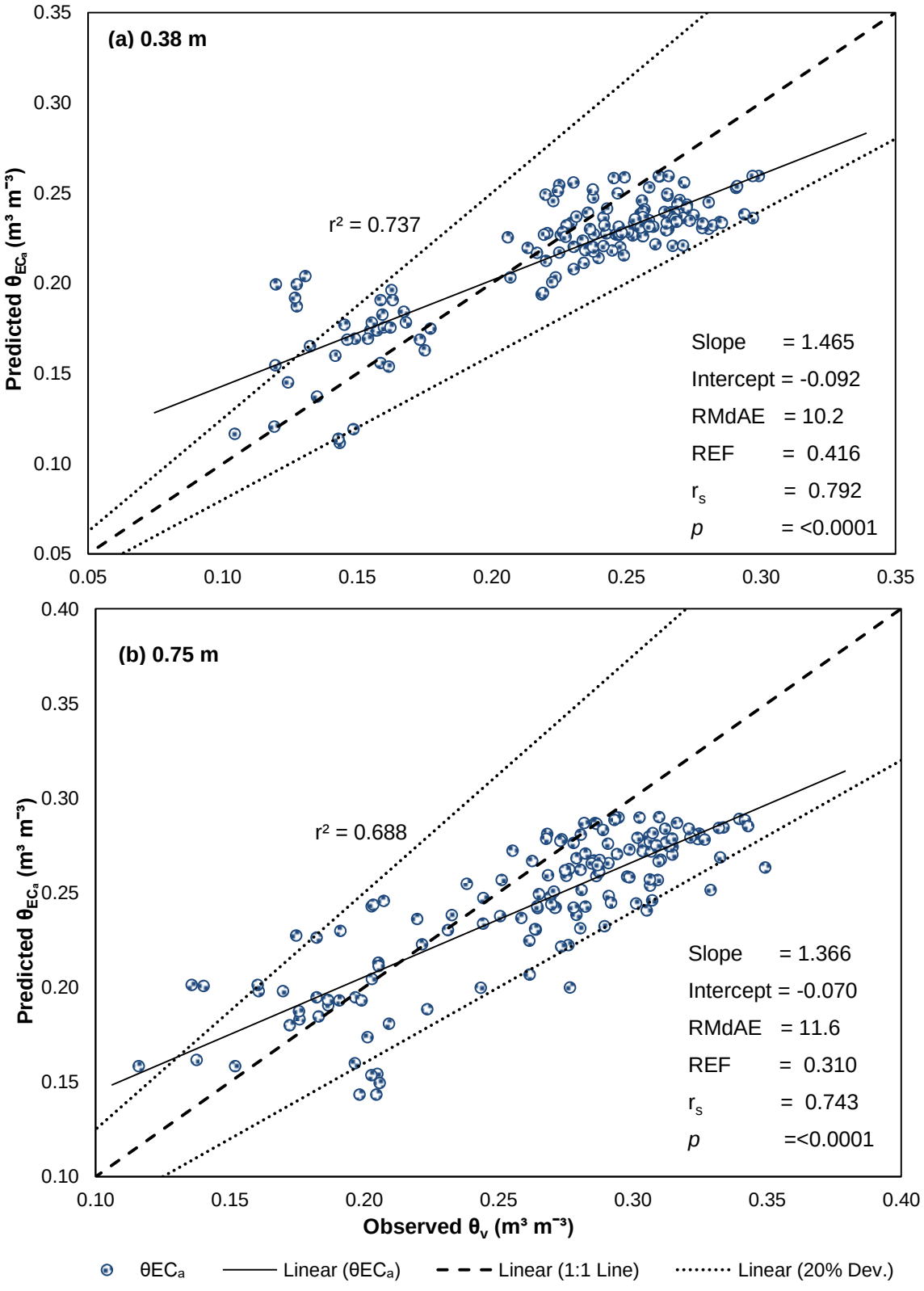

Figure 5.6 Validation results for the general model showing comparison of predicted (θ_{ECa}) and observed water content (θ_V) at (a) 0.38 m depth and (b) 0.75 m depth (RMdAE = relative median absolute error; REF = relative modelling efficiency; and r_s = Spearman's rank correlation).

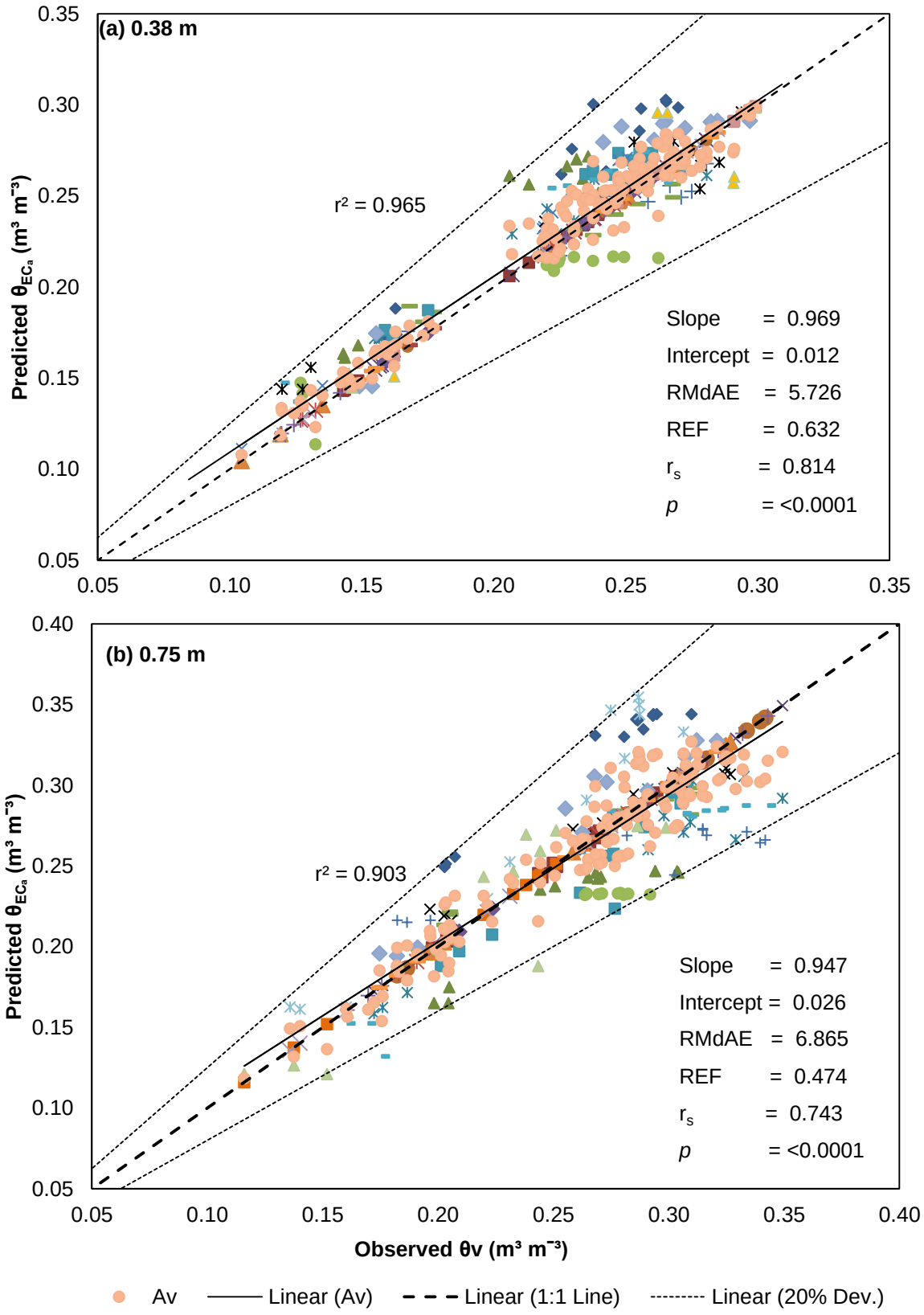

Figure 5.7 Validation results for individual plot models showing comparison of predicted (θ_{ECa}) and observed water content (θ_V) at (a) 0.38 m and (b) 0.75 m depths (RMdAE = relative median absolute error; REF = relative modelling efficiency; and r_s = Spearman's rank correlation). Detailed statistical in Appendix 5.6.

Several studies related EC_a measured with the EM38 to soil water content measured with various soil water instruments, including TDR (Kachanoski *et al*., 1988), NWM (Kachanoski *et al.*, 1990; Reedy & Scanlon, 2003; Stanley *et al*., 2014) and ERT (Lavoué *et al.*, 2010). Among these, only Reedy & Scanlon (2003) presented mathematical models to predict soil water content from measured EC_a values. On a 2 m deep engineered soil cover of sandy clay loam, Reedy & Scanlon (2003) successfully predicted soil water content up to 1.5 m depth at point locations (R^2 = 0.80), when calibrating the EM38 using NWM readings. With the general models in the current study EC_a values could spatially predict 74% and 69% of the volumetric soil water content at 0.38 m and 0.75 m, respectively (Figure 5.6a and b). This is in line with results of Reedy & Scanlon (2003), especially considering the fact that, soils in this study was substantially more heterogeneous than the engineered soil cover used in the other study.

As was expected, individual plot models predicted soil water content much better than the general models. The estimated water content explained on average 97% and 90% of variation in soil water content, at 0.38 m and 0.75 m, respectively (Figure 5.7a and b). However, from a practical point of view, spatial characterization of soil water content at field scale with the EM38-MK2 will require a general calibration model incorporating all soil forms present in the survey area. From the validation results it is clear that the general models developed in this study were sufficiently accurate for soil water estimation. Therefore, the general model in Figure 5.5 can be used to spatially estimate water content over the entire field scale. This calibration models, could also be periodically updated by directly relating spatial or temporal field measured values from EM38-MK2 and DFM probes.

5.4 Conclusion

This study successfully estimated soil water content from EC_a measured with the EM38-MK2, after site specific calibration with DFM capacitance probes.

The general models show promise for use in real-time, non-invasive soil water content estimation using apparent electrical conductivity. Variations of soil properties in this study affected the performance of the general models. The individual plot calibration models were more accurate but for practical application at field scales, the general model is required. Although the precision is less, it was able to produce water content to an acceptable degree of accuracy. Therefore, on this heterogeneous soil comprising of four different soil forms, it was possible to generate EC_a-based model that can be used for future characterization of soil water variation over the field scale.

CHAPTER 6. GENERAL CONCLUSIONS AND RECOMMENDATIONS FOR FUTURE RESEARCH

6.1 Conclusions

Maintaining a balance between water use and food production has received great attention in precision agriculture, with considerable focus on more accurate methods to monitor water distribution at large spatial and temporal scales over depths beneficial to agriculture. This has resulted in a wide interest in EMI instruments. Of the EMI instruments that are commercially available, the EM38 devices have been most widely used for various applications in agriculture. The instrument and its newer version "EM38-MK2" are non-invasive, relatively easy to use and have the ability to survey on large field scale in a small time frame. These EM-devices can provide information on soil water distribution through its measured apparent electrical conductivity (EC_a), after calibration on a specific soil using the standard volumetric method. This is both time consuming and extremely laborious considering the focus of precision agriculture. Therefore, various studies have adopted a two-step process to relate EC_a measured with EM-devices to water content using other indirect soil water measuring instruments. These studies included the use of time domain reflectometry (TDR) and neutron water meter (NWM) by first calibrating these instruments and using the estimated water content to calibrate the EM38 device. The present study wanted to evaluate the use of DFM capacitance probes in calibrating the EM38-MK2 for soil water estimation.

It should be noted that, the two selected sites for this study were non-saline soils. The calculated EC_a were much in line with the clay and soil water values, as the two variables increase or decrease. Therefore, it was expected that the EM38-MK2 measured EC_a will relate mostly with the soil water content during calibration without any influence from salinity. However, the clay content will enhance the ability of the soil to hold water during soil wetting.

A major drawback in the application of EM-devices in agricultural is that, it is very sensitive to metallic objects, and may therefore be affected by any soil water instruments used to calibrate it. Hence, it was first examined whether the proposed use of capacitance probes would interfere with EC_a measurements, since it is necessary to measure EC_a very close to the soil water measuring point for accurate calibration. In addition, possible interference from steel NWM access tubes and trenches that might be present on the experimental site, was also investigated. An experiment was designed placing these interferences at the center of four transects, one at a time, while operating the EM38-MK2 from 10 m away, then moving over each interference and continuing a further 10 m away. The first intension was to determine how

far away the EM38-MK2 can be operated from these interferences in the field before any influence was detected. Secondly, if there was an effect, would EC_a still be measured accurately without first re-zeroing the EM-device. The experiment was conducted on Bainsvlei soils of Kenilworth Experimental Farm that are homogenous over the area, allowing effects of the interferences to be clearly visible.

It was suspected that trenches could cut off current flow from the EM38-MK2 since most of the magnetic field would be circulating in the air, however, this study found no interference from trenches on EC_a measured in both vertical and horizontal dipole modes. DFM capacitance probes and steel access tubes interfered with EC_a readings when the EM38-MK2 was moved closer than 1 m. The interference from the steel tubes was much more pronounced than that from the DFM probes, and extremely variable, reading either negative or positive EC_a values. This was probably due to the fact that the steel access tubes contain considerably more metal than DFM probes.

Without zeroing the EM-device, there was either inconsistency or reduction in EC_a readings after encountering the metal-containing interferences. Inconsistent EC_a readings were only observed in the vertical mode for DFM probes. For DFM probes in the horizontal mode and steel tubes in both modes, there was a significant decrease in mean EC_a readings after encountering these interferences. Although these effects were statistically significant, the magnitude thereof was so small that it is of little practical importance.

Therefore, this study concludes that the EM38-MK2 should not be operated closer than 1 m to these soil water measuring instruments. Furthermore, if the operator accidently used the EM-device too close to these instruments, it is would probably not be necessary to go back to the initial calibration point to re-zero the instrument. It should be sufficient keeping to the recommendation of re-zeroing the instrument hourly during a field survey.

In the second part of the study the EM38-MK2 was calibrated using soil water estimated from DFM capacitance probes. The experiment was carried out on heterogeneous soils of Paradys Experimental Farm. Calibration was performed on 12 controlled plots under three varying soil water conditions, i.e. dry, wet and very wet soil. All data required for calibration was collected from these plots and EC_a readings were corrected for temperature before data use.

The DFM probes were successfully calibrated with θ_V and validation of the models indicated high precision in estimating soil water content. Results suggested single plot calibration of the probes for better accuracy on such a heterogeneous soil. The resulting DFM-based water content was used to calibrate EC_a measured with the EM38-MK2, to develop general calibration models for 0.38 m and 0.75 m soil depths. The estimated water content from the

DFM probes related well to the EC_a measured with the EM38-MK2 and was significant both for single plot and the generalized field models. The models produced from this second relationship were validated, and despite the heterogeneity of this site, the results from calibrating EM38-MK2 with DFM probes were comparable to studies that used other instruments to calibrate EM38 device.

The last objective was to apply general calibration models that were developed to characterize soil water content over the field scale. DFM-based and EC_a-based general models were spatially applied using a different data set. Notwithstanding the soil heterogeneity, EC_a-based general models were able to show the spatial and temporal variation in soil water over the experimental area. The spatial distribution of EC_a and soil water content were temporally stable however, variation in EC_a was able to reflect the absolute differences in water content. The spatio-temporal soil water maps produced an accurate representation of topographical effects on soil water distribution over the area.

Therefore, the main finding of this study was that the estimated soil water content from calibrated DFM capacitance probes can be used, in a two-step process, to calibrate apparent electrical conductivity (EC_a) readings measured with the EM38-MK2 *in situ* for soil water characterization at field scale. With the EC_a-based model already developed for this specific site, one only need to spatially measure EC_a to update soil water information over time.

6.2 Recommendations for future research

This study was purposely conducted on relatively large study area with four different soil types that are extremely non-uniform both spatially and over depth, to quantify soil water distribution using EC_a-based models calibrated with the DFM probes. While the result shows successful implementation of this proposed method, an extension of this study to different areas with different ranges of agricultural soil types are required to generalize the results presented.

- In this study, each DFM probe was individually calibrated due to soil differences over the area. If the same study should be conducted on a homogeneous soil, a general model for all DFM probe readings may be generated to save time and costs.
- Calibration of DFM probes was conducted on controlled plots before models were developed. If calibration is to be done under uncontrolled conditions, results may not be similar to this study.
- Should calibration be done on controlled plots on heterogeneous clay soils, the researcher should first make a monolith, wrap the walls with plastic sheeting and refill the soil. This is to avoid lateral flow of water, thus ensuring vertical infiltration.

- The study focused on spatial and temporal characterization of soil water content with the two selected depths modelled separately. The proposed calibration method can also be tested in studies focusing on depth of water variation.
- The general models produced in this study should be apply to spatially map soil water content on a larger field scale

References

ATKINS, R.T., PANGBURN, T., BATES, R.E. & BROCKETT, B.E., 1998. Soil moisture determinations using capacitance probe methodology. U.S. Army Cold Regions Research and Engineering Laboratory, Spacial Report 98-2, Hanover, New Hamphshire 03755 - 1290.

AUDUN, K., HUGH, R., SIGRUN, H.K. & LIVE, S.V., 2003. Relations between a commercial soil survey map based on soil apperent electrical conductivity and measured soil properties on a Morainic soil in Southeast Norway. In: Alllred, B.J., Daniels, J.J., Ehsani, M.R., (eds), Handbook of Agricultural Geophysics. Soils, Plant and Enviroment, CRC Press, pp. 225 - 231.

AUERSWALD, K., SIMON, S. & STANJEK, H., 2001. Influence of soil properties on electrical conductivity under humid water regimes. *Soil Sci.* 166, 382 - 390.

BANTON, O., SEGUIN, M.K. & CIMON, M.A., 1997. Mapping field-scale physical properties of soil with electrical resistivity. *Soil Sci. Soc. Am. J.* 61, 1010 - 1017.

BARRY, J.A., DOUGLAS GROOM, M., REZA, E. & JEFFREY, J.D., 2008. Resistivity methods: In Barry, J.A., Jeffery, J.D., Ehsani, M.R. (Eds). Handbook of Agricultural Geophysics, Boca Raton, FL: CRC Press, pp. 86 - 91.

BATTE, M., 2000. Factors influencing the profitability of precision farming systems. *J. Soil Water Conserv.* 55, 12 - 18.

BELL, K., BLANCHARD, B.J., SCHMUGGE, T. & WITCZAK, M., 1980. Analysis of surface moisture variations within large-field sites. *Water Resour. Res.* 16, 796 - 810.

BESSON, A., COUSIN, I., DORIGNY, A., DABAS, M. & KING, D., 2008. The Temperature Correction for the electrical resistivity measurements in undisturbed soil samples: Analysis of the existing conversion models and proposal of a new model. *Soil Sci.* 173, 707 - 720.

BEVAN, B.W., 1983. Electromagnetics for mapping buried earth features. *J. Field Archaeo.* 10, 47 - 54.

BEVAN, B.W., 1998. Geophysical exploration for archaelogy: an introduction to geophysical exploration. Midwest Archaelogical Center, National Park Service, US Department of interior, Report No. 1:13.

BLAKESTON, A., 2015. Broken column and bar charts. http://plus.google.com/104553959934905819059?rel=author

BOTHMA, C.B., 2009. In-field runoff and soil water storage on duplex soils at Paradys Experimental Farm. MSc. thesis, University of the Free State, South Africa.

BOWLING, S.D., SCHULTE, D.D. & WOLDT, W.E., 1997. A geophysical and geostatistical methodology for evaluating potential subsurface contamination from feedlot runoff retention ponds. ASAE Paper No 972087, ASAE Winter Meeting, Chicago, IL, ASAE, St Joseph, MI.

BREVIK, E.C. & FENTON, T.E., 2002. The relative influence of soil water content, clay, temperature and carbonate minerals on soil electrical conductivity readings taking with an EM38 along a mollisol catena in central Iowa. *Soil Surv. Horiz*. 49, 9 - 13.

BREVIK, E.C., FENTON, T.E. & HORTON, R., 2004. Effect of daily soil temperature fluctuations on soil electrical conductivity as measured with the Geonics, EM38. *Precis. Agric*. 5, 145 - 152.

BREVIK, E.C., FENTON, T.E. & JAYNES, D., 2003. Evaluation of the accuracy of a central Iowa soil survey and implications for precision soil management. *Precis. Agric*. 4, 323 - 334.

BREVIK, E.C., FENTON, T.E. & JAYNES, D.B., 2012. Use of electrical conductivity to investigate soil homogeneity in Story County, Iowa, USA. Soil Surv. Horiz. 53, 50 - 54.

BREVIK, E.C., FENTON, T.E. & LAZARI, A., 2006. Soil electrical conductivity as a function of soil water content and implications for soil mapping. *Precis. Agric.* 7, 393 - 404.

BROCCA, L., MELONE, F. & MORAMARCO, R., 2009. Soil moisture temporal stability over experimental areas in central Italy. *Geoderma* 148, 364-374.

BROCCA, L., MELONE, F., MORAMARCO, T. & MORBIDELLI, R., 2010. Spatial- temporal variability of soil moisture and its estimation across scales. *Water Resour. Res*. 46, p. W02516.

BROCCA, L., TULLO, T., MELONE, F., MORAMARCO, T. & MORBIDELLI, R., 2012. Catchment scale soil moisture spatial-temporal variability. *J. Hydrol.* 422, 63 - 75.

BRUNE, D.E. & DOOLITTLE, J., 1990. Locating lagoon seepage with radar and electromagnetic survey. *Environ. Geol. Water Sci.* 16, 195 - 207.

BRUS, D.J., KNOTTERS, M., VAN DOOREMOLEN,W.A., VAN KERNEBEEK, P. & VAN SEETERS, R.J.M., 1992. The use of electromagnetic measurements of apparent soil electrical conductivity to predict the boulder clay depth. *Geoderma* 55, 79 - 93.

CA, 2007. A comprehensive assessment of water management in agriculture. In: M. David, (Ed.) Water for food, Water for life. London and International Water Management, Colombo Institute: *Earthscan*.

CAMPBELL, G.S., 1985. Soil physics with besic. *Elsevier*, New York.

CHIMUNGU, J.G., 2009. Comparison of feild and laboratory measured hydraulic properties of selected diagnostic soil horizons. MSc. thesis, University of the Free State, South Africa.

CHRISTENSEN, R., JOHNSON, W. & PEARSON, L.M. 1992. Prediction diagnostics for spatial linear models. Biometrika, 79, 583 – 591.

CLAY, R.B., 2005. Conductivity (EM) Survey: A Survival Manual. Cultural Resource Analysts, Inc. auvergne@earthlink.net; rbclay@CRAI-KY.com

CORWIN, D.L., KAFFKA, S.R., HOPMANS, J.W., MORI, Y., Van GROENIGEN, J.W., Van KESSEL, C. LESCH, S.M. & OSTER, J.D., 2003a. Assessment and field-scale mapping of soil quality properties of a saline-sodic soil. *Geoderma* 114, 231 - 259.

CORWIN, D.L. & LESCH, S.M., 2003. Application of soil electrical conductivity to precision agriculture: theory, principles, and guidelines. *Agron. J*. 95, 455 – 471.

CORWIN, D.L., LESCH, S.M., SHOUSE, P.J., SOPPE, R. & AYARS, J.E., 2003b. Soil Management: Identifying Soil Properties that Influence Cotton Yield Using Soil Sampling Directed by Apparent Soil Electrical Conductivity. *Agron. J.* 95, 352 – 364

CORWIN, D.L., 2008. Past, present and future trends of soil electrical Conductivity measurement using Geophysical Methods. In: BARRY, A., JEFFREY, J. & REZA, M.E., (Ed.) Handbook of Agricultural Geophysics. U S: Taylor and Francis Group, CRC Press, pp. 17 - 44.

CORWIN, D.L. & LESCH, S.M., 2005a. Apparent soil electrical conductivity measurements in agriculture. *Comput. Electron. Agric*. 46, 11 - 43.

CORWIN, D.L. & LESCH, S.M., 2005b. characterizing soil spatial variability with apparent soil electrical conductivity: Survey protocol 1. *Comput. Electron. Agric*. 46, 103-133.

CORWIN, D.L. & LESCH, S.M., 2010. Delineating site-specific management units with proximal sensors. In: Geostatistical applications for precision agriculture. USA: Springer Science+Business Media, pp. 139 - 165.

CORWIN, D.L., LESCH, S.M. & FARAHANI, H.J., 2008. Theoritical insight on the measurment of soil electrical conductivity. In: Handbook of Agricultural Geophysics. USA: Taylor and Francis Group, CRC Press, pp. 59 - 82.

CORWIN, D.L. & Lesch, S.M., 2013. Protocols and guidelines for field-scale measurement of soil salinity distribution with EC_a-directed soil sampling. *J. Environ. Eng. Geophys*. (JEEG) 18, 1 - 25.

COX, D.R. & HINKLEY, D.V., 1974. Theoritical statistics. Chapman and Hall 1st (Edn)

COSH, M.H., JACKSON, T.J., BINDLISH, R. & PRUEGER, J., 2004. Watershed scale temporal persistence of soil moisture and its role in validating satellite estimates. *Rem. Sens. Environ*. 92, 427 - 435.

DABAS, M., GEBBERS, R., LUCK, E. & DOMSCH, H., 2003. A comparison of different sensors for soil mapping: the ATB case study. http://precision.agri.umn.edu/conference/edits/121Dabas%5B1%5D_edt.doc

DALGAARD, M., HAVE, H. & NEHMDAHL, H., 2001. Soil clay mapping by measurement of electromagnetic conductivity. In: Proceedings of 3rd European conference on precision agriculture. Grenier, G. & Blackmore, S., (Eds) Agro Montpellier, France. pp. 367 - 372.

DALLIGER, T.E., 2006. Geometric and temperature effects on Time-domain reflectometry measurements in soils. MSc. Thesis, Purdue University, West Lafayette, IN.

DANIELS, J.J., VENDI, M., ESHANI, M.R. & ALLRED, B.J., 2008. Electromagnetic Induction Methods. In: Allred B.J., Daniels, J.J. & Eshani, M.R., (Eds) Handbook of Agricultural Geophysics. pp. 109 - 128.

DE FRAITURE, C., SMAKHTIN, V., BOSSIO, D., McCORNICK, P., HOANH, C., NOBLE, A., MOLDEN, D., GICHUKI, F., GIORDANO, M., FINLAYSON, M. & TURRAL, H., 2007. Facing climate change by securing water for food, livelihood and ecosystems. SAT e-Journal.icrisat.org, 4.

DOMSCH, H. & GIEBEL, A., 2004. Estimation of soil textural features from soil electrical conductivity recorded using the EM38. *Preci. Agric*. 5, 389 - 409.

DOOLITTLE, J.A. & BREVIK, E.C., 2014. The use of electromagnetic techniques in soils studies. *Geoderma* 223 - 225, 33 - 45.

DOOLITTLE, J.A., SUDDUTH, K.A., KITCHEN, N.R. & INDORANTE, S.J., 1994. Estimating depths to clay pans using electromagnetic induction methods. *J. Soil Water Conserv*. 49, 572 - 575.

DOOLITTLE, J.A., WINDHORN, R.D., WITHERS, D.L. & MCLEESE, R.L., 2009. High-intensity soil mapping with the aid of EMI in northern Illinois. *Soil Surv. Horiz*. 50, 68 - 74.

DOOLITTLE, J.A., WINDHORN, R.D., WITHERS, D.L., ZWICKER, S.E., HEISNER, F.E. & MCLEESE, B.L., 2008. Soil scientists revisit a high-intensity soil survey in Northwest Illinois with electromagnetic induction and tradition methods. *Soil Surv. Horiz*. 49, 102 - 108.

DURLESSER, H., 1999. Detemination of the spatial and temporal variability of physical soil parameters using electromagnetic induction.

EAGLESON, P.S., 1978. Climate, soil and vegetation 1: Introduction to water-balance dynamics. *Water Resour. Res.* 14, 705 - 712.

EIGENBERG, R.A., DORAN, J.W., NIENABER, J.A., FERGUSON, R.B. & WOODBURY, B.L., 2002. Electrical conductivity monitoring of soil condition and available N with animal manure and a cover crop. *Agric. Ecosyst. Environ*. 88, 183 - 193.

EIGENBERG, R.A., KORTHALS, R.L. & NIENABER, J.A., 1998. Geophysical electromagnetic survey methods applied to agricultural waste sites. *J. Environ. Qual.* 27, 215 - 219.

EIGENBERG, R.A. & NIENABER, J.A., 1998. Electromagnetic survey of cornfield with repeated manure applications. *J. Environ. Qual.* 27, 1511 - 1515.

EIJKELKAMP, 2003. Operating instruction: EC-probe set for soil conductivity measurements. Agrisearch equipment.

FRAENKEL, C., 2008. Spatual variability of selected soil properties in and between map units. MSc. thesis, University of the Free State, South Africa.

FRIEDMAN, S.P., 2005. Soil properties influencing apparent electrical conductivity: A review. *Comput. Electron. Agric*. 46, 45 - 70.

FULTON, A., SCHWANKL, L., LYNN, K., LAMPINEN, B., EDSTROM, J. & PRICHARD, T., 2011. Using EM and VERIS technology to assess land suitablility for orchard and vineyard development. *Irrig. Sci*. 29 497 - 512.

GANGRADE, S., 2012. Evaluation of use of EM38-MK2 as a tool to understand field scale changes in soil properties. MSc. thesis, Clemson University, United States.

GARDNER, W., 1986. Chapter 21 Water content: physical and mineralogical methods, Part 1. In: KLUTE, A. (Ed.) Methods of soil analysis. Madison, Wisconsin: *Soil Sci. Soc. Am. J.* 493 - 544.

GEBBERS, R., LUCK, E. & HEIL, K., 2007. Depth soundong with the EM38 detection of soil layering by inversion of apparent electrical conductivity measurements. 6th European Conference on Precision Agriculture 2007. Skiathos, Greece. 2-6, pp. 95 - 102.

GEBBERS, R., LUCK, E. & DABAS, M., 2009. Comparison of instruments for geoelectrical soil mapping at the field scale. European Association of Geoscientists & Engineers, *Near surf. Geophys.* 7, 179 - 190.

GEONICS LIMITED, 2003. EM38B Ground conductivity Meter: Dual Output Version, operating manual. Leaders in Electomagnetics, Mississauge, Ontario, Canada.

GEONICS LIMITED, 2010. Operating instructions: EM38-MK2 data logging system for field computers Archer and Allegro MX, EM38-MK2 Version 2.02., Mississauga, Ontario, Canada.

GEONICS LIMITED, 2012. Geophysical instrumentation for exploration and the environment: 50th Anniversary, Geonics Catalogue: leaders in electromagnetics. Mississauga, Ontario Canada L5T 1C6. Website: http://www.geonics.com.

GRISSO, R., ALLEY, M., HOLSHOUSER, D. & ThOMASON, W., 2009. Precision farming tools: Soil electrical conductivity. Virginia Coop. Ext. , 18, pp. 442 - 508.

HAYASHI, M., 2004. Temperature-Electrical Conductivity Relation of Water for Environmental Monotoring and Geophysical data Inversion. *Environ. Monit. Assess*. 96, 119 - 128.

HEERMANN, D. F., HOETING, J., DUKE, H. R., WESTFALL, D. G., BUCHLEITER, G. W., WESTRA, P., PEAIRS, F. B., & FLEMING, K. (2000). Irrigated precision farming for corn production. Proceedings of 2nd International Conference on Geospatial Information in Agriculture and Forestry, pp. 144 - 151, Lake Buena Vista, Florida.

HEIL, K. & SCHMIDHALTER, U., 2012. Characterisation of soil texture variability using apparent electrical conductivity at a highly variable site. *Comput. Geosci*. 39, 98 - 110.

HEIL, K. & SCHMIDHALTER, U., 2015. Comparison of the EM38 and EM38-MK2 electromagnetic induction-based sensors for spatial soil analysis at field scale. *Comput. Electron. Agric.* 110, 267-280.

HEIMOVAARA, T.J., FOCKE, A.G., BOUTE, W. & VERSTRATEN, J.M., 1995. Assessing Temporal Variations in Soil Water Composition with Time Domain Reflectometry. *Soil Soil Sci. Soc. Am. J.* 59, 689 - 698.

HEINIGER, R.W., McBRIDE, R.G., CLAY, D.E., 2003. Using soil electrical conductivity to improve nutrient management. *Agron. J*. 95, 508-519.

HENDRICKX, J.M.H., 1990. Determination of hydraulic soil properties, in process studies in Hillslop hydrology. pp. 43 - 92.

HENDRICKX, J. ET AL., 1992. Soil Salinity assessment by electromagnetic induction of irrigated land. *Soil Sci. Soc. Am. J.* 56, 1933-1941.

HERRERO, J., BA, A.A. & ARAGUES, R., 2003. Soil salinity and its distribution determined by soil sampling and electromagnetic techniques. *Soil Use Manage*. 19, 119 - 126.

HILLEL, D., 1998. Environmental soil physics. Academic press Inc. New York.

HOSSIAN, M.B., LAMB, D.W., LOCKWOOD, P.V., FRAZIER, P., 2010. EM38 for volumetric soil water content estimation in the root-zone of deep vertosol soils. *Comput. Electrons. Agric.* 74, 100-109.

HU, W., TALLON, L.K., BISWAS, A. & CHENG S.B., 2013. Time stability of soil water content. Advances in Agrophysical Research, pp. 47 - 78.

HUTH, N. & POULTON, P., 2007. An electromagnetic induction method for monitoring variation in soil moisure in agroforestry systems. *Aust. J. Soil Res*. 45, 63 - 72.

JAMES, I.T., WAINE, T.W., BRADLEY, R.I., GODWIN, R.J. & TAYLOR, J.C., 2000. A comparison between traditional methods and EMI scanning for determining soil textural boundaries. AGENG 2000, Paper 00-PA-014, Warwick, UK.

JAYNES, D.B., 1996. Mapping the areal distribution of soil parameters with geophysical techniques. In: Corwin, D.L., Loague, K. (Ed.), Applications of GIS to the Modeling of

Non-point Source Pollutants in the Vadose Zone. SSSA Special Publication No. 48. SSSA, Madison, WI, USA, pp. 205 - 216.

JAYNES, D.B., 2008. Mapping pesticide partition coefficients by Electromagnetic Induction. In: Handbook of Agricultural Geophysics. CRC Press, pp. 233-240.

JAYNES, D.B., COLVIN, T.S. & AMBUEL, J., 1993. Soil type and crop yeild determinations from ground conductivity surveys. ASAE, paper No 933552. ASAE, St. Joseph, MI, USA.

JOHNSON, C.K., DORAN, J.W., DUKE, H.R., WEINHOLD, B.J., ESKRIDGE, K.M. & SHANAHAM, J.F., 2001. Fiel-scale Electrical Conductivity Mapping for Delineating Soil Condition. *Soil Sci. Soc. Am. J*. 65, 1829 - 1837.

JOHNSON, C.K., DORAN, J.W., EGHBALL, B., EIGENBERG, R.A., WEINHOLD, B.J. & WOODBURY, B.L., 2003. Status of soil electrical conductivity studies by central state researchers. ASAE Paper No 032339, Annual International Meeting, Las Vegas, NV, ASAE, St Joseph, MI.

JURY, W.A., GARDNER, W.R. & GARDNER, W.H. 1991. Soil Physics, 5th edn., John Wiley and Sons,Inc.

KACHANOSKI, R.G., De JONG, E. & Van WESENBEECH, I.J.V., 1990. Feild scale patterns of soil water storage from non-contacting measurements of bulk electrical conductivity. *Can. J. Soil Sci. Soc*. 70, 537-541.

KACHANOSKI, R.G., GREGORICH, E.G. & Van WESENBEECK, I.J.V., 1988. Estimating spatial variations of soil water content using non-contacting electromagnetic inductive methods. *Can. J. Soil Sci. Soc*. 68, 715 - 722.

KELLENERS, T.J., ROBINSON, D.A., SHOUSE, P.J., AYARS, J.E. & SKAGGS, T.H., 2005. Frequency dependency of the complex permittivity and its impact on dielectric sensor calibration in soils. *Soil Sci. Sc. Am. J*. 69, 67 - 76.

KITCHEN, N.R, SUDDUTH, K.A. & DRUMMOND, S.T., 1999. Soil electrical conductivity as a crop productivity measure for claypan soils. *J. Prod. Agric*. 12, 607- 617.

KITCHEN, N.R, SUDDUTH, K.A. & DRUMMOND, S.T., 1996. Mapping of sand deposition from 1993 Mid-west floods with electrimagnetic induction measurements. *J. Soil Water Conserv.*, 51, 336 – 340.

KIZITO, F., 2008. Frequency, electrical conductivity and temperature analysis of a low cost capacitance soil moisture sensor. *J. Hydrol*. 352, 367 - 378.

KOSSEVA, C. & WEBB, M.R., 2013. Introduction: Causes and chanllenges of food wastage. In: Webb, M.R. & Kosseva, C. (Eds), Food industry wastes: Assessment and recuperation of commodities. Academic press, pp. xv - xxiv.

KRAVCHENKO, A., 2008. Mapping of Drainage classes Using Soil Electrical Conductivity. In: Handbook of Agricultural Geophysics. CRC Press. Boca Raton, FL., pp. 255 - 263.

KRAVCHENKO, A., BOLLERO, G., OMONODE, R. & BULLOCK, D., 2002. Quantitative mapping of soil drianage classes using topographical data and soil electrical conductivity. *Soil Sci. Soc. Am. J.* 66, 235 - 243.

KWEON, G., 2012. Toward the ultimate soil survey: sensing multiple soil landscape properties in one pass. Agron. J. 104, 1547-1557. Doi: 10.2134/agronj2012.0156

LAHOCHE, F., GODARD, T., FOURTY,T., LELANDAIS, V. & LEPOUTRE, D., 2002. A multi-sensor approach for generating in-field pedological variability maps. *Geosyst*., France.

LAVOUE, F., VAN DER KRUK, J., RINGS, J., ANDRE, F., MOGHADAS, D., HUISMAN, J.A., LAMBOT, S., WEIHERMULLER, L., VANDERBORGHT, J. & VEREECKEN, H., 2010. Electromagnetic induction calibration using apparent electrical conductivity modelling based on electrical resistivity tomography. *Near surf. Geophys*. 8, 553 - 561.

LESCH, S.M., 2005. Sensor-directed response surface sampling designs for characterizing spatial variation in soil properties. *Comput. Electron. Agric*. 46, 153 - 179.

LESCH, S.M. & CORWIN, D.L., 2003. Predicting EM/soil property correlation estimates via the dual pathway parallel conductance model. *Agron. J.* 95, 365 - 379.

LESCH, S.M., CORWIN, D. & ROBINSON, D., 2005. Apparent electrical conductivity mapping as an agricultural management tool in arid zone soils. *Comput. Electron. Agric.* 46, 351 - 378.

LESCH, S.M., RHOADES, J.D. & CORWIN, D.L., 2000. ESAP-95 version 2.0IR: User manual and totorial guide. Research Report 146. USDA-ARS, George E. Brown, Jr., Salinity Laboratory, Riverside, California.

LESCH, S.M., RHOADES, J.D., LUND, L. & CORWIN, D.L., 1992. Mapping soil salinity using calibrated electromagnetic measurements. *Soil Sc. Sc. Am. J.* 56, 540 - 548.

LESCH, S.M., STRAUSS, D.J. & RHOADES, J.D., 1995a. Spatial prediction of soil salinity using electromagnetic induction techniques. 1. Statistical prediction models: a comparison of multiple linear regression and cokriging. *Water Resour. Res.* 31, 373 - 386.

LESCH, S.M., STRAUSS, D.J & RHOADES, J.D., 1995b. Spatial prediction of soil salinity using electromagnetic induction: 2. An efficient spatail sampling algorithm suitable for multiple linear regression model identification and estimation. *Water Resour. Res*. 31, 387 - 398.

LI, J. & HEAP, A.D., 2011. A review of comparative studies of spatial interpolation methods: performance and impact factors. *Ecol. Inform*. 6, 228 - 241.

LONG, D.S., 1998. Spatial autoregression modelling of site-specific wheat yield. *Geoderma* 85, 181 – 197.

LUCK, E., RUHLMANN, J. & SPANGENBERG, U., 2005. Physical background of soil EC mapping: Laboratory, theoretical and feild studies. In: STAFFORD, J., (Ed.) Preci. Agric., Netherlands: Wageningen Academic, pp. 417 - 424.

LUND, E.D., CHRISTY, C.D. & DRUMMOND, P.E., 1999. Practical appilication of soil electrical conductivity mapping. In: Proceedings of the 2nd European Conference on Precision Agriculture.

MA, R., McBRATNEY, A., WHELAN, B., MINASNY, B. & SHORT, M., 2010. Comparing temperature correction models for soil electrical conductivity measurment. *Preci. Agric*., Australia.

MARTINEZ-FERNANDEZ, J. & CEBALLOS, A., 2003. Temporal stability of soil moisture in a larg field experiment in Spain. *Soil Sci. Soc. Am. J.* 67, 1647 - 1656.

MARTINI, E., WERBAN, U., ZACHARIAS, S., POHLE, M., DIETRICH, P. & WOLLSCHLÄGER, U., 2016. Repeated electromagnetic induction measurements for mapping soil moisture at the field scale: validation with data from a wireless soil moisture monitoring network. *J. Hydrol. Earth Syst. Sci*.

MAVIMBELA, S.S.W. & VAN RENSBURG, L.D., 2013. Estimating hydraulic conductivity of internal drainage for layered soils in situ. *J. Hydrol. Earth Syst. Sci* 17, 4366 - 4366.

MAVIMBELA, S.S.W. & VAN RENSBURG, L.D., 2011. In-situ evaluation of internal drainage in layered soils (Tukulu, Sepane and Swartland). *J. Hydrol. Earth Syst. Sci.* 8, 979 7 - 9841.

MCKENZIE, R.C., CHOMISTEK, W. & CLARK, N.F., 1989. Convertion of electromagnetic inductnce readings to saturated paste extract values in soils for different temperature, texture and moisture conditions. *Can. J. Soil Sci.* 69, 25 - 32.

MCKENZIE, R.C., TRAVIS, G., HERRON, W., CLARK, N.F. & CHOMISTEK, W., 1988. Rapid collection of EM38 (ECa) data for preperation of ECe contour maps of soil salinity. Proceedings of the 25th Alberta Soil Science Workshop, Lethbridge, Alta. pp. 246 - 250.

MCNEILL, J.D., 1980. Electromagnetic terrain conductivity measurement at low induction numbers. Technical Note TN-6.

MCNEILL, J.D., 1992. Rapid, accurate mapping of soil salinity by electromagnetic ground conductivity meters. In TOP, G.C. REYNOLDS, W.D., GREEN, R.E. (Eds), Advances in measurement of soil physical properties: Bringing theory into practice. Madison: SSSA special publication No. 30, pp. 209 - 229.

MCNEILL, J.D., 1996. Why doesn't geonics limited build a multi-freguency EM31 or EM38? Technical Note TN-30, GEONICS LIMITED, URL:http://www.geonics.com.

MCROBERTS, R., 2010. Probablity and model-based approaches to inference for proportion forest using satellite imagery as ancillary data. *Rem. Sens. Environ*. 114, 1017 - 1025.

MISRA, R.K., & PADHI, J., 2014. Assessing field-scale soil water distribution with electromagnetic induction meter. *J. Hydrol*. 516, 200 - 209.

MULLER, W., 2001. Collecting spatial data: Optimum design of experiments for random fields. Heidelberg, Germany: Physica-Verlag.

MUÑOZ-CARPENA, R., SHUKLA, S. & MORGAN, K., 2004. Field Devices for Monitoring Soil Water Content: For The Irrigation Water Management Program Team of the Southern Regional Water Program, University of Florida.

NADLER, A. and FRENKEL, H. 1980. Determination of soil electrical conductivity from bulk soil electrical conductivity measurements by the Four-electrode method. Soil Sc. Soc. Am. J. 44, 1216 - 1221.

NEUDERKER, E., SCHIDHALTER, U., SPERL, C. & SELIGE, T., 2001. Site-specific soil mapping by electromagnectic Induction. European Conference Precision Agriculture, Montpellier, pp. 271 - 276.

NON-AFFILIATED SOIL ANALYSIS WORK COMMITTEE, 1990. Handbook of standard soil testing methods for advisory purposes. Soil Science Society of South Africa.

NUGTEREN, W. ., MALO, D. D., SCHUMACHER, T. E., SCHUMACHER, J. A., CARLSON, C.G., CLAY, D.E., CLAY, S.A. & DALSTED, K.J. 2000. Hillslope chronosequence of electromagnetic induction readings as influenced by selected soil properties. In: Proceedings of the 5th International Conference on Precision Agriculture. Roberts, P.C., Rust, R.H. & Larson, W.E. (ASA, CSSA, SSSA, Madison, WI, USA), Published on CD-ROM, p. 8.

PADHI, J. & MISRA, R.K., 2011. Sensitivity of EM38 in determining soil water distribution in an irrigated wheat field. *Soil Till. Res*. 117, 93 -102.

PERSSON, M. & BERNDTSSON, R., 1998. Texture and electrical conductivity effects on temperature dependency in time domain reflectometry. *Soil Sc. Soc. Am. J.* 62, 887 - 893.

PERRY, M.A. & NIEMANN, J.D., 2008. Generation of soil moisture patterns at the catchment scale by EOF interpolation. *J. Hydrol. Earth Syst. Sci*. 12, 39 - 53.

PORPORATO, A., LAIO, F., RIDOLFI, L. & RODRIGUEZ-ITURBE. 2001. Plants in water-controlled ecosystems: active role in hydrologic processes and response to water stress III. Vegetation Water Stress, *Adv. Water Resour*. 24, 725 - 744.

RAYMENT, G.E., HIGGINSON, F.R., 1992. Electrical conductivity. In: Australian Laboratory Handbook of Soil and Water Chemical Methods. Inkata Press, Melbourne.

REEDY, R.C. & SCANLON, B.R., 2003. Soil water content monitoring using electromagnetic induction. *J. Geotech. Geoenviron. Eng*. 129, 1028 - 1039.

RHOADES, J.D., 1982. Soluble salts. In A.L. Page *et al.* (Eds) Methods of soil analysis, Part 2. *Agron. J*. 9, 167 - l 78.

Rhoades, J.D., 1989. Determining soil salinity from measurements of electrical conductivity presented at the EM Confrence, April 1989, Mooroopna. Department of Agriculture and Rural Affair, Victoria, Australia.

RHOADES, J.D., SHOUSE, P.R., ALVES, W.J., MANTRGHI, N.M. & LESCH, S.M., 1990. Determining soil salinity from soil electrical conductivity using different models and estimates. Soil SSci. Soc. Am. J., 54, 46 – 54.

RHOADES, J.D., CHANDUVI, F. & LESCH, S.M., 1999. Soil salinity assessment: Methods and interpretation of electrical conductivity measurements. FAO Irrigation and Drianage Paper No 57. Food and Agriculture Organization of United Nations, Rome, Italy.

RHOADES, J.D. & CORWIN, D.L., 1981. Determining soil electrical conductivity-Depth relation using induction electromagnetic soil conductivity meter. *Soil Sc. Soc. Am. J.* 45, 255 - 260.

RHOADES, J.D., MANTEGHI, N.A., SHOUSE, P.J. & ALVES, W.J., 1989a. Estimating soil salinity from saturated soil-paste electrical conductivity. *Soil Sci. Soc. Am. J*. 53, 428 - 433.

RHOADES, J.D., MANTEGHI, N.A., SHROUSE, P.J. & ALVES., W.J., 1989b. Soil electrical conductivity and soil salinity: new formulations and calibrations. *Soil Sci. Soc. Am. J.* 53, 433 - 439.

RHOADES, J.D., RAATS, P.A. & PRATHER, R.J., 1976. Effect of liquid-phase electrical conductivity, water content and surface conductivity on bulk soil electrical conductivity. *Soil Sci. Soc. Am. J.* 40, 651 - 655.

RICHARDSON, J.L., WILDING, L.P. & DANIELS, R.B., 1992. Recharge and discharge of groundwater in aquic conditions illustrated with flow analysis. *Geoderma* 53, 65-78.

ROBINSON, D.A., ABDU, H., JONES, S.B., SEYFRIED, M., LEBRON, I. & KNIGHT, R., 2008. Eco-geophysical imaging of watershed-scale soil pattern links with plant community spatial patterns. *Vados zone J. Soil Sci. Soc. Am.* 7, 1132 - 1138.

ROBINSON, D.A., LEBRON, I., LESCH, S.M. & SHOUSE, P., 2004. Minimizing drift in electrical conductivity measurements in high temperature environments using the EM38. *Soil Sci. Soc. Am. J.* 68, 339 - 345.

SAS INSTITUTE Inc., 1999. SAS/STAT User's Guide, Version 8, Cary, NC: SAS Institute Inc., USA. http://www.math.wpi.edu/saspdf/stat/chap67.pdf

SCOLLER, I., TABBAGH, A., HESSE, A. & HERZOG, I., 1990. Archaeological prospecting and remote sensing. New York: The Press Syndicate of the University of Cambridge.

SHAINBERG, I., RHOADES, J.D. & PRATHER, R.J., 1980. Effect of ESP, cation exchange capacity and soil solution concentration on soil electrical conductivity. *Soil Sci. Soc. Am. J.* 44, 469 - 473.

SHEETS, K.R. & HENDRICKX, J.M.H., 1995. Non- inversive soil water content measurement using electromagnetic induction. *Water Resour. Res*. 31, 2401 - 2409.

SEIFI, M.R., ALIMARDANI, R. & SHARIFI, A., 2010. How can soil electrical conductivity measurements control soil pollution? *J. Environ. Earth Sci.*, 2, 235 – 238.

SINGH, V.P. & FIORENTINO, M., 1996. Geographical information systems in hydrology, Kluwer Academic Publication, Dordrecht.

SOIL CLASSIFICATION WORKING GROUP, 1991. A Taxonomic System for South Africa. Soil and Irrigation Research Institute, Department of Agricultural Development.

STANLEY, J.N., LAMB, D.W, IRVINE, S.E. & SCHNEIDER, D.A., 2014. Effect of aluminum neutron probe access tubes on the apparent electrical conductivity recorded by electromagnetic soil survey sensor. IEEE, *GeoSci. Rem. Sens.* 11, 333 - 336.

STOGRYN, A., 1971. Equations for calculating the dielectric constant of saline water. Transactions of microwave theory and techniques, IEEE 19, 733 - 736.

SUDDUTH, K.A., DRUMMOND, S.T. & KITCHEN, N.R., 2001. Accuracy issues in electromagnetic induction sensing of soil electrical conductivity for precision agriculture. *Comput. Electron. Agric*. 31, 239 - 264.

SUDDUTH, K.A. & KITCHEN, N.R., 1993. Electromagnetic induction sensing of claypan depth. ASAE paper No 931531, pp. 12 - 17.

SUDDUTH, K.A., KITCHEN, N.R., BOLLERO, G.A., BULLOCK, D.G. & WIEBOLD, W.J., 2003. Comparison of electromagnetic induction and direct sensing of soil electrical conductivity. *Agron. J*. 95, 472 - 482.

SUDDUTH, K.A., KITCHEN, N.R., HUGHES, DF. & DRUMMOND, S.T., 1995. Electromagnetic induction sensing as an indicator of productivity on claypan soils. In: Robert, P.C., Rust, R.H. & Larson, W.E., (Ed.) Second International Conference on site-specific management of Agricultural systems. *ASA-CSSA-SSSA*.

SUDDUTH, K.A., KITCHEN, N.R., WIEBOLD, W.J., BATCHELOR, W.D., BOLLERO, G.A., BULLOCK, D.G., CLAY, D.E., PALM, H.L., PIERCE, F.J., SCHULER, R.T. & THELEN,

K.D., 2005. Relating apparent electrical conductivity to soil properties across the north-central USA. *Comput. Electron. Agric.* 46, 263 - 283.

TESFUHUNEY, W.A., 2012. Optimising runoff to basin ratios for maize production within-field rainwater harvesting. Phd. thesis, University of the Free State, South Africa.

TEULING, A.J., UIJLENHOET, R., HUPET, F., Van LOON, E.E. & TROCH, P.A., 2006. Estimating spatial mean root-zone soil moisture from point-scale observations. *J. Hydrol. Earth Syst. Sci.* 10, 755 - 767.

TOPP, G.C., DAVIS, J.L. & ANNAN, A.P., 1980. Electromagnetic determination of soil water content: measurements in coaxial transmission lines. *Water resour. Res*. 16, 574 - 582.

TOPP, G.C. & FERRE, P.A., 2002. The soil solution phase: In: Methods of soil Analysis. Madison: *Soil Sci. Soc. Am. J.* 417 - 534.

TOUSHMALANI, R., 2010. Application of geophysical methods in agriculture. *Aust. J. Basic appli. Sci.* 4, 6433 - 6439.

TRIANTAFILIS, J., AHMED, M.F. & ODEH, I.O.A., 2002. Application of a mobile electronic sensing system (MESS) to assess cause and management of soil Salinazation in an irrigated cotton-growing feild. *Soil use manage*. 18, 330 - 339.

TRIANTAFILIS, J. & LESCH, S.M., 2005. Mapping clay content variation using electromagnetic induction techniques. *Comput. Electron. Agric*. 46, 203 - 237.

TRIANTAFILIS, J., ODEH, I.O.A., JARMAN, A.L., SHORT, M. & KOKKORIS, E., 2004. Estimating and mapping deep drainage risk at the district level in the lower Gwydir and Macquarie valleys. *Aust. J. Exp. Agric*. 44, 893 - 912.

UNITED STATES SALINITY STAFF, 1969. Diagnosis and improvement of saline and alkaline soils. U.S. Laboratory Handbook 60, USDA, Washington.

U.S. SALINITY LABORATORY STAFF, 1954. Diagnosis and improvement of saline and alkali soils. In: Handbook 60. Washington, DC: U.S. Government printing office, pp. 1 - 160.

VACHAUD, G., PASSERAT DE SILANS, A., BALABANIS, P. & VAUCLIN, M., 1985. Temporal stability of spatially measured soil water probability density function. *Soil Sci. Soc. Am. J.* 822 - 828, p. 49.

VLOTMAN, W.F. (Ed.), 2000. EM-38 Workshop Proceedings. New Delhi, February 4, 2000, Special Reports, vol. 10. ILRI, The Netherlands.

WAINE, T.W., BLACKMORE, B.S. & GODWIN, R.J., 2000. Mapping available water content and estimating soil textural class using electromagnetic induction. U.K, Warwick, Paper Number 00-SW-044.

WALKER, S. & TSUBO, M., 2003. Estimation of rainfall intensity for potential crop production on clay soil within in-field water harvesting practices in a semi-arid area., Pretoria: WRC Report No. 1049/1/02 .

WELLS, C.B., 1978. Electrolytic conductivity of soil solutions and wares: Conversion from field to standard temperatures: Division of Soils Technical Paper No 37. Commonwealth Scientific and Industrial Research Organization, Australia, pp. 1 -17.

WESTERN, A.W., ZHOU, S.L., GRAYSON, R.B., McMAHON, T.A., BLOSCHI, G. & WILSON, D.J., 2004. Spatial correlation of soil moisture in small catchments and its relationship to dominanat spatial hydrological processes. *J. Hydrol*. 286, 113 - 134.

WHITE, M.L., SHAW, J.N., RAPER, R.L., RODEKOHR, D. & WOOD, C.W., 2012. A multivariate approach for high-resolution soil survey development. *Soil Sci*. 177, 345 - 354.

WILLIAMS, B.G. & BAKER, G.C., 1982. An electromagnetic induction technique for reconnaissance surveys of soil salinity hazards. *Aust. J. Soil Res.* 20, 107 - 118.

WILLIAMS, B.G. & HOEY, G.C., 1987. The use of electromagnetic induction to detect the spatial variability of the salt and clay content of soils. *Aust. J. Soil Res*. 25, 21 - 28.

WOLLENHAUPT, N.C., RICHARDSON, J.L., FOSS, J.E. & DOLL, E.C., 1986. A rapid method for estimating weighted soil salinity from apparent soil electrical conductivity measured with an aboveground electromagnetic induction meter. *Can. J. Soil Sci*. 66, 315 - 321.

WRAITH, J.M. & OR, D., 1999. Temperature effects on soil bulk dielectric permittivity measured by time domain reflectometry: Experimental evidence and hypothesis development. *Water Resour. Res*. 35, 361 - 369.

ZERIZGHY, M.G., 2013. Comparison of the DFM capacitance and neutron water meter to measure soil water evaporation. *Water SA* 39, 56 - 76.

ZHU, Q., Lin, H.S. & Doolittle, J.A., 2010. Repeated electromagnetic induction surveys for improved soil mapping in an agricultural landscape. *Soil Sci. Soc. Am. J.* 74, 1750 - 1762.

Appendix

Appendix 4.1 Descriptive statistics of the ECa measured values (mS m^{-1}) before, over and after the DFM probes, NWM steel access tubes and trenches at vertical and horizontal modes, n = 40

	Before interference						Point of interference				After interference					
Interferences	*Min	*Max	Mean	*SD	*CV	*Std Err	*Min	*Max	Mean	*SD	*Min	*Max	Mean	*SD	*CV	*Std Err
DFM V-mode	13.00	24.00	18.75	2.808	14.98	0.444	-122.0	22.00	-43.50	71.50	10.00	29.00	19.40	5.391	27.79	0.852
DFM H-mode	7.000	12.00	10.10	1.215	12.03	1.215	-92.00	-61.00	-79.50	13.90	7.000	12.00	9.225	1.330	14.42	1.330
Steel tubes V-mode	14.00	22.00	16.93	1.760	10.40	0.278	-111.0	115.0	-30.00	102.8	12.00	21.00	14.85	2.237	15.06	0.354
Steel tubes H-mode	7.000	14.00	9.625	2.072	21.52	0.328	-1595	-179.0	-1041	654.6	6.000	14.00	8.350	1.889	22.62	0.299
Trench V-mode	14.00	19.00	16.60	1.236	7.447	0.196	11.00	18.00	15.30	3.10	14.00	19.00	16.53	1.569	9.49	0.248
Trench H-mode	7.000	16.00	8.325	1.575	18.92	0.249	7.00	10.00	7.50	0.58	6.000	10.00	7.950	0.932	11.73	0.147

*Min = minimum
*Max = Maximum
*SD = Standard deviation
*CV = Coefficient of variation
*Std Err = Standard error

Appendix 4.2 Statistically evaluating the difference between measurements before and after the treatments, N = 40

	Difference (After-Before)							
Interferences	Mean	SD	Std Err	Method	Variances	DF	t value	*Pr* > |t|
DFM, V-mode	0.65	4.2983	0.9611	Cochran	Unequal	39	0.68	0.5029
DFM, H-mode	-0.875	1.2739	0.2848	Pooled	Equal	78	-3.07	0.0029
Steel tubes, V-mode	-2.075	2.0124	0.45	Pooled	Equal	78	-4.61	<.0001
Steel tubes, H-mode	-1.275	1.9822	0.4432	Pooled	Equal	78	-2.88	0.0052
Trench, V-mode	-0.075	1.4123	0.3158	Pooled	Equal	78	-0.24	0.8129
Trench, H-mode	-0.375	1.2943	0.2894	Cochran	Unequal	39	-1.3	0.2027

*SD = Standard deviation

*Std Err = Standard error

Appendix 5.1 Relationship between bulk density (ρd) and gravimetric water content (θv, $m^3\ m^{-3}$) for individual selected plots, n = 12

	A-horizon				B-horizon				C-horizon			
Plots	Slope	Intercept	r^2	Std Error	Slope	Intercept	r^2	Std Error	Slope	Intercept	r^2	Std Error
1	-0.402	0.784	0.94	0.012	-0.795	1.431	0.94	0.026	-0.388	0.771	0.95	0.012
2	-0.321	0.650	0.90	0.010	-0.398	0.801	0.95	0.013	-0.760	1.398	0.90	0.024
3	-0.273	0.561	0.95	0.005	-0.478	0.919	0.96	0.011	-0.465	0.901	0.95	0.013
4	-0.388	0.773	0.96	0.008	-0.358	0.726	0.96	0.011	-0.534	1.027	0.92	0.018
5	-0.506	0.971	0.95	0.014	-0.593	1.119	0.94	0.025	-0.462	0.905	0.96	0.012
6	-0.318	0.648	0.94	0.006	-0.532	0.994	0.93	0.009	-0.444	0.862	0.93	0.011
7	-0.388	0.775	0.94	0.009	-0.530	1.005	0.97	0.014	-0.409	0.810	0.95	0.007
8	-0.498	0.946	0.94	0.007	-0.431	0.842	0.96	0.011	-0.494	0.947	0.93	0.018
9	-0.275	0.561	0.92	0.016	-0.271	0.563	0.93	0.012	-0.327	0.664	0.93	0.011
10	-0.408	0.785	0.94	0.011	-0.516	0.977	0.93	0.019	-0.588	1.080	0.93	0.015
11	-0.296	0.598	0.94	0.006	-0.540	1.023	0.94	0.012	-0.551	1.034	0.93	0.009
12	-0.524	0.990	0.97	0.009	-0.421	0.842	0.92	0.012	-0.521	1.008	0.95	0.009

Appendix 5.2 Range, mean and coefficient of variation (CV%) of soil bulk density and gravimetric water content measured over dry and wet conditions for A-, B- and C-horizons

Recorded soil bulk density from dry to wet conditions (Mg m^{-3})									
Profile no.	A (0.35 m)		B (0.75 m)		C (0.90 - 110 m)		CV (Mg m-3)		
	Range	Mean	Range	Mean	Range	Mean	AB	AC	BC
1	1.41 - 1.77	1.58	1.38 - 1.69	1.55	1.42 - 1.80	1.61	0.01	0.01	0.03
2	1.47 - 1.82	1.66	1.42 - 1.75	1.52	1.39 - 1.69	1.58	0.06	0.03	0.03
3	1.57 - 1.79	1.65	1.43 - 1.78	1.59	1.40 - 1.78	1.6	0.03	0.02	0.00
4	1.51 - 1.82	1.65	1.42 - 1.79	1.57	1.45 - 1.78	1.6	0.04	0.02	0.01
5	1.40 - 1.72	1.59	1.36 - 1.74	1.54	1.36 - 1.76	1.59	0.02	0.00	0.02
6	1.52 - 1.74	1.63	1.51 - 1.68	1.59	1.45 - 1.75	1.61	0.02	0.01	0.01
7	1.60 - 1.85	1.69	1.30 - 1.74	1.54	1.49 - 1.69	1.59	0.07	0.04	0.02
8	1.32 - 1.85	1.63	1.43 - 1.79	1.6	1.35 - 1.79	1.61	0.01	0.01	0.00
9	1.58 - 1.76	1.67	1.43 - 1.89	1.61	1.47 - 1.86	1.64	0.03	0.01	0.01
10	1.61 - 1.87	1.7	1.40 - 1.90	1.61	1.38 - 1.71	1.53	0.04	0.07	0.04
11	1.57 - 1.81	1.68	1.46 - 1.69	1.58	1.46 - 1.69	1.58	0.04	0.04	0.00
12	1.51 - 1.91	1.68	1.57 - 1.85	1.66	1.60 - 1.80	1.68	0.01	0.00	0.01
Recorded gravimetric water content from dry to wet conditions (g)									
Profiles no.	A (0.35 m)		B (0.75 m)		C (0.90 - 110 m)		CV (g)		
	Range	Mean	Range	Mean	Range	Mean	AB	AC	BC
1	0.08 - 0.23	0.15	0.06 - 0.37	0.20	0.06 - 0.21	0.15	0.20	0.00	0.20
2	0.06 - 0.17	0.12	0.10 - 0.25	0.19	0.11 - 0.34	0.20	0.32	0.35	0.04
3	0.08 - 0.13	0.11	0.07 - 0.23	0.16	0.08 - 0.25	0.16	0.26	0.26	0.00
4	0.08 - 0.20	0.13	0.09 - 0.22	0.16	0.08 - 0.26	0.17	0.15	0.19	0.04
5	0.09 - 0.25	0.17	0.09 - 0.34	0.20	0.10 - 0.30	0.17	0.11	0.00	0.11
6	0.10 - 0.17	0.13	0.11 - 0.20	0.15	0.08 - 0.23	0.15	0.10	0.10	0.00
7	0.06 - 0.17	0.12	0.09 - 0.31	0.19	0.11 - 0.21	0.16	0.32	0.20	0.12
8	0.07 - 0.16	0.11	0.08 - 0.23	0.15	0.07 - 0.29	0.15	0.22	0.22	0.00
9	0.04 - 0.20	0.11	0.05 - 0.19	0.13	0.07 - 0.19	0.13	0.12	0.12	0.00
10	0.02 - 0.13	0.09	0.02 - 0.27	0.14	0.06 - 0.26	0.18	0.31	0.47	0.18
11	0.06 - 0.14	0.1	0.10 - 0.25	0.17	0.11 - 0.24	0.17	0.37	0.37	0.00
12	0.03 - 0.17	0.11	0.06 - 0.18	0.14	0.08 - 0.18	0.14	0.17	0.17	0.00

Calibration and validation on individual plots at Paradys Experimental Farm

Appendix 5.3 Statistical measures evaluating the accuracy of the relationship between DFM probes output verses volumetric water content.

Soil forms	Depths (m)	DFM model performance					
		Slope	Intercept	*RMdAE	*REF	*rs	*p*-values
Plot 1	0.38	1.088	0.004	9	0.37	0.97	0.010
	0.75	1.151	-0.015	9	0.07	0.96	0.014
Plot 2	0.38	1.044	-0.016	5	0.61	0.92	0.007
	0.75	1.055	-0.026	7	0.34	0.93	0.011
Plot 3	0.38	0.877	0.008	8	0.45	0.98	0.008
	0.75	1.209	-0.080	5	0.62	0.97	0.013
Plot 4	0.38	0.907	0.003	7	0.56	0.99	0.009
	0.75	0.826	0.019	10	0.31	0.99	0.013
Plot 5	0.38	0.928	0.012	4	0.65	0.94	0.009
	0.75	0.851	0.032	4	0.68	0.96	0.012
Plot 6	0.38	1.208	-0.050	7	0.45	0.96	0.009
	0.75	0.983	0.007	4	0.65	0.93	0.012
Plot 7	0.38	1.195	-0.021	11	0.39	0.99	0.009
	0.75	0.858	0.048	6	0.61	0.92	0.013
Plot 8	0.38	1.034	-0.008	4	0.75	0.97	0.008
	0.75	0.915	0.006	6	0.42	0.95	0.010
Plot 9	0.38	1.021	-0.021	8	0.57	0.98	0.008
	0.75	0.987	-0.004	5	0.70	0.97	0.013
Plot 10	0.38	1.068	-0.016	5	0.69	0.97	0.010
	0.75	0.971	0.025	6	0.58	0.97	0.013
Plot 11	0.38	1.001	-0.021	6	0.67	0.97	0.010
	0.75	1.048	-0.022	7	0.61	0.94	0.009
Plot 12	0.38	0.817	0.025	8	0.57	0.96	0.009
	0.75	0.960	-0.010	7	0.64	0.97	0.009

*RMdAE = Relative median absolute error
*REF = Relative model efficiency
*rs = Spearman's' rank correlation

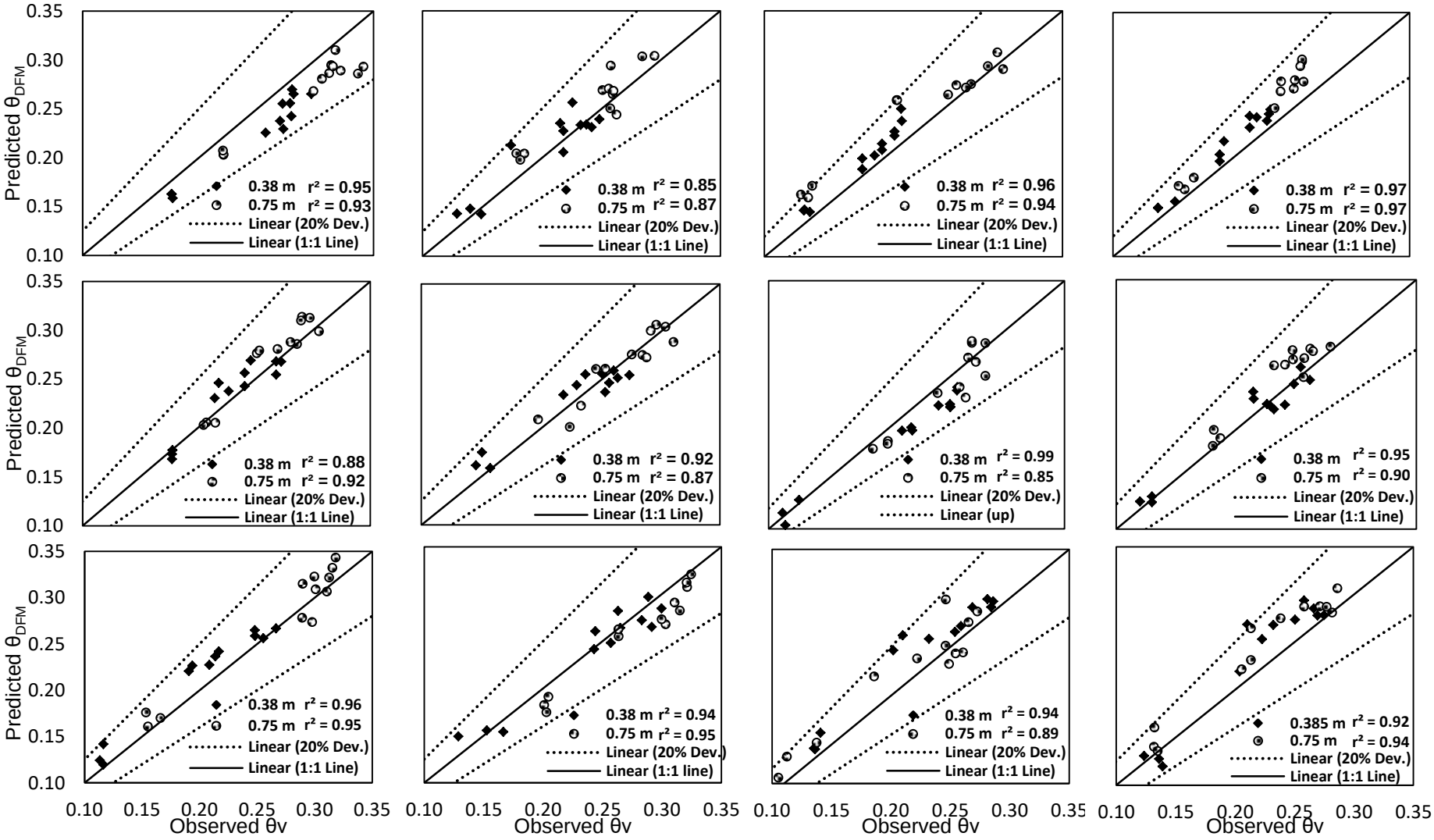

Appendix 5.4 Regression line of DFM-probes predicted soil water content (θ_{DFM}, $m^3\ m^{-3}$) and the observed soil water content ($m^3\ m^{-3}$) at 0.38 m and 0.75 m depths for individual plots.

Appendix 5.5 Calibration model equations and statistical indices between EC_a measured with the EM38-MK2 and calibrated DFM capacitance probes output (θ_{DFM}), n=12 per plot

Depth (m)	Plot No.	Model Name	EC_a vs θ_{DFM}		
			Model Function	r^2	*p*-value
0.38	1	Poly.	$\theta_{ECa} = -0.0007(EC_a)^2 + 0.0458(EC_a) - 0.4427$	0.973	0.000
	2	Poly.	$\theta_{ECa} = -0.0002(EC_a)^2 + 0.014(EC_a) + 0.0382$	0.907	0.000
	3	Poly.	$\theta_{ECa} = -0.0009(EC_a)^2 + 0.0484(EC_a) - 0.3876$	0.899	0.000
	4	Power	$\theta_{ECa} = 0.013(EC_a)^{0.899}$	0.979	0.000
	5	Power	$\theta_{ECa} = 0.0285(EC_a)^{0.6636}$	0.906	0.000
	6	Poly.	$\theta_{ECa} = -0.0005(EC_a)^2 + 0.0291(EC_a) - 0.1439$	0.953	0.000
	7	Poly.	$\theta_{ECa} = -0.0005(EC_a)^2 + 0.0291(EC_a) - 0.1442$	0.948	0.000
	8	Poly.	$\theta_{ECa} = -0.0003(EC_a)^2 + 0.0206(EC_a) - 0.1368$	0.910	0.000
	9	Power	$\theta_{ECa} = 0.0096(EC_a)^{1.0191}$	0.955	0.000
	10	Poly.	$\theta_{ECa} = -0.0014(EC_a)^2 + 0.0741(EC_a) - 0.6893$	0.840	0.002
	11	Power	$\theta_{ECa} = 0.0134(EC_a)^{0.8546}$	0.813	0.003
	12	Power	$\theta_{ECa} = 0.0001(EC_a)^{2.4205}$	0.854	0.001
0.75	1	Poly.	$\theta_{ECa} = -0.0005(EC_a)^2 + 0.0351(EC_a) - 0.2719$	0.919	0.000
	2	Poly.	$\theta_{ECa} = -0.0003(EC_a)^2 + 0.0157(EC_a) + 0.0416$	0.870	0.000
	3	Power	$\theta_{ECa} = 0.0134(EC_a)^{0.9558}$	0.955	0.000
	4	Poly.	$\theta_{ECa} = -0.0003x^2 + 0.0172x + 0.0269$	0.970	0.000
	5	Power	$\theta_{ECa} = 0.0427(EC_a)^{0.5802}$	0.894	0.000
	6	Power	$\theta_{ECa} = 0.0222(EC_a)^{0.8429}$	0.726	0.003
	7	Power	$\theta_{ECa} = 0.0993(EC_a)^{0.3352}$	0.912	0.000
	8	Poly.	$\theta_{ECa} = -0.001(EC_a)^2 + 0.0413(EC_a) - 0.1931$	0.887	0.000
	9	Poly.	$\theta_{ECa} = -0.0005(EC_a)^2 + 0.0317(EC_a) - 0.2149$	0.969	0.000
	10	Power	$\theta_{ECa} = 0.0089(EC_a)^{1.0496}$	0.966	0.000
	11	Poly.	$\theta_{ECa} = -0.0004(EC_a)^2 + 0.0258(EC_a) - 0.1154$	0.915	0.000
	12	Poly.	$\theta_{ECa} = -0.0007(EC_a)^2 + 0.0484(EC_a) - 0.4232$	0.815	0.000

Appendix 5.6 Statistical measures evaluating the accuracy of the relationship between field measured EC_a and θ_{DFM}

Soil forms	Depths (m)	EM38-MK2 model performance					
		Slope	Intercept	RMdAE	REF	rs	p-values
Plot 1	0.38	1.107	-0.007	7	0.50	0.97	0.001
	0.75	0.862	0.068	12	-0.29	0.98	0.014
Plot 2	0.38	0.877	0.035	6	0.48	0.95	0.000
	0.75	1.107	-0.045	7	0.32	0.94	0.003
Plot 3	0.38	0.708	0.053	4	0.69	0.96	0.000
	0.75	0.883	0.007	8	0.47	0.95	0.003
Plot 4	0.38	0.796	0.043	4	0.75	0.98	0.000
	0.75	0.475	0.130	12	0.19	0.95	0.008
Plot 5	0.38	0.798	0.047	4	0.70	0.96	0.000
	0.75	0.733	0.070	3	0.73	0.98	0.000
Plot 6	0.38	0.993	0.013	4	0.65	0.99	0.000
	0.75	1.051	-0.031	6	0.46	0.94	0.000
Plot 7	0.38	1.067	0.000	7	0.59	0.99	0.000
	0.75	0.753	0.070	5	0.71	0.98	0.000
Plot 8	0.38	0.973	0.019	8	0.52	0.97	0.000
	0.75	0.616	0.088	6	0.49	0.97	0.000
Plot 9	0.38	0.970	0.025	10	0.49	0.98	0.000
	0.75	1.103	-0.027	3	0.84	0.96	0.000
Plot 10	0.38	1.091	-0.010	6	0.65	0.97	0.010
	0.75	0.997	0.017	4	0.70	0.97	0.000
Plot 11	0.38	1.021	-0.005	2	0.88	0.94	0.000
	0.75	0.933	-0.008	6	0.63	0.92	0.000
Plot 12	0.38	0.842	0.041	6	0.67	0.98	0.000
	0.75	1.265	-0.029	11	0.45	0.97	0.000

*RMdAE = Relative median absolute error

*REF = Relative model efficiency

*rs = Spearman's' rank correlation

Calibration based on soil forms of Paradys Experimental Farm

Appendix 5.7 Polynomial and power equations describing the relationship between DFM probes measured scale frequency (*SF*) and volumetric water content (θ_V) for the soil forms of Paradys Experimental Farm

		SF vs θv			
Soil forms	Depth (m)	Model Function	r²	*p*-value	*n*
Sepane	0.38	$\theta_{DFM} = -0.0004(SF)^2 + 0.0348(SF) - 0.5449$	0.720	$3E^{-08}$	
	0.75	$\theta_{DFM} = -7E\text{-}05(SF)^2 + 0.0135(SF) - 0.3187$	0.780	$3E^{-14}$	36
Swartland	0.38	$\theta_{DFM} = 0.0384(SF)^{0.4598}$	0.574	$2E^{-06}$	
	0.75	$\theta_{DFM} = 0.0026(SF)^{1.1164}$	0.900	$4E^{-14}$	24
Tukulu	0.38	$\theta_{DFM} = -8E\text{-}05(SF)^2 + 0.0108(SF) - 0.0851$	0.683	$2E^{-16}$	
	0.75	$\theta_{DFM} = -1E\text{-}05(SF)^2 + 0.006(SF) - 0.0451$	0.795	$2E^{-23}$	57
Bloemdal	0.38	$\theta_{DFM} = 0.0001(SF)^2 - 0.0033(SF) + 0.1649$	0.820	$2E^{-10}$	
	0.75	$\theta_{DFM} = 0.0786e^{0.0187(SF)}$	0.802	$4E^{-07}$	24

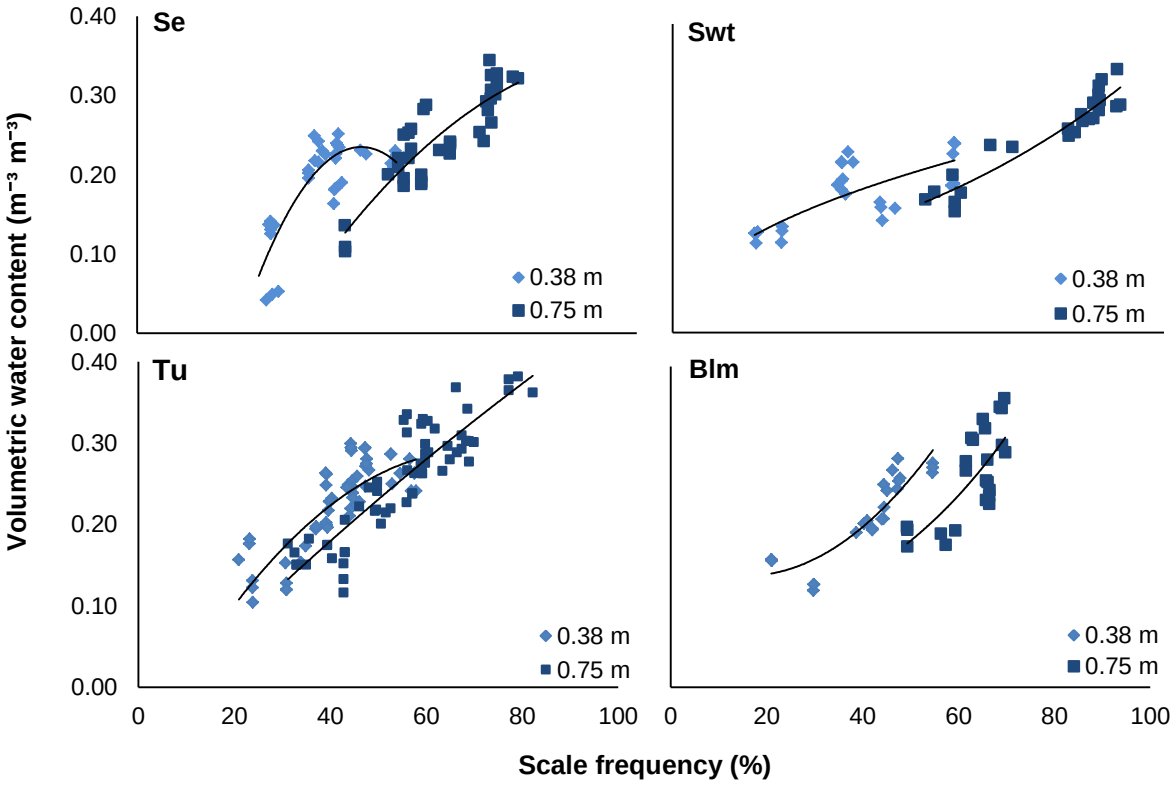

Appendix 5.8 Regression trend between DFM output (SF, %) versus volumetric water content at 0.38 m and 0.75 m depths, for Sepane (Se), Swartland (Swt), Tukulu (Tu) and Bloemdal (Blm) soil forms.

Appendix 5.9 Statistical measures evaluating the accuracy of the relationship DFM probes *SF* versus volumetric water content θ_V

Soil forms	Depths (m)	DFM model performance					
		Slope	Intercept	*RMdAE	*REF	*r_s	*p*-value
Sepane	0.38	0.657	0.041	22	-0.17	0.84	0.000
	0.75	0.973	-0.008	5	0.59	0.73	0.000
Swartland	0.38	0.895	0.010	9	0.44	0.76	0.000
	0.75	0.960	-0.007	5	0.68	0.53	0.007
Tukulu	0.38	0.686	0.065	10	0.37	0.81	0.000
	0.75	0.842	0.037	8	0.52	0.75	0.000
Bloemdal	0.38	1.051	-0.019	5	0.62	0.85	0.000
	0.75	1.507	-0.132	21	-0.68	0.38	0.060

*RMdAE = Relative median absolute error

*REF = Relative model efficiency

*r_s = Spearman's rank correlation

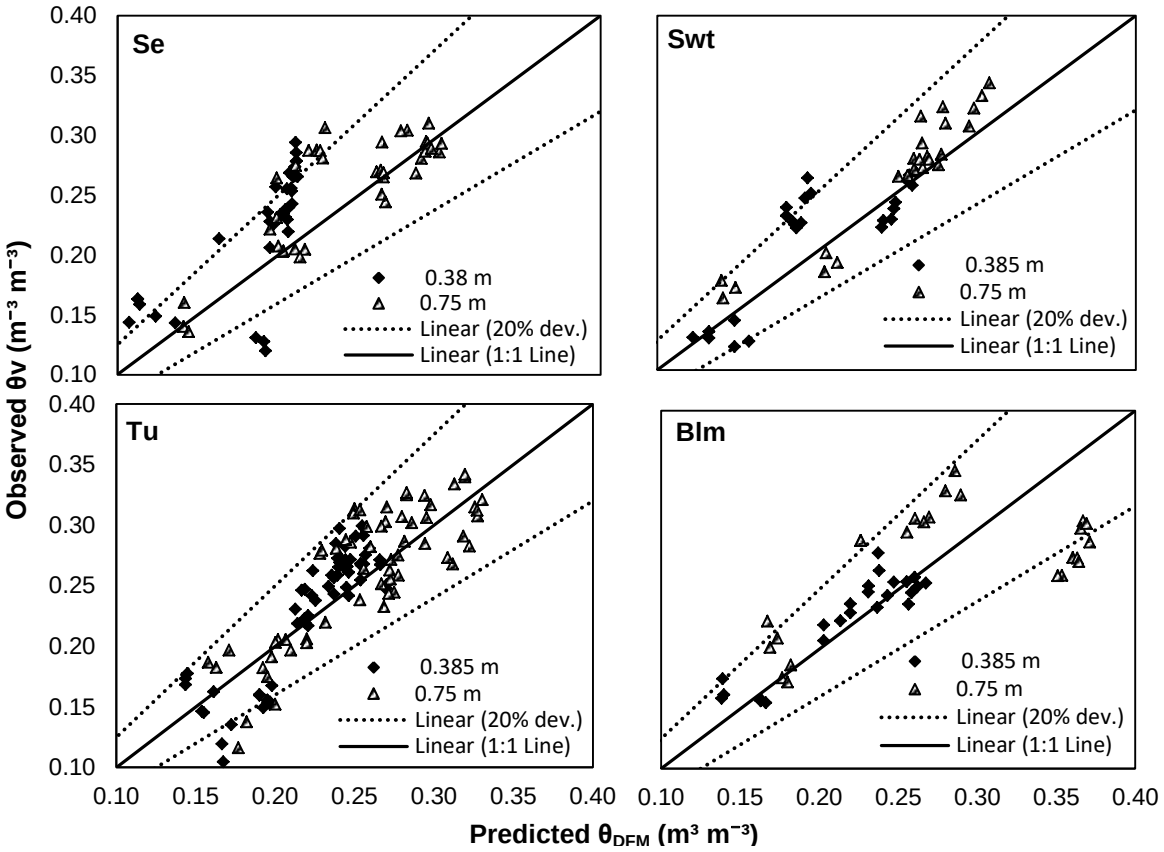

Appendix 5.10 Regression line of DFM predicted soil water content (θ_{DFM}, $m^3\ m^{-3}$) and the observed soil water content ($m^3\ m^{-3}$) at 0.38 m and 0.75 m depths for individual soil forms.

Appendix 5.11 Linear, power and polynomial equations that described soil water content determined from the relationship between EC_a and water content estimated from DFM probe calibration (θ_{DFM}) for the soil forms of Paradys Experimental Farm (n =Sample sizes)

ECa vs θ_{DFM}					
Soil forms	Depth (m)	Model Function	R^2	*P*-value	*n*
Sepane	0.38	θ_{ECa} = 0.007(EC_a) + 0.0639	0.903	$6E^{-18}$	36
	0.75	θ_{ECa} = 0.0063(EC_a) + 0.1049	0.907	$2E^{-18}$	
Swartland	0.38	θ_{ECa} = -0.0004(EC_a)^2 + 0.0246(EC_a) - 0.1294	0.929	$1E^{-13}$	24
	0.75	θ_{ECa} = $-6E^{-05}$(EC_a)^2 + 0.012(EC_a) + 0.021	0.900	$2E^{-12}$	
Tukulu	0.38	θ_{ECa} = 0.0159(EC_a)$^{0.8453}$	0.874	$8E^{-24}$	60
	0.75	θ_{ECa} = 0.0068(EC_a) + 0.0978	0.890	$9E^{-26}$	
Bloemdal	0.38	θ_{ECa} = 0.0088(EC_a) + 0.0308	0.813	$6E^{-09}$	24
	0.75	θ_{ECa} = -0.0007(EC_a)^2 + 0.0395(EC_a) - 0.2263	0.859	$8E^{-08}$	

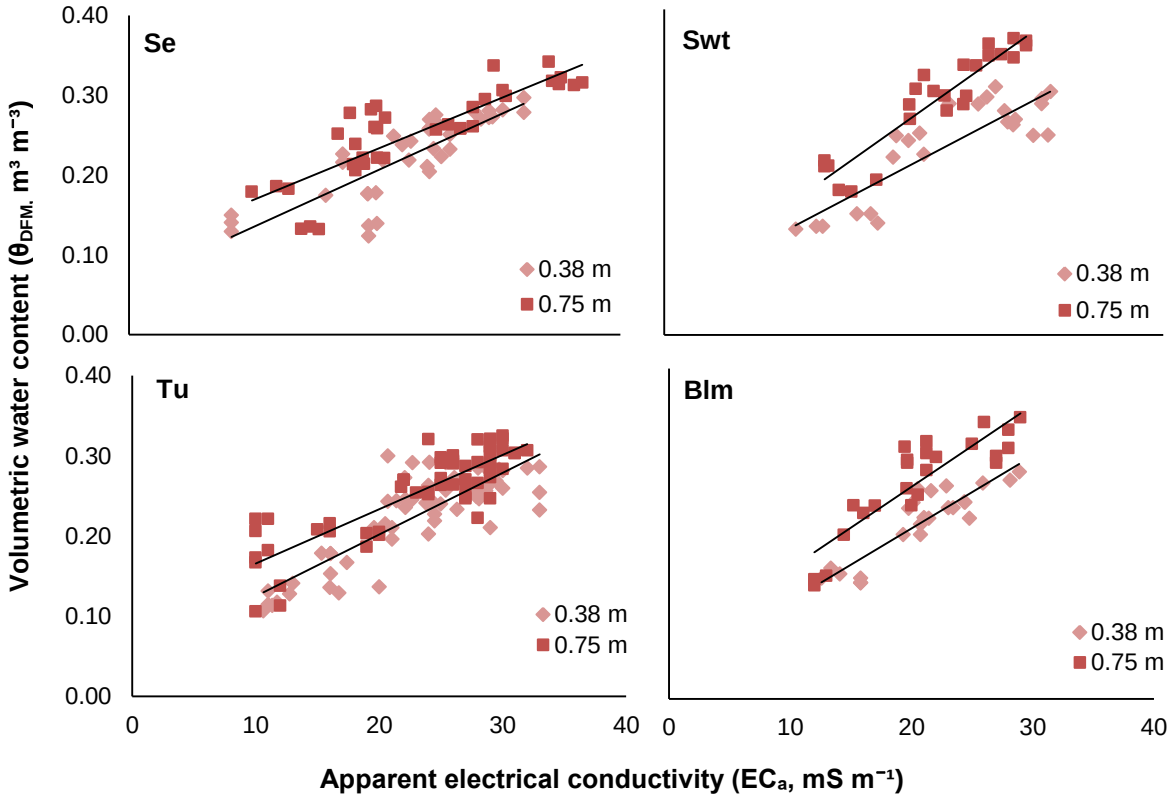

Appendix 5.12 Regression trend between EM38-MK2 readings (EC_a, mS m^{-1}) versus DFM estimated water content (θ_{DFM}, m^3 m^{-3}) at 0.38 m and 0.75 m depths, for Sepane (Se), Swartland (Swt), Tukulu (Tu) and Bloemdal (Blm) soil forms.

Appendix 5.13 Statistical measures evaluating the accuracy of the relationship between EC_a verses DFM volumetric water content (θ_{DFM}),

Soil forms	Depths (m)	EM38-MK2 model performance					
		Slope	Intercept	*RMdAE	*REF	*rs	*p*-value
Sepane	0.38	0.703	0.074	7.79	0.569	0.80	0.000
	0.75	0.917	0.021	9.60	0.572	0.78	0.000
Swartland	0.38	0.733	0.066	8.10	0.490	0.89	0.002
	0.75	1.027	-0.013	6.60	0.596	0.91	0.008
Tukulu	0.38	1.018	-0.002	6.10	0.603	0.89	0.000
	0.75	0.842	0.039	7.50	0.564	0.87	0.000
Bloemdal	0.38	0.847	0.034	4.00	0.703	0.96	0.000
	0.75	1.141	-0.045	4.90	0.619	0.93	0.001

*RMdAE = Relative median absolute error

*REF = Relative model efficiency

*rs = Spearman's' rank correlation

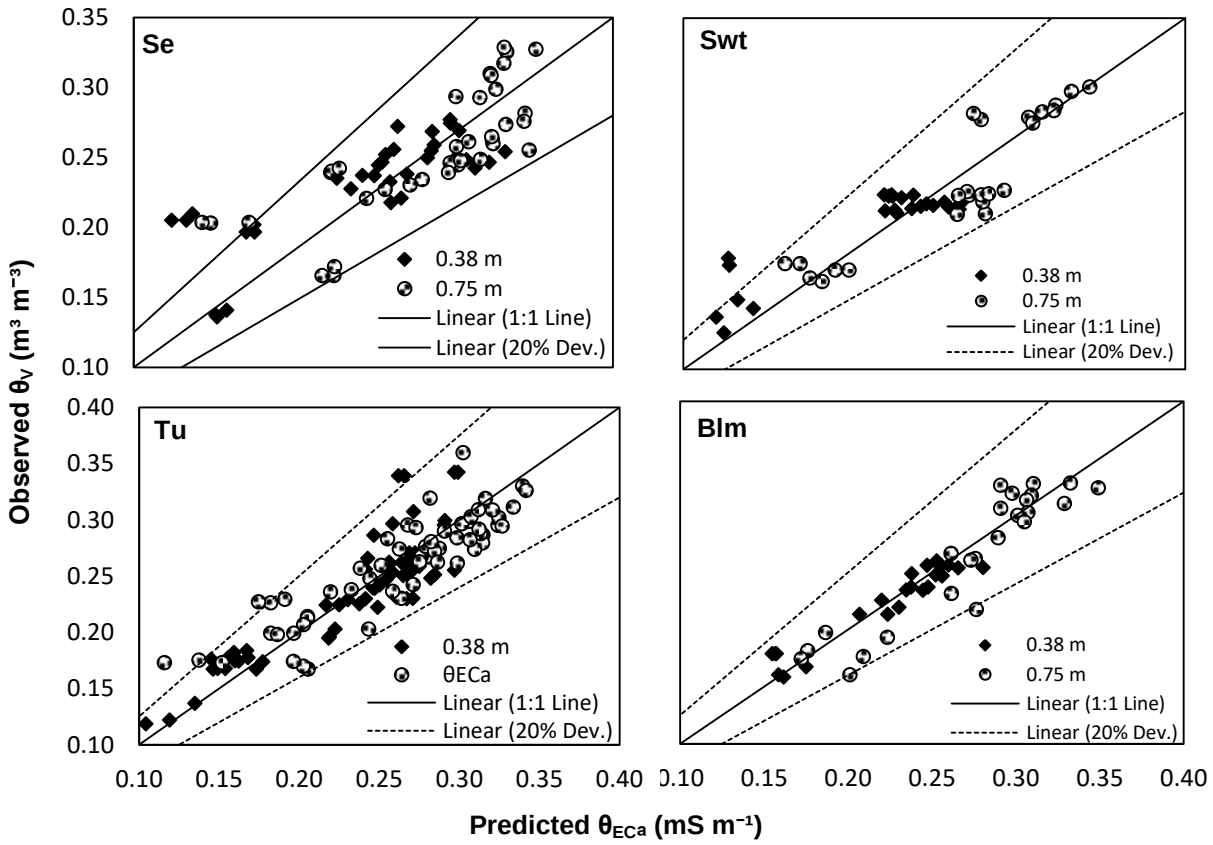

Appendix 5.14 Regression line of EM38-MK2 predicted soil water content (θ_{ECa}, $m^3\ m^{-3}$) and the observed soil water content ($m^3\ m^{-3}$) at 0.38 m and 0.75 m depths for individual soil forms.